

NATIONAL BUREAU OF STANDARDS REPORT

NBS Report 10 568

TEST AND EVALUATION OF THE PREFABRICATED LEWIS BUILDING AND ITS COMPONENTS PHASE II

and

NBS Report 10 193

HAIL RESISTANCE TESTS OF ALUMINUM SKIN HONEYCOMB PANELS FOR THE RELOCATABLE LEWIS BUILDING, PHASE II

for
Naval Civil Engineering Laboratory
Port Hueneme, California



U.S. DEPARTMENT OF COMMERCE
NATIONAL BUREAU OF STANDARDS

NATIONAL BUREAU OF STANDARDS

The National Bureau of Standards¹ was established by an act of Congress March 3, 1901. Today, in addition to serving as the Nation's central measurement laboratory, the Bureau is a principal focal point in the Federal Government for assuring maximum application of the physical and engineering sciences to the advancement of technology in industry and commerce. To this end the Bureau conducts research and provides central national services in four broad program areas. These are: (1) basic measurements and standards, (2) materials measurements and standards, (3) technological measurements and standards, and (4) transfer of technology.

The Bureau comprises the Institute for Basic Standards, the Institute for Materials Research, the Institute for Applied Technology, the Center for Radiation Research, the Center for Computer Sciences and Technology, and the Office for Information Programs.

THE INSTITUTE FOR BASIC STANDARDS provides the central basis within the United States of a complete and consistent system of physical measurement; coordinates that system with measurement systems of other nations; and furnishes essential services leading to accurate and uniform physical measurements throughout the Nation's scientific community, industry, and commerce. The Institute consists of an Office of Measurement Services and the following technical divisions:

Applied Mathematics—Electricity—Metrology—Mechanics—Heat—Atomic and Molecular Physics—Radio Physics²—Radio Engineering²—Time and Frequency²—Astrophysics²—Cryogenics.²

THE INSTITUTE FOR MATERIALS RESEARCH conducts materials research leading to improved methods of measurement standards, and data on the properties of well-characterized materials needed by industry, commerce, educational institutions, and Government; develops, produces, and distributes standard reference materials; relates the physical and chemical properties of materials to their behavior and their interaction with their environments; and provides advisory and research services to other Government agencies. The Institute consists of an Office of Standard Reference Materials and the following divisions:

Analytical Chemistry—Polymers—Metallurgy—Inorganic Materials—Physical Chemistry.

THE INSTITUTE FOR APPLIED TECHNOLOGY provides technical services to promote the use of available technology and to facilitate technological innovation in industry and Government; cooperates with public and private organizations in the development of technological standards, and test methodologies; and provides advisory and research services for Federal, state, and local government agencies. The Institute consists of the following technical divisions and offices:

Engineering Standards—Weights and Measures—Invention and Innovation—Vehicle Systems Research—Product Evaluation—Building Research—Instrument Shops—Measurement Engineering—Electronic Technology—Technical Analysis.

THE CENTER FOR RADIATION RESEARCH engages in research, measurement, and application of radiation to the solution of Bureau mission problems and the problems of other agencies and institutions. The Center consists of the following divisions:

Reactor Radiation—Linac Radiation—Nuclear Radiation—Applied Radiation.

THE CENTER FOR COMPUTER SCIENCES AND TECHNOLOGY conducts research and provides technical services designed to aid Government agencies in the selection, acquisition, and effective use of automatic data processing equipment; and serves as the principal focus for the development of Federal standards for automatic data processing equipment, techniques, and computer languages. The Center consists of the following offices and divisions:

Information Processing Standards—Computer Information—Computer Services—Systems Development—Information Processing Technology.

THE OFFICE FOR INFORMATION PROGRAMS promotes optimum dissemination and accessibility of scientific information generated within NBS and other agencies of the Federal government; promotes the development of the National Standard Reference Data System and a system of information analysis centers dealing with the broader aspects of the National Measurement System, and provides appropriate services to ensure that the NBS staff has optimum accessibility to the scientific information of the world. The Office consists of the following organizational units:

Office of Standard Reference Data—Clearinghouse for Federal Scientific and Technical Information³—Office of Technical Information and Publications—Library—Office of Public Information—Office of International Relations.

¹ Headquarters and Laboratories at Gaithersburg, Maryland, unless otherwise noted; mailing address Washington, D.C. 20234.

² Located at Boulder, Colorado 80302.

³ Located at 5285 Port Royal Road, Springfield, Virginia 22151.

NATIONAL BUREAU OF STANDARDS REPORT

10 568

TEST AND EVALUATION OF THE PREFABRICATED LEWIS BUILDING AND ITS COMPONENTS PHASE II

Report to

Naval Civil Engineering Laboratory
Port Moresby, California



U.S. DEPARTMENT OF COMMERCE
NATIONAL BUREAU OF STANDARDS

NATIONAL BUREAU OF STANDARDS

The National Bureau of Standards ¹ was established by an act of Congress March 3, 1901. Today, in addition to serving as the Nation's central measurement laboratory, the Bureau is a principal focal point in the Federal Government for assuring maximum application of the physical and engineering sciences to the advancement of technology in industry and commerce. To this end the Bureau conducts research and provides central national services in four broad program areas. These are: (1) basic measurements and standards, (2) materials measurements and standards, (3) technological measurements and standards, and (4) transfer of technology.

The Bureau comprises the Institute for Basic Standards, the Institute for Materials Research, the Institute for Applied Technology, the Center for Radiation Research, the Center for Computer Sciences and Technology, and the Office for Information Programs.

THE INSTITUTE FOR BASIC STANDARDS provides the central basis within the United States of a complete and consistent system of physical measurement; coordinates that system with measurement systems of other nations; and furnishes essential services leading to accurate and uniform physical measurements throughout the Nation's scientific community, industry, and commerce. The Institute consists of an Office of Measurement Services and the following technical divisions:

Applied Mathematics—Electricity—Metrology—Mechanics—Heat—Atomic and Molecular Physics—Radio Physics ²—Radio Engineering ²—Time and Frequency ²—Astrophysics ²—Cryogenics.²

THE INSTITUTE FOR MATERIALS RESEARCH conducts materials research leading to improved methods of measurement standards, and data on the properties of well-characterized materials needed by industry, commerce, educational institutions, and Government; develops, produces, and distributes standard reference materials; relates the physical and chemical properties of materials to their behavior and their interaction with their environments; and provides advisory and research services to other Government agencies. The Institute consists of an Office of Standard Reference Materials and the following divisions:

Analytical Chemistry—Polymers—Metallurgy—Inorganic Materials—Physical Chemistry.

THE INSTITUTE FOR APPLIED TECHNOLOGY provides technical services to promote the use of available technology and to facilitate technological innovation in industry and Government; cooperates with public and private organizations in the development of technological standards, and test methodologies; and provides advisory and research services for Federal, state, and local government agencies. The Institute consists of the following technical divisions and offices:

Engineering Standards—Weights and Measures—Invention and Innovation—Vehicle Systems Research—Product Evaluation—Building Research—Instrument Shops—Measurement Engineering—Electronic Technology—Technical Analysis.

THE CENTER FOR RADIATION RESEARCH engages in research, measurement, and application of radiation to the solution of Bureau mission problems and the problems of other agencies and institutions. The Center consists of the following divisions:

Reactor Radiation—Linac Radiation—Nuclear Radiation—Applied Radiation.

THE CENTER FOR COMPUTER SCIENCES AND TECHNOLOGY conducts research and provides technical services designed to aid Government agencies in the selection, acquisition, and effective use of automatic data processing equipment; and serves as the principal focus for the development of Federal standards for automatic data processing equipment, techniques, and computer languages. The Center consists of the following offices and divisions:

Information Processing Standards—Computer Information—Computer Services—Systems Development—Information Processing Technology.

THE OFFICE FOR INFORMATION PROGRAMS promotes optimum dissemination and accessibility of scientific information generated within NBS and other agencies of the Federal government; promotes the development of the National Standard Reference Data System and a system of information analysis centers dealing with the broader aspects of the National Measurement System, and provides appropriate services to ensure that the NBS staff has optimum accessibility to the scientific information of the world. The Office consists of the following organizational units:

Office of Standard Reference Data—Clearinghouse for Federal Scientific and Technical Information ³—Office of Technical Information and Publications—Library—Office of Public Information—Office of International Relations.

¹ Headquarters and Laboratories at Gaithersburg, Maryland, unless otherwise noted; mailing address Washington, D.C. 20234.

² Located at Boulder, Colorado 80302.

³ Located at 5285 Port Royal Road, Springfield, Virginia 22151.

NATIONAL BUREAU OF STANDARDS REPORT

NBS PROJECT

4215421

April 1971

NBS REPORT

10 568

TEST AND EVALUATION OF THE PREFABRICATED LEWIS BUILDING AND ITS COMPONENTS PHASE II

BY

Edgar V. Leyendecker and Thomas W. Reichard
Structures Section
Building Research Division
Institute for Applied Technology

for

Naval Civil Engineering Laboratory
Port Hueneme, California

IMPORTANT NOTICE

NATIONAL BUREAU OF STANDARDS
for use within the Government. Be
and review. For this reason, the p
whole or in part, is not authorize
Bureau of Standards, Washington,
the Report has been specifically pr

Approved for public release by the
director of the National Institute of
Standards and Technology (NIST)
on October 9, 2015

accounting documents intended
bjected to additional evaluation
sting of this Report, either in
Office of the Director, National
the Government agency for which
ies for its own use.



U.S. DEPARTMENT OF COMMERCE
NATIONAL BUREAU OF STANDARDS



ABSTRACT

A two bay, 20 ft wide by 48 ft long, Mark III-A Relocatable Lewis Building was tested in the laboratory to determine the structural behavior of the building while resisting lateral loads and to suggest modifications. In addition various Lewis Building components were tested. Test data and their significance are presented in the report.

TABLE OF CONTENTS

	Page
ABSTRACT	i
1. INTRODUCTION	1
1.1 Objective and Scope.	1
1.2 General.	2
1.3 SI Conversion Units.	4
2. TEST STRUCTURE	5
2.1 General.	5
2.2 Components	5
2.2.1 Panels	5
2.2.2 Aluminum Extrusions.	7
2.2.3 Ridge and Transverse Beams	7
2.2.4 End Wall Panels.	8
2.2.5 Aluminum I-Beams	8
2.3 Building Erection.	8
2.3.1 General.	8
2.3.2 Modifications.	11
2.3.3 Erection Problems.	12
2.3.4 Erection Time.	12
3. TEST PROGRAM	14
3.1 General.	14
3.2 Test Series S1, Panel Tests.	14
3.2.1 Test S1a, Single Panel with Air Bag Loading.	14
3.2.2 Test S1b, Three-Panel Tests.	15
3.2.3 Test S1c, Single Panel with Vacuum Loading.	15
3.2.4 Instrumentation.	16
3.3 Test Series S2, Full-Scale Building Tests.	16
3.3.1 General.	16
3.3.2 Test S2a and S2c	16
3.3.3 Test S2b	17
3.3.4 Loading.	17
3.3.5 Instrumentation.	18
3.4 Test Series S3, Shear and Flexural Properties	18
3.4.1 Test Series S3a, 3/4 in Cell Honeycomb.	18
3.4.2 Test Series S3b, 1/2 in Cell Honeycomb.	19
3.5 Test Series S4, Flatwise Compression Tests	20
3.5.1 Test Series S4a, 3/4 in Cell Honeycomb.	20
3.5.2 Test Series S4b, 1/2 in Cell Honeycomb.	20

TABLE OF CONTENTS (Cont.)

3.6	Test Series S5b, Indentation Test.	20
3.7	Test Series S6, Ridge Beam Test.	21
3.8	Test Series S7, Hardware Tests	22
3.9	Test Series S8, Flatwise Tension Tests	22
4.	TEST RESULTS	24
4.1	General	24
4.2	Test Series S1, Panel Tests	24
4.2.1	General.	24
4.2.2	Test Series S1a, Single Panel with Air Bag Loading.	25
4.2.3	Test Series S1b, Three Panel Tests	25
4.2.4	Test Series S1c, Single Panel with Vacuum Loading	29
4.2.5	Discussion	30
4.3	Test Series S2, Full-Scale Building Tests.	32
4.3.1	General.	32
4.3.2	Test S2a	32
4.3.3	Test S2c	34
4.3.4	Discussion of Test S2a and S2c	35
4.3.5	Modified S2b Tests	36
4.3.6	Test S2b(1) and S2b(2)	37
4.3.7	Discussion of Test S2b(1) and S2b(2)	39
4.3.8	Performance & Appearance of Building After Tests.	42
4.4	Test Series S3, Shear and Flexural Properties	43
4.4.1	Test Series S3a, 3/4 in Cell Honeycomb.	43
4.4.2	Test Series S3b, 1/2 in Cell Honeycomb.	44
4.4.3	Discussion	44
4.5	Test Series S4, Flatwise Compression Strength	46
4.5.1	Test Series S4a, 3/4 in Cell Honeycomb	46
4.5.2	Test Series S4b, 1/2 in Cell Honeycomb	47
4.5.3	Discussion	47
4.6	Test Series S5b, Indentation Tests	47
4.7	Test Series S6, Ridge Beam Test.	49
4.8	Test Series S7, Hardware Tests	49
4.9	Test Series S8, Flatwise Tension Tests	49
5.	CONCLUSIONS AND RECOMMENDATIONS.	50
5.1	Erection	50
5.2	Structural	50
6.	ACKNOWLEDGEMENTS	53

TEST AND EVALUATION OF THE PREFABRICATED LEWIS
BUILDING AND ITS COMPONENTS
PHASE II

By

Edgar V. Leyendecker*

and

Thomas W. Reichard**

1. INTRODUCTION

1.1 Objective and Scope

The objective of this study was to evaluate a Mark III-A model of the Lewis Relocatable Building and its components when subjected to loadings suggested by the Naval Civil Engineering Laboratory (NCEL) at Port Hueneme, California. A proposed test program was described in a letter dated July 31, 1969 to E. O. Pfrang of the National Bureau of Standards (NBS) from W. F. Burkart of NCEL. The proposed program, which included structural and limited environmental testing, was modified in a letter dated September 19, 1969 to Mr. Burkart from I. A. Benjamin of the National Bureau of Standards. The subsequent structural tests performed and reported

* Structural Research Engineer, Building Research Division, Institute of Applied Technology, National Bureau of Standards.

**Physicist, Building Research Division, Institute of Applied Technology, National Bureau of Standards.

herein are summarized in table 1.1.^{1/} Test Series S2 was performed on a full-scale building without end walls in order to study the resistance of the building to lateral load. The tests were designed to determine the behavior of the standard two module 48 foot long building and to determine the behavior of an expanded building consisting of an indefinite number of modules. The remaining tests were performed to obtain component and small specimen data. The complete structural test program is described in detail in section 3.

Since numerous tests were performed on the Mark III-A it was necessary to prevent serious overloading in any one test. Such overloading might invalidate data obtained in subsequent tests. Hence, the data obtained from the full-size building, was not necessarily intended to include ultimate load data.

1.2 General

The basic design of the Lewis Building is detailed in NAVFAC Drawing No. 065-012, dated November 1, 1968. The Mark III model of the Lewis Building was described in a set of eight drawings entitled "Relocatable 20 ft 6 in x 48 ft 9 in Lewis Building for the Department of the Navy." The set of

^{1/} The NBS Hailstone Test on component materials, designated as Test S5a in the test program, was described in NBS Report No. 10193 which is attached to this report.

drawings, dated February 17, 1969, was prepared by the manufacturer of the building. The Mark III was tested in the laboratories of the Building Research Division of the National Bureau of Standards and three reports were issued [1,2,3].^{2/}

The Mark III-A model (modified Mark III) of the Lewis Building, tested and reported herein, was prefabricated in Florida using 4 ft wide aluminum sandwich panels and was made by the manufacturer of the Mark III. The erection procedure and structural details for the Mark III-A are described in a set of eight drawings entitled, "Navy MK III-A Lewis Building, F. O. No. 2856-2." These drawings were prepared by the manufacturer of the building [4].

The Mark III-A was designed on a 24 ft long module, 20 ft wide. Two such modules made up the 20 ft by 48 ft building^{3/}. A full-scale building, modified by removing the end walls, was tested in the laboratory.

^{2/}Numbers in brackets refer to references in the bibliography.

^{3/}The Mark III was designed on a 16 ft long module, 20 ft wide. Three such modules made up the 20 ft by 48 ft building.

1.3 SI Conversion Units

In view of present accepted practice in this country in this technological area, common U. S. units of measurement have been used throughout this paper. In recognition of the position of the USA as a signatory to the General Conference on Weights and Measures, which gave official status to the metric SI system of units in 1960, we assist readers interested in making use of the coherent system of SI units, by giving conversion factors applicable to U. S. units used in this paper.

Length	1 in = 0.0254* meter 1 ft = 0.3048* meter
Area	1 in ² = 6.4516* x 10 ⁻⁴ meter ² 1 ft ² = 0.09290 meter ²
Force	1 lb (lbf) = 4.448 newton 1 kip = 4448 newton
Pressure, Stress	1 psi = 6895. newton/meter ² 1 ksi = 6.895 x 10 ⁶ newton/meter ²
Mass Volume	1 lb/ft ³ (lbm/ft ³) = 16.02 ₃ kilogram/ meter ³
Moment	1 kip-in = 113.0 newton-meter

* Exactly

2. TEST STRUCTURE

2.1 General

The building plans are contained in reference 4. Technical specifications and erection instructions are in references 5 and 6, respectively.

2.2 Components

The major components of the building were:

- 1.. 4 ft x 8 1/2 ft wall panels.
2. 4 ft x 20 1/2 ft floor panels.
3. 4 ft x 11 1/2 ft roof panels.
4. 24 ft long ridge beams.
5. 20 ft long, gable shaped, transverse beams.
6. End wall panels with sloping top.
7. Eight different aluminum extrusions.
8. Aluminum I-Beams (extruded).
9. Extruded rigid vinyl "locking cleat."

2.2.1 Panels

The wall, floor, and roof panels were three inch thick, symmetrical sandwich panels. The sandwich core was 11

percent phenolic impregnated, 99 lb kraft paper fabricated into a 3/4 in cell size honeycomb. The honeycomb core was positioned with the ribbon perpendicular to the panel length. The floor panel facings were .050 in (nominal) mill-finish, sheet aluminum. The wall and roof panel facings were 0.024 in nominal (0.0245 in actual) prefinished, stucco embossed, coiled sheet aluminum. Facings were 3105-H264 aluminum with a yield strength of 24,000 psi and an ultimate strength of 26,000 psi. The facings were pressure bonded to the honeycomb with a neoprene-phenolic contact adhesive containing 25 to 30 percent solids. The solvent was evaporated in a flash oven.

The lengthwise edges of the wall and roof panel facings were bent into a "J" shaped, internal lock groove, during fabrication. Figure 2.1 illustrates the use of the rigid vinyl extrusion to connect the "J" shaped edges of two adjacent panels.

The floor panel edges were reinforced and sealed with a special factory-installed aluminum channel (extrusion G, figure 2.2). The paper honeycomb core was exposed at the edges of the roof and wall panels.

2.2.2 Aluminum Extrusions

The purpose, shape and scaled size of the extrusions used in the Mark III-A are shown in figure 2.2. These extrusions are the same as those used in the Mark III with a few exceptions. For convenience in comparison, the same designations used in a previous report [2] have been used. Extrusion "D" used in the Mark III was replaced in the Mark III-A by extrusion F which was also still used for its original purpose. These extrusions were aluminum alloy 6063-T5.

2.2.3 Ridge and Transverse Beams

The ridge and transverse beams were fabricated from the sandwich panel material described in section 2.2.1. Extrusions A and G were used as the top and bottom flanges of the transverse beam as well as the bottom and end flanges of the ridge beam. The top flange of the ridge beam consisted of several extrusions as shown in figure 2.3.

The beam extrusions were connected to the sandwich panel material with 1/8 in diameter aluminum pop rivets with steel mandrels at about one inch on center in the transverse beam and two inches on center in the ridge beam.

2.2.4 End Wall Panels

The end wall panels were fabricated from the same materials and in the same manner as the side wall panels. These panels extend full length from the floor to the roof with the top edge cut to the roof angle. These end wall panels were not installed in the tests described herein.

2.2.5 Aluminum I-Beams

Aluminum I-Beams served as the foundation for the building. These beams were extrusions apparently made for some other purpose as they had several special purpose projections on the web and one flange. Neglecting these projections, the dimensions of the beams were:

Depth	- 10 in
Width	- 4 in
Web Thickness	- 3/32 in
Flange Thickness	- 5/32 in
Weight	- 2.56 lb/ft (Including projections)
Aluminum Type	- 6063-T5

2.3 Building Erection

2.3.1 General

The building components were prefabricated in Florida and shipped by rail to Gaithersburg, Maryland in six crates. The

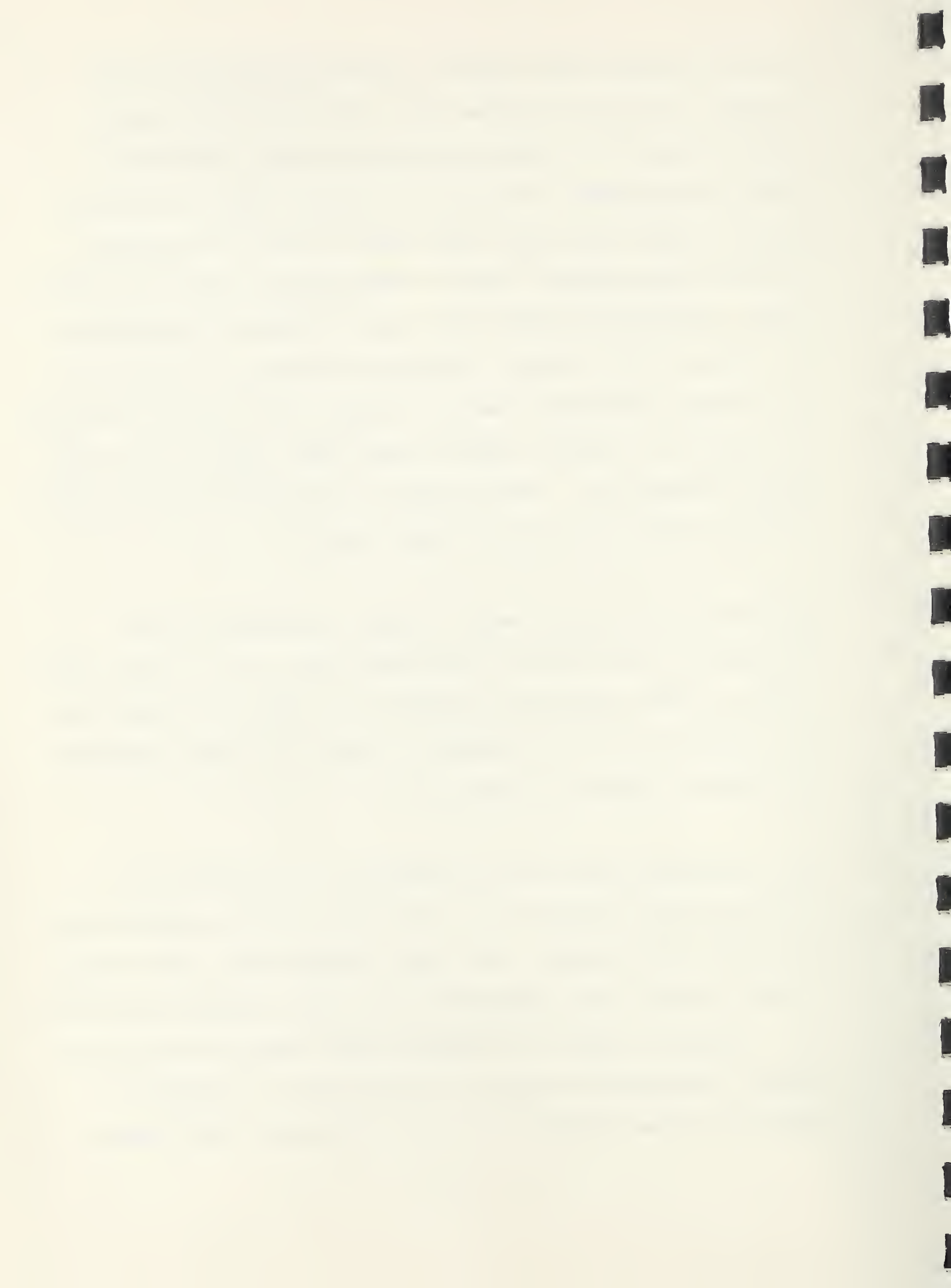
crates and their contents were received in good condition. The crates were well built and suitable for reuse with the contents protected from the weather. The shipment packing list is in appendix A. The packing list contains the weight, dimensions and contents of each of the six crates. The crate contents were arranged so that only one crate at a time needed to be opened during erection of the designed building.

The 20 ft x 48 ft modified (no end walls) building was erected by laboratory personnel on the laboratory test floor. The beginning of erection is shown in figure 2.4. All of the aluminum I-Beams are shown connected and ready for placement on fourteen steel-plywood supports anchored to the test floor. The supports simulated piers called for by the building plans. The I-Beams rested on 10 in squares of 3/4 in plywood (simulating 10 in concrete piers) which, in turn, rested on steel channels. Bolts passed through the bottom flange of the I-Beam, the plywood and the channel to provide attachment to the floor. The steel-plywood piers were attached to the floor at additional points to prevent their movement during testing. The I-Beams are shown attached to the simulated piers in figure 2.5.

The floor panels were placed, starting at one end of the building, after the I-Beams were connected to the "pier" plates (figure 2.5, note the shipping crate on the left side of the figure). Six 1/4 in aluminum stove bolts were used to fasten the first floor panel at each intersection with the longitudinal I-Beams (three bolts on each 20 1/2 ft side). Subsequent panels were laid in order by connecting the edges of the factory installed extrusion G (figure 2.2) in a tongue and groove fashion. Three 1/4 in bolts were used to connect the leading edge of each floor panel to the floor beam intersections. Twelve four ft wide panels and one seven inch wide panel made up the floor length.

After the floor panels were in place, extrusion F was fastened to the floor with stainless steel No. 12 sheet metal screws. These screws were placed in a double row along the extrusion at six in on centers in each row. This completed operation is shown in figure 2.6.

The wall panels were set into extrusion F starting at a building corner (figure 2.7). The rigid vinyl extrusion was inserted, from the top, into each vertical wall joint except at the corners where extrusion C was used (normally extrusion H). Stainless steel No. 12 sheet metal screws at six in on centers fastened both faces of each panel to extrusion F. Extrusion B was placed on the top of the side wall panels.



The transverse beams and the longitudinal ridge beams were then placed and connected to each other with 1/4 in stove bolts. The completed installation is shown in figure 2.8.

The roof panels were then installed using extrusion E at the ridge and extrusion F at the eave. No. 12 sheet metal screws were used at six inches on centers (inside and out) to fasten the extrusions to the panels. The completed structure is shown in figure 2.9.

2.3.2 Modifications

The Mark III-A erected in the laboratory was modified by replacing the end walls with a typical transverse beam. This was done in order to obtain data on a building consisting of an indefinite number of 24 ft modules. This required a slight modification to the building as shown in figure 2.10. Figures 2.10a and b are enlarged drawings of the area shown in figure 2.10c. Figure 2.10a is the normal detail and figure 2.10b is the modified detail in the test structure. Ordinarily the wall panels are fastened to the panel seats in extrusion C and a vinyl cleat. As erected, there was a one inch gap between the panel and the panel seat in the end extrusions as shown in figure 2.10b. The wall panels were fastened to the end extrusions with No. 12 screws. Allowance must be made for this slight dimensional difference if this

building is to be used with a variable number of modules.

One possible solution is to modify the vinyl extrusion connecting the wall panel to extrusion C when more than two modules are used. Another possible solution would be to use two vinyl cleat extrusions connected by a very narrow wall panel. This 1-in wide wall panel would be in reality two sheet aluminum channels with legs bent to engage the vinyl extrusions.

Optional knee braces were installed on the building for test S2c. Details of the braces are shown in figure 2.11. The braces were fabricated by NBS personnel from panel material described in section 2.2.1.

2.3.3 Erection Problems

Erection problems encountered in the Mark III [2] were eliminated in the Mark III-A. The only difficulty encountered was the dimensional problem described in section 2.3.2 due to erecting the building without end walls.

2.3.4 Erection Time

Overall, 20 man days (7 1/2 hr days) were used in erecting the Mark III-A. This compares with 36 man days (7 1/2 hr

days) required to erect the Mark III [2] in which considerable erection difficulties were encountered.

This was the second time this particular building had been erected. Disassembly and erection at still another location would not be difficult.

3. TEST PROGRAM

3.1 General

The test program included full-scale building tests and component tests. These tests are summarized in table 1.1 and discussed in more detail below.

3.2 Test Series S1, Panel Tests

Test Series S1 were tests on full-size panels. The various tests conducted are described below and summarized in figure 3.1.

3.2.1 Test S1a, Single Panel with Air Bag Loading

Three 4 ft by 8 ft panels were tested individually as uniformly loaded beams, simply supported on a 7 ft 8 in span, as shown in figure 3.1a. The panels were tested in an inverted position by inserting an air bag between the panel and the laboratory test floor. The panel was held to the floor at 7 ft 8 in centers to provide the simple supports. The purpose of the test was to determine the load capacity of a single panel.

3.2.2 Test Slb, Three-Panel Tests

Two specimens consisting of three 4 ft by 14 ft panels joined together with vinyl cleats were tested as a uniformly loaded beam (only the two outside panels were loaded) as shown in figure 3.1b. The panels were tested in an inverted position by inserting an air bag between each of the two outside panels and the floor. The panels were held to the floor at 13 ft 8 in centers to provide the simple supports. The purpose of the test was to determine the load that could be transferred through the vinyl cleats to an unloaded panel.

3.2.3 Test Slc, Single Panel with Vacuum Loading

Three 4 ft by 8 ft panels were tested individually as uniformly loaded beams simply supported on a 7 ft 8 in span as shown in figure 3.1c. This test differed from test Sla in that the uniform load was provided by a vacuum on the tension face rather than an air bag loading on the compression face. During these tests the compression facing was open to atmospheric pressure. The purpose of the tests was to determine if the tension facing would pull away from the honeycomb material before the panel reached the maximum load as determined in test Sla.

3.2.4 Instrumentation

Deflections were measured with LVDT linear displacement gages at the locations shown in figure 3.1. In addition, two of the three Slc test specimens had five strain gages (one inch gage length) mounted at midspan; one in the middle, two at three inches from each edge and two at twelve inches from each edge.

3.3 Test Series S2, Full-Scale Building Tests

3.3.1 General

Test Series S2 were conducted on a modified (as described in section 2) full-scale building. Three types of tests (S2a, S2b and S2c) were conducted in this series as described below.

3.3.2 Test S2a and S2c

Tests S2a and S2c were performed with the loading shown in figure 3.2. The purpose of these tests was to determine the resistance of an interior length of the building to lateral loads such as winds. Test S2c differed from S2a in that S2c had the optional knee braces described in section 2.3.2.

3.3.3 Test S2b

Test S2b was performed with the loading shown in figure 3.3. The purpose of the test was to determine the bending resistance of the roof in the horizontal plane. Load was applied with a single ram at the midlength of the building. Two rams at the ends of the building provided reaction support in the horizontal plane.

3.3.4 Loading

The Mark III-A is shown ready for testing in figure 3.4. Three test frames are shown in the photograph with hydraulic rams in position for loading.

- (a) Tests S2a and S2c - Each of the three identical rams were operated from a common hydraulic oil supply insuring equal load at each load application point. The test frames were held in position by attaching them to the laboratory tie-down floor.
- (b) Test S2b - The building was loaded only by the ram attached to the center test frame. The oil supply was disconnected from the two end rams. The two end transverse beams were restrained by passing a closed yoke around them. One end of the yoke was attached to the test frame through the disconnected rams and the other end of the yoke was fastened to the north end of the transverse beams.

3.3.5 Instrumentation

The various measuring devices are described below. Their locations are shown in figure 3.5. The analog signals from all instrumentation were fed into a 100 channel data processor and recorded on perforated paper tape as well as a printed copy.

- (a) Lateral Deflection Measurements - The lateral movements of the side walls in the plane of the end walls were measured at twenty locations using LVDT linear displacement gages. (2-in measuring range).
- (b) Vertical Roof Deflection Measurements - Vertical roof ridge movements were measured with LVDT's at five locations.
- (c) Vertical Uplift Deflection Measurements - Vertical uplift at the base of the walls were measured at six locations using LVDT's.
- (d) Load Measurements - Loads were measured at five locations, but only three during any one test. Loads were measured at the three rams on the south wall during test S2a and S2c.

The load was measured at the center ram of the south wall and the end reactions on the north wall during test S2b.

3.4 Test Series S3, Shear and Flexural Properties

3.4.1 Test Series S3a, 3/4 inch Cell Honeycomb

Six specimens, with 3/4 inch cell honeycomb core, conditioned at 50 percent relative humidity (RH) and 73°F, were tested in

flexure to determine core shear strength, shear modulus, and bending stiffness. The same tests were performed on an equal number of specimens conditioned at 100 percent RH and 73°F. Flexural test apparatus, specimen size, and loading conformed to ASTM C393-62. In addition three 6" x 24" specimens conditioned at 50 percent RH and 73°F were tested in compressive shear using the plate shear method of ASTM C-273. These loading conditions are shown in figure 3.6.

The core was 11 percent phenolic impregnated, 99 lb (99 lb per 3000 sq ft) kraft paper fabricated into a 3/4 inch cell size honeycomb. This was the same type core used in the 4 ft x 8 ft panels, and building, previously described. The core ribbon was perpendicular to the test span.

3.4.2 Test Series S3b, 1/2 inch Cell Honeycomb

These tests were the same as test series S3a (section 3.4.1) except that 1/2 inch cell honeycomb core was used in the specimens. The core was 11 percent phenolic impregnated, 70 lb per 3000 sq ft) kraft paper fabricated into a 1/2 inch cell size honeycomb. The core ribbon was perpendicular to the test span.

3.5 Test Series S4, Flatwise Compression Tests

3.5.1 Test Series S4a, 3/4 inch Cell Honeycomb

Six specimens with 3/4 inch cell honeycomb core conditioned at 50 percent RH and 73°F were tested to determine the flatwise compressive strength. The same tests were also performed on six specimens conditioned at 100 percent RH and 73°F. Test apparatus, specimen size and loading conformed to ASTM C365-57. The loading condition is shown in figure 3.6.

3.5.2 Test Series S4b, 1/2 inch Cell Honeycomb

These tests were the same as Test Series S4a (section 3.5.1) except 1/2 inch cell honeycomb core was used.

3.6 Test Series S5b, Indentation Tests^{4/}

Indentation tests were performed on typical floor panels with tile in place, which is the actual use case since the

^{4/}Test S5a, Hailstone Test, is described in reference 7 (copy attached).

floor tile is factory installed. Test procedure was similar to ASTM E72. A one inch diameter steel probe (area = .785 sq. in.) was used to apply loads of 200, 400, 600, 800, and 1000 lb (255, 510, 764, 1020, and 1274 psi) in five locations along the length of the building directly under the ridge beam. Thus, the point of load application was directly over an aluminum I-Beam running the length of the building. The test loads were applied using a hydraulic ram, with the reaction carried through a timber post into the ridge beam.

Permanent indentation was measured with a dial gage mounted on a tripod arrangement, as recommended by ASTM E72. The test procedure was to record a base reading, then load to a predetermined test load (200, 400, 600, 800 or 1000 lb). The load was removed and final indentation readings were taken after time intervals of one minute and one hour. In addition the indentation under load was measured with a similar tripod arrangement mounted on the probe.

3.7 Test Series S6, Ridge Beam Test

A typical ridge beam was tested with a uniform load on a 23 ft 6 in simply supported span. The beam was loaded by applying air pressure to a fire hose placed between the beam and the laboratory test floor. The beam was held to the floor at 23 ft 6 in centers to provide the simple supports. With

this loading system the ridge beam was inverted from its normal position in the building but the load was applied as in actual use. The beam was tested on simple supports with the reactions bearing on the bottom extrusion.

Air pressure in the fire hose, end reactions, and end and midspan deflections were measured. The purpose of the test was to determine the beam strength under roof loading.

In actual practice the support reactions are carried by shear through the extrusion at the end of the beam rather than bearing on the bottom flange. There is probably some continuity effect.

3.8 Test Series S7, Hardware Tests

This series of tests was to determine the strength of extrusions, rivets, and other connecting hardware, as deemed necessary. No tests were performed.

3.9 Test Series S8, Flatwise Tension Tests

This test procedure was as described in ASTM C297. Steel blocks (3 in x 3 in x 1 in thick) were bonded to both skins of 3 in x 3 in specimens with a "hot glue." Universal joints were connected to both blocks. The tensile load was applied

through the universal joints to the specimen by using 3/8 in pull rods gripped in the heads of a hydraulic testing machine. No measurements were made other than the maximum load. This test evaluates the strength of the skin-to-core bond or the tensile strength of the core, depending on the type of failure.



b = panel width = 48 in
t = facing thickness = 0.0245 in
h = sandwich panel thickness = 3 in

h-t = lever arm between centroids of facings

M = 24 ksi x 48 in x 0.0245 in x (3 in - 0.0245 in x
1/12

M = 7.00 kip-ft

4.2.2 Test Series Sla, Single Panel with Air Bag Loading

The load-deflection curves for the 4 ft x 8 ft panels uniformly loaded with an air bag are shown in figure 4.1 (along with curves from Test Series Slc). A dual scale is used for the ordinate. One scale is the applied load in psf, the second scale is the midspan bending moment.

The three specimens failed by wrinkling of the compression facing near midspan at almost identical loads. The average failure load was 157 psf (average facing stress = 15,640 psi; average core shear stress = 17.3 psi) which was 65.9 percent of the computed flexural capacity. The load response was virtually linear up to the point of failure.

4.2.3 Test Series Slb, Three Panel Tests

The deflection profiles for the three panel (4 ft x 14 ft panels) tests are shown in figures 4.2 and 4.3 for specimens 1 and 2 respectively. The midspan load-deflection curves

for locations 1, 2, and 3 (as identified in figures 4.2 and 4.3) are shown in figure 4.4 for the two specimens tested. Both specimens failed by splitting of the vinyl cleat connecting one of the loaded panels with the unloaded center panel. As indicated by the load-deflection curves in figure 4.4 and the deflection profiles, the unloaded center panel carried a significant portion of the applied load. The percents of flexural capacity tabulated in table 4.1 indicate that if the center panel carried no load, then the two loaded panels reached 115 to 120 percent of the calculated flexural capacity. If the three panels are equally effective in resisting load then each panel carried 75 to 80 percent of the calculated flexural capacity. The true case lies between these two extremes. This will be discussed later. The above data indicate that the panels did attain a larger percent of their flexural capacity without wrinkling of the compression facing than the single panels (table 4.1).

The center panel is loaded, as shown in figure 4.5, by shear transferred across the joint by the vinyl extrusions. The approximate amount of bending moment carried by the center panel may be determined by assuming a pin joint between panels and a sinusoidal distribution of shear loading at the joint. The bending moment may then be calculated by

$$M_1 = \frac{q_1 L^2}{\pi^2} \quad (4.2)$$

where:

M_1 = midspan bending moment

q_1 = intensity of loading per foot at midspan

L = span length

π = 3.14 ...

and:

$$W_1 = \frac{M_1 L^2}{\pi^2 EI} \quad (4.3)$$

where:

W_1 = midspan deflection

EI = flexural rigidity

Eq. 4.1 and 4.2 are approximate since they neglect shear deflections.

The modulus of elasticity, E , was assumed as 10,000,000 psi (typical for aluminum of the type used). The moment of inertia, I , was computed assuming all flexural bending is resisted by the facings. Plate action (Poisson's ratio effect) was neglected in computing the flexural rigidity, EI . Midspan bending moments were computed using eq 4.3 with midspan deflections, W_1 , obtained from figure 4.4. The load intensity, q_1 , was computed using eq 4.2.

The calculated midspan moments on the center panels were 4.13 kip-ft (using an extrapolated $W_1 = 2.62$ in) and 4.16 kip-ft

(using $W_1 = 2.60$ in) for specimens 1 and 2 respectively. The resulting load intensities, q_1 , were 218 and 220 lb/ft. Moments on the exterior panels were computed by subtracting the above moments from the total moments listed in table 4.1. The difference was assumed to be equally distributed between the two exterior panels. Thus the exterior panel moment was 5.99 kip-ft on specimen 1 and 6.33 kip-ft on specimen 2. In both specimens the above data indicate that the center panel was carrying about 2/3 of the bending moment of each exterior panel. Thus, considerable load was being transferred through the vinyl extrusion.

Based on the above analysis, the exterior panels in specimen 1 carried 85.6 percent of its calculated flexural yield moment and specimen 2 carried 90.5 percent. Both of these percents are larger than the average 65.9 percent obtained in test series Sla for a single panel. At these percents, the test specimen capacity was limited by splitting in the vinyl cleat rather than wrinkling in the aluminum facing as in series Sla. Wrinkling did occur in the single outer loaded panel as a secondary effect after the vinyl extrusion split. The increased capacity per panel, when compared with isolated panel strengths, is attributed to the elastic restraint along the panel edges. Thus the flexural load carrying capacity of each of a series of panels is probably 85 to 90 percent of the calculated flexural capacity of an individual panel. If the



vinyl extrusion had not split, the panels might have reached their yield moment capacity.

4.2.4 Test Series Slc, Single Panel With Vacuum Loading

The load-deflection curves for specimens I and J are shown in figure 4.1 along with curves for Series Sla specimens. Deflection data for specimen H was considered invalid because of difficulties in maintaining a constant load while reading gages due to leakage in the loading system.

The failure loads for this series were not as consistent as in Series Sla and Slb. Specimen H failed at a load of 117 psf. This was a shear failure at a "dry" core splice^{5/} located about three inches from a support. Specimen I failed in shear at 116 psf (average facing stress = 11,550 psi; average core shear stress = 12.8 psi), a load almost the same as specimen H. This was a true shear failure with no evidence of a splice or any other defect. The reason for this failure is not known. Specimen J failed by wrinkling of the compression facing as in Series Sla at a load of 141 psf (average facing stress = 14,030 psi; average core shear stress = 12.8 psi). The tension facing did not separate from the paper honeycomb.

^{5/}A dry core splice is where two individual sheets of core are used in a panel with no attempt being made to provide structural continuity between the two.

4.2.4 Discussion

The test results indicate that individual panels fail by wrinkling of the compression face under uniform load at about 65 percent of the yield load. Test results further indicate that when panels are joined together with the vinyl extrusions they may reach 85 to 90 percent of their calculated yield moments due to the elastic restraint of the extrusions preventing wrinkling until after the vinyl extrusions fail.

If the isolated panel strength is taken as the design limit then the strength of a typical wall panel, under uniform loading, is about 153 psf on an eight foot span and 68 psf on a twelve foot span. Both of these exceed the design requirement of 20 psf wind load and 30 psf snow load by substantial margins. However, the failures are sudden and without warning.

The panels tested on an eight foot span loaded with a vacuum indicate that the failure mode may be either by shear or buckling of the compression skin. Thus this loading condition may result in a borderline stress condition where the final failure mode depends on slight strength variations.

Test Series Slc indicated that the panels fail by either shear or compression facing buckling before pulling the facing from the core. The flexural failure in specimen J occurred at 141

psf which was lower than the 153 psf average for Test Sla. The shear failure occurred at a load of 116 psf. These results lead to the following conclusions.

- (a) The compression facing is partially restrained from wrinkling when the load is applied directly to that surface (153 psf vs 141 psf).
- (b) A shear type failure is restrained from occurring when the load is applied directly to the compression facing (no shear failures occurred in Test Sla).
- (c) Either a core shear or compression facing buckling failure may occur when the load is applied to the tension facing, depending on panel strength variation.

A comparison of the facing stresses (where wrinkling occurred) and core shear stresses (where shear failure occurred) of these panel tests with the flexural and shear tests described in section 4.4.1 indicates the following at 50% RH and 73°F.

- (a) Facing wrinkling stresses are larger in uniformly loaded panels than in small specimens loaded with concentrated loads (15,640 psi and 14,030 psi versus 12,600 psi).
- (b) Core shear stresses are about the same in uniformly loaded panels and small specimens loaded with concentrated loads (12.8 psi vs 13.5 psi).

Thus, for design purposes, the stresses determined from tests such as those described in section 4.4.1 may be safely used.



4.3 Test Series S2, Full-Scale Building Tests

4.3.1 General

Seven tests were conducted on the full-scale building described in section 2.3. Since numerous loadings were involved, it was not the objective to obtain ultimate load data in each test. The first test corresponds to test condition S2a and is referred to as such. Similarly, the second test is referred to as S2c. The sixth test corresponds to test condition S2b and is referred to as S2b(1). The seventh test was the same as the sixth except a higher load level was applied. This latter test is referred to as S2b(2). The third, fourth and fifth tests were loaded as in S2b except the six optional knee braces were still in place after test S2c. These three tests were conducted to perfect the loading system used in tests S2b(1) and S2b(2) and are referred to as modified S2b tests. The location of damages which occurred during the various tests are shown in figure 4.6. Damages are discussed in detail under individual tests.

4.3.2 Test S2a

The load-deflection response for test S2a is shown in figure 4.7 (along with S2c). The relative lateral deflections at the top of the wall are shown in plots one through five.

Two curves for S2a are shown in each of the five plots. The south wall (loaded wall) data are shown by solid circles connected by solid lines. The north wall deflections are shown by open circles connected by dashed lines. Only south wall data are shown when deflections for both wall coincide. Both curves for each plot are for the same building cross section.

Two load scales are used in figure 4.7. The scale on the left is the total lateral load applied at the eave line. The scale on the right is the equivalent uniform load which causes the total eave reaction shown on the left scale. This assumes that one half the uniform load goes into the base and the other half into the eave.

The north and south wall deflections are about the same for each cross section, furthermore the deflection is uniform (or nearly so) for the building length. The south wall deflection at section five is an exception. At that location, the deflection gage was apparently stuck until a load of 1100 lb was reached when the gage came loose. An error in the unloaded reference reading also occurred due to the stuck gage.

The load-deflection response was essentially linear, up to the maximum total applied load of 2160 lb with lateral

deflections of about two inches. At this load level, there were numerous popping noises. Loading was halted due to the large deflections and observed damage. Although the maximum possible load was not applied, some damage was noted as follows (the damage locations are shown in figure 4.6):

Location No. 1 - Screws attaching extrusion E (ridge extrusion) to the roof panels were showing signs of pulling out. Several screws did pull out near the west end of the building. This was probably at the load level of 2160 lb when the popping noises were heard.

Extrusion E was rippled between screws for its entire length.

Location No. 2 - The exterior facing of the panel adjacent to the center extrusion C wrinkled near the panel-to-panel joint.

Location No. 3 - Screws fastening extrusion C to the panel facing pulled out at the extrusion base (both ends of the building).

Location No. 4 - Extrusion C buckled locally just above the bottom flange of the ridge beam at the beam-to-wall junction.

4.3.3 Test S2c

The load-deflection response for test S2c is shown in figure 4.7 (along with S2a). This plot was described in section 4.3.2. As in the case for no knee braces (test S2a) the north and south wall deflections are about the same for each cross section. Cross sections 1, 3 and 5 have about the same load-deflection response. Similarly, sections 2 and 4 are about the same but slightly less than 1, 3 and 5.

The load-deflection response was essentially linear, up to the maximum total applied load of 5190 lb with lateral deflections of about one inch. At this point there was a drop in load. Further loading was halted due to the indication of possible damage to the building. Although the maximum possible load was probably not applied and no new permanent damage was noted, one potential damage area was found as follows:

Location No. 5 - The base of all three optional knee braces on the loaded wall were separating from extrusion F. This indicated the likelihood of pulling out screws if loading had been continued.

4.3.4 Discussion of Test S2a and S2c

Tests S2a and S2c were done for comparison of the behavior of a typical interior length of the building with and without knee braces when subjected to lateral loads.

Comparison of the curves for S2a and S2c indicates that the addition of the six knee braces increased the stiffness of the building about 4 1/2 times with regard to lateral load. Without the knee braces, a uniform load of 10 psf caused a lateral deflection of two inches. This is a net lateral deflection of about two percent of the wall height and is unacceptable under many codes and would certainly be unacceptable under a combination of roof and wind loading.

Based on this test it is concluded that the Mark III-A, as built, is unacceptable for a building of indefinite length.

With the knee braces installed, a load of about 25 psf was reached with indications that this may have been approaching the maximum load. Thus, it is concluded that the "frames" consisting of the knee braces and transverse beam should be spaced no further apart than 24 ft. Also the knee braces should be designed to insure joint continuity and increase strength. With the use of adequate knee braces, the building could probably be made an indefinite length.

4.3.5 Modified S2b Tests

The third, fourth and fifth tests were performed to perfect the loading system used in S2b(1) and (2). Test results are reported only to the extent of damages and maximum load.

In the third test, the center ram was loaded to 6040 lb. The restraining yokes at the ends of the building were not adjusted properly to give symmetrical end reactions. The maximum load, reached in the fourth and fifth tests were 6460 and 3050 lb respectively. A faulty load cell prevented accurate measurement of one end reaction in both tests. No new damages occurred in the third and fifth tests respectively. However, in the fourth test, the following damages

occurred at the locations identified in figure 4.6.

Location No. 6 - The facing on the transverse beam in the center knee brace wrinkled diagonally.

Location No. 7 - The transverse beam facings wrinkled adjacent to extrusion C for the full depth of the transverse beam.

The damaged area was repaired by installing 1/16 in thick aluminum plates over the entire damage zone. The plates were installed on both facings and attached on all four edges to the surrounding extrusions on three sides and the beam facings on the fourth side. Comparison of limited data between tests four and five indicated similar load-deflection response. Hence it is assumed that the repair did not affect the behavior in tests S2b(1) and (2).

4.3.6 Test S2b(1) and S2b(2)

The load-deflection response for tests S2b(1) and (2) are shown in figures 4.8 and 4.9 respectively. The maximum center load was 4500 lb during test S2b(1) and 7000 lb during S2b(2). The load response was almost the same for both tests up to 4500 lb, hence the following remarks apply to both tests. The north and south walls deflected about the same for each cross section except at section 5. At that location the gage measuring the loaded wall movement was apparently defective in both tests. Deflections were symmetrical about

the building midlength with the restraint forces at sections 1 and 5 permitting a movement of about $2/3$ the midlength deflection.

The slope of the load-deflection curves decreases at 5 kips in test S2b(2). Although the maximum possible load was not reached, the following damages were found during the test:

Location No. 8 - Roof panels were deflecting inward between the top of the loaded wall and the ridge. Some panels, particularly near the midlength of the building, had differential deflections of as much as $1/2$ inch at the panel-to-panel joints.

The center load versus measured end reactions are plotted in figure 4.10. The following remarks apply to both tests. In figure 4.10a the total reaction is the sum of the measured east and west reactions. Note that the data are linear, but that the applied load is not equal to the measured reaction which was 75 and 72.5 percent of the applied load in tests S2b(1) and (2) respectively. This difference was caused by the movement at the restraints. The movement allowed some of the applied load (about 25 percent) to be carried into the base of the building. Figures 4.10b indicate that the east and west reactions were equal throughout both tests.

4.3.7 Discussion of Test S2b(1) and S2b(2)

In order for the S2b tests to be a measure of the roof resistance as a deep beam, the movement at the end restraints must be accounted for.

Consider the roof as a beam on elastic supports as in figure 4.11. The roof system is shown in the right hand side of figure 4.11. An analogous beam is shown in the left hand side of the figure. Some of the applied force is resisted by the "frames" at the middle and ends of the building rather than the roof system. Consider in figure 4.11a a beam, simply supported at the ends by elastic supports with a spring constant k_2 . These are analogous to the end restraint yokes at the ends of the building. These forces are known quantities since they were measured and are known to be about 75 percent of the applied load. Next consider the beam to be simply supported by three springs of equal spring constants, one at each end and one in the middle. These are analogous to the transverse beam system in the building. Under a midpoint loading, the beam deflects as shown in figure 4.11b. If the spring constants are known, and the deflections are measured, then forces may be computed. The forces are shown in figure 4.11c (only lateral forces are shown on the building). The R_1 reactions are known in the case of the building since they were measured. The difference between load P_1

and the measured reactions R_1 may be distributed among the "frames" according to their deflections. This may be done since the "frames" exhibited essentially the same stiffness in test S2a. The loads may be combined as in figure 4.11d. Thus, the true beam deflection, is the midspan movement, minus the end movements. The effective midspan load is the applied load minus the portion of the load required to stretch the "spring".

The net deflection at the midlength of the building may be found by subtracting the average end restraint deflections from the midlength deflection. The effective midlength force P_2 may be found as

$$P_2 = P_1 - kw_2 = 0.75 P_1 + 2 kw_1 \quad (4.4)$$

Where the above equation was obtained from figure 4.11c.

Note that R_1 plus R_1 was measured as approximately $0.75 P_1$. The "missing" $0.25 P_1$ may then be distributed according to deflections. That is:

$$P_2 = P_1 - 0.25 P_1 \left(\frac{W_2}{W_1 + W_2 + W_1} \right) \quad (4.5)$$

The effective midlength load versus the effective midlength roof deflection is shown in figure 4.12.

The Mark III-A with its 48 ft roof span in the horizontal plane, may be compared with the Mark III which was tested with a 32 ft roof span in the horizontal plane [2]. The comparison is made in figure 4.13, where midspan bending moment was computed for both structures. Bending moment was used as a comparison since the structures had different loading and span lengths. In both buildings, the roofs were assumed to be simply supported in the horizontal plane. The Mark III-A was assumed supported at the end restraint forces. The Mark III was assumed supported at the end walls. Mid-length deflection was corrected for end wall movement. A predicted load-deflection curve is shown for the Mark III based on the Mark III-A curve assuming equal bending stiffness for both structures. The agreement between the actual and predicted curves is good, even though several assumptions were made.

Moment may be related to uniform load for the 32 ft and 48 ft span lengths by the two scales shown in the right side of figure 4.13. These two scales are intended only to relate the bending moment scale to uniform load. The moment-deflection curves shown were not obtained using uniform loads. The plot indicates that the roof system is adequate to transfer the present design load of 20 psf into the end walls or into a system of frames such as the transverse beam and knee brace used in test S2c.

Based on figure 4.13 and damage observed during test S2b, it is concluded that the roof system should not be loaded with bending moment exceeding 55 kip-ft in the horizontal plane. If the building were expanded in the modules of 24 ft, three modules would result in a span of 62 ft between end walls. A uniform wall load of about 27 psf will result in a moment of 55 ft-kip. This is felt to be marginal. Thus the roof span should be limited to 48 ft maximum. Without interior frames, this limits the building length to 48 ft. If interior frames are used they can be spaced no farther apart than 48 ft based on the roof capacity. Other considerations discussed later limit the spacing of the "frames" to 24 ft.

4.3.8 Performance and Appearance of Building after Testing

Following the Series S2 Tests a cyclic load varying between 0.5 and 2.0 kips was applied at the center and the ends were partially restrained. This is the same loading as for test S2b. After more than 100,000 cycles the performance of the building did not appear to have deteriorated although deflection measurements were not made.

In fact, following this test, the building had not changed in appearance, except for the repairs mentioned above, since erection.



4.4 Test Series S3, Shear and Flexural Properties

The data for midpoint and quarter point tests are tabulated in tables 4.2 and 4.3 respectively. All specimens subjected to midpoint loading failed by compression-skin-wrinkling near the load point. Wrinkling occurred at the facing stresses tabulated in table 4.2. All specimens subjected to quarter point loading, failed by core shear in the shear span. The core shear stresses are tabulated in table 4.3. The load-deflection curve slopes are tabulated for each test in tables 4.2 and 4.3. These are secant slopes expressed in inches per 100 lb of load. The secant lines were drawn through the load-deflection curves at one half the failure load.

The various formulas used for analyzing these specimens are contained in appendix B.

4.4.1 Test Series S3a, 3/4 in Cell Honeycomb

The load-deflection curves for midpoint and quarter point loading tests for the 3/4 in cell size are shown in figure 4.14 for 50% RH - 73°F conditioning and 100% RH - 73°F conditioning. In most cases the entire curves are not shown since deflection data were not usually obtained at the abrupt failure loads.

The data for 50% and 100% RH conditioning form two separate groups for both loading conditions, indicating the effect of humidity on the load-deflection curves.

4.4.2 Test Series S3b, 1/2 in Cell Honeycomb

The data for the 1/2 in cell size are shown in figure 4.15 in a manner similar to figure 4.14. The difference between the 100% and 50% RH is not as pronounced as in the case of the 3/4 in cell core, indicating that humidity either does not affect, or did not penetrate through, the 1/2 in cell honeycomb, as much as the 3/4 in honeycomb.

4.4.3 Discussion

- (a) Core Shear Strengths - The average core shear strengths are compared in figure 4.16. As expected, the 100% RH strength was lower than the 50% RH strength. The 100% RH shear strength was 62 and 80 percent of the 50% RH strength for the 3/4 in and 1/2 in cell honeycomb respectively. Under both conditions, the 1/2 in cell honeycomb was superior to the 3/4 in cell honeycomb at 50% RH and 100% RH respectively.
- (b) Facing Stresses - The flexural specimens failed by wrinkling of the compression facing as a result of loss of skin-to-core bond. Thus, the facing stress should be higher in the 1/2 in cell honeycomb than in the 3/4 in all honeycomb since there is more bond per unit area of facing. The test results bear this out as indicated in figure 4.17. The 3/4 in cell honeycomb facing stress was 87 percent and 71 percent of the 1/2 in cell honeycomb facing stress for 50% RH and 100% RH respectively.
- (c) Flexural Rigidity - The experimental flexural rigidity may be determined as described in appendix B.4 using data from the center point and quarter

point loading conditions. As shown in figures 4.14 and 4.15, there is some scatter in the various load-deflection curves. The reason for the scatter is not known.

Average flexural rigidities are tabulated in table 4.4 and compared in figure 4.18. The calculated value was obtained by assuming only the aluminum facings as effective in resisting flexure. The experimental rigidities for the 1/2 in and 3/4 in cells are about the same at 50% RH but less than the calculated value. At 100% RH both rigidities exceed the calculated values but are not in agreement with each other. It is likely that at the 100% RH conditions, the assumptions used in deriving the formulas in appendix B are not valid. It is probably just as accurate to calculate a flexural rigidity as it is to determine an experimental value for this type of sandwich panel.

- (d) Shear Modulus - An experimental modulus may be determined as described in appendix B.5 using the data in figures 4.14 and 4.15.

Average moduli are tabulated in table 4.4 and compared in figure 4.19. Three types of moduli are shown and tabulated. Type 1 is an experimental value determined as described in appendix B.5. Type 2 is based on the results of the midpoint loading using a calculated flexural rigidity (eq. B.9a). Type 3 is the same as type 2, except the quarter point loading data was used (eq. B.10a). As can be seen in figure 4.19, there is little difference among the three methods and no apparent pattern. Hence, for these panels, it is simpler and just as accurate to use a calculated flexural rigidity and only one type of test to determine the shear modulus, at least for the 50% RH condition.

- (e) Additional Tests - Examination of the results (tables 4.3 and 4.4), indicate that the 1/2 in cell honeycomb had a smaller shear modulus but greater shear strength than the 3/4 in cell honeycomb. This was confirmed by using the plate shear test described in ASTM C273. Three samples of each cell size were tested at 50% RH - 73°F. The 3/4 in cell had an average shear strength of 17.2 psi (compared to 13.5 psi in the quarter point loading) with a shear modulus of 1845 psi (compared to 1189 psi obtained by method 3). The 1.2 inch cell had an average shear strength of 24.1 psi (compared to 18.2 psi in the quarter point

loading) with a shear modulus of 1690 psi (compared to 898 psi obtained by method 3). These results follow the same trend as the quarter point data but the values are higher. The data obtained from the quarter point loading data are considered better since these were obtained from a combination of bending and shear.

- (f) Tests on full size panels indicated higher stresses could be reached depending on how the panel was loaded. Thus, the small specimen stresses are conservative.

4.5 Test Series S4, Flatwise Compression Strength

The data from this test series are tabulated in table 4.5. Average results are shown in figure 4.20. Detailed results are discussed below.

4.5.1 Test Series S4a, 3/4 inch Cell Honeycomb

The average test results for the specimens from Panel A are consistently lower than those from Panel B. It may be seen, by reference to table 4.5, that test results for specimens from a single panel (such as A) were very consistent. At 50 percent RH the average Panel A strength was 73 percent ($\frac{42.5 \text{ psi}}{58.3 \text{ psi}} \times 100\%$) of the average Panel B specimen strength. At 100 percent RH the average Panel A strength was 72 percent ($\frac{16.9 \text{ psi}}{23.5 \text{ psi}} \times 100\%$) of the average Panel B specimen strength. The average for all Panel A and Panel B specimens was 50.4 psi at 50% RH and 20.2 psi at 100% RH.

4.5.2 Test Series S4b, 1/2 inch Cell Honeycomb

The average test results for the specimens from Panel C were consistently lower than those from Panel D. The difference is not as great as between Panels A and B with 3/4 in cells. At 50 percent RH the average Panel C strength was 94 percent ($\frac{84.4 \text{ psi}}{89.9 \text{ psi}} \times 100\%$) of the average Panel D specimen strength. At 100 percent RH the average Panel C strength was 92 percent ($\frac{56.6 \text{ psi}}{61.4 \text{ psi}} \times 100\%$) of the average Panel D strength. The average for all Panel C and D specimens was 87.2 psi at 50 percent RH and 59.0 psi at 100% RH.

4.5.3 Discussion

- (a) Effect of Moisture Content - The relative effect of the conditioning method of flatwise compressive strength is shown in figure 4.21 for 3/4 in and 1/2 in cells. At 100 percent RH the 3/4 in cell attained only 40 percent of the strength at 50 percent RH. The 1/2 in cell specimen strength at 100 percent RH attained 68 percent of the 50 percent RH strength.
- (b) Effect of Cell Size - The effect of cell size on flatwise compression strength is shown in figure 4.22 for both curing conditions. The 1/2 in cell specimens were 1.73 and 2.94 times as strong as the 3/4 in cell specimens at 50 percent and 100 percent RH respectively.

4.6 Test Series S5b, Indentation Tests

The results of the indentation tests are plotted in figure 4.23. Each data point represents one test. The left hand

curves show the amount of indentation remaining after removing the load for time intervals of one minute and one hour. The right hand curve gives the ratio of recovered indentation to indentation at the full load level. Thus, for complete recovery, the ratio would be one.

The following damages were observed after removal of each load:

- 200 lb - No visual damage (255 psi)
- 400 lb - No visual damage (510 psi)
- 600 lb - Some indentation in tile (764 psi)
- 800 lb - Indentation apparent with some dimpling around the load point (1020 psi)
- 1000 lb - Deep indentation mark in tile with considerable dimpling around the load point (1274 psi)

Service loads can be as great as 1200 psi for a grand piano being moved on two casters. In contrast, a 300-lb man balancing himself on the back legs of a straight chair would impose concentrated loads of about 375 psi.

The above qualitative observations agree with the data in figure 4.23. That is, for loads exceeding 400 lb the amount of indentation is increasing at a more rapid rate than for loads 400 lb and less.

Hail damage indentation tests on roof panels are contained in reference [7] which is attached to this report.

4.7 Test Series S6, Ridge Beam Test

The load-deflection curve for the one ridge beam tested, is shown in figure 4.24. Uniform load per ft is plotted as the left scale. The equivalent uniform roof load is shown as the right hand scale. The ridge beam failed at an equivalent roof load of 30 psf. The actual beam capacity, as used, is greater since the beam failed by buckling of the flange extrusion at the reaction. In use, this type of failure would not occur since the reactions are carried by shear into the web rather than by bearing on the flange.

4.8 Test Series S7, Hardware Tests

No tests were performed in this category.

4.9 Test Series S8, Flatwise Tension Tests

Flatwise tensile tests performed on 3/4 in cell specimens gave consistent test results. Six specimens tested from Phase II panels averaged 10.5 psi. Six specimens tested from Phase I panels after being stacked horizontally outside and exposed to weather for a period of one year averaged 10.5 psi. Specimens reported in reference [1] averaged 10 psi when tested at 50% RH - 73°F.

5. CONCLUSIONS AND RECOMMENDATIONS

5.1 Erection

The Mark III-A building, described in this report, had been previously erected at another location. No major difficulties were encountered in the second erection, described herein, at the National Bureau of Standards Laboratories. The total erection time was 20 man days (7 1/2 hr days). There would be no difficulty in disassembling, repacking and assembling the structure at another location.

Minor dimensional changes described in section 2 would make the building suitable for expansion in modules of 24 ft. This is not practical in the building as presently designed.

5.2 Structural

The following conclusions were reached, based on the structural tests described in this report:

- (a) Ultimate loads for single panels with 3/4 in cell honeycomb (50% RH - 73°F) are 153 and 68 psf for 8 ft and 14 ft long panels respectively. Failures are caused by sudden wrinkling of the compression facing.
- (b) Single panels tested in flexure by vacuum loading indicated some difference in the capacity listed in (a), although still much larger than the design loads. This indicates that there should be no



problem with skins being peeled off during high winds before general panel failure.

- (c) Tests on three panels, connected by vinyl extrusions and tested in flexure with only the outside panels loaded, indicated that the unloaded panel resisted $2/3$ of the bending moment resisted by a loaded panel. This indicates that the vinyl extrusions can transmit considerable shear.
- (d) Tests on the panels described in (c) indicate that the vinyl extrusion enables panels to carry higher loads than those listed in (a). Apparently, the clamping action of vinyl extrusions and its behavior as an elastic support increases the load capacity. It is recommended that this be neglected in design since it was not fully evaluated.
- (e) The properties of $3/4$ and $1/2$ in cell honeycomb core panels are listed in table 5.1. As can be seen, the $1/2$ in cell honeycomb core was superior to the $3/4$ cell honeycomb core in all cases except for the shear modulus. The $3/4$ in cell honeycomb appears adequate for the Mark III-A, however.

The flexural rigidity listed in table 5.1, was computed assuming only the facings as effective in resisting bending. The shear modulus was determined using the quarter point loading data and the computed flexural rigidity. This is considered as accurate as using the ASTM C393 procedure and is simpler. Use of the quarter point loading also permits the determination of shear strength.

- (f) As presently built, the Mark III-A should be limited to a length of 48 ft due to the limited ability of the roof to transfer lateral loads into the end walls. The addition of knee braces to the transverse beams at 24 ft centers to form a "frame" would allow the expansion of the building in 24 ft modules. The knee braces described in this report were not intended as an optimum design and should not be used. The braces were intended merely to demonstrate the feasibility of expansion. If knee braces are used they should be designed with adequate continuity at the brace-to-transverse beam connection.
- (d) Floor indentation tests with the $1/8$ in vinyl asbestos floor tile in place indicates that loads larger than 400 lb concentrated on a one inch

diameter area will cause visible damage to the floor.

- (h) The 24 ft ridge beam is adequate to carry a roof load of at least 30 psf. The ridge beam capacity is one reason for limiting the Mark III-A to 24 ft modular construction.

6. ACKNOWLEDGEMENTS

The work described herein was carried out in the structural laboratories of the Building Research Division at the National Bureau of Standards. The program was sponsored by the Naval Facilities Engineering Command. The Naval Civil Engineering Laboratory (NCEL) at Port Huenene, California was responsible for program coordination. Monitoring was provided by W. A. Kennan, NCEL. L. J. Davis, on temporary assignment from the Institute for Basic Standards at the National Bureau of Standards, provided assistance in the test program and data reduction.



7. REFERENCES

1. Reichard, T. W. and Leyendecker, E. V., "Test and Evaluation of the Prefabricated Lewis Building and Its Components, Phase I Part 1, Evaluation of Sandwich Panel Components," National Bureau of Standards Report 10163, March 1970.
2. Reichard, T. W. and Leyendecker, E. V., "Test and Evaluation of the Prefabricated Lewis Building and Its Components, Phase I Part 2, Full-Scale Building Tests," National Bureau of Standards Report 10164, February 1970.
3. Phillips, C. W. and Kuklewicz, M. E., "Thermal Performance of a Mark III Relocatable Lewis Building," National Bureau of Standards, NBS Project 4214442, June 1969.
4. "Navy MK III-A Building, F. O. No. 2856-2," Set of Eight Drawings, Bellaire Products, Inc., Bradenton, Florida.
5. "Manufacture and Technical Specifications, Mark III Lewis Building," Bellaire Products, Inc., Bradenton, Florida.
6. "Erection Manual for Mark III Lewis Building," Bellaire Products, Inc., Bradenton, Florida.
7. Mathey, R. G., "Hail Resistance Tests of Aluminum Skinned Honeycomb Panels for the Relocatable Lewis Building," National Bureau of Standards Report 10193, April 1970 (copy attached).

8. TABLES

Test No.	Test Description	Number of Tests	Test Arrangement
Sl a	Uniform lateral loading of 4' x 8' panel	3	
Sl b	Uniform lateral loading of the outer panels of a three panel assembly consisting of 4' x 14' panels joined with cleats	3	
Sl c	Uniform lateral "tension" loading of 4' x 8' panel	3	

Table 1.1a Test Program

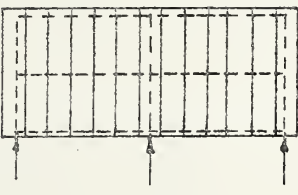
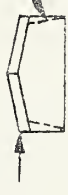
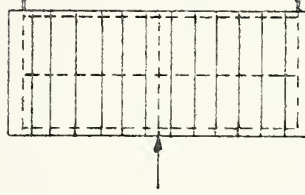
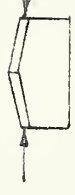
Test No.	Test Description	Number of Tests	Test Arrangement
S2a	Resistance of 48 ft long building without end walls to lateral load	1	  <p data-bbox="660 173 719 318">OPTIONAL KNEE BRACE</p>
S2c	Same as S2a except optional knee braces in place	1	
S2b	Resistance of 48 ft roof to lateral load. Roof acting as a beam in the horizontal plane.	2	 

Table 1.1b Test Program

Test No.	Test Description	Number of Tests	Test Arrangement
S3a	Core shear modulus, core shear strength, and bending stiffness of sandwich specimens with 3/4 inch cell honeycomb core. Apparatus, specimen size, and loading conformed to ASTM C 393-62. Six specimens were conditioned at 50% RH and 73°F; the other six at 100% RH and 73°F.	6 - 8 in x 32 in specimens 6 - 8 in x 64 in specimens	ASTM C 393-62
S3b	Same as S3a but with 1/2 inch cell honeycomb core.	6 - 8 in x 32 in specimens 6 - 8 in x 64 in specimens	ASTM C 393-62
S4a	Flatwise compressive strength of sandwich with 3/4 inch paper honeycomb core. Apparatus, specimen size, and loading conformed to ASTM C 365-57. Six specimens were conditioned at 50% RH and 73°F; the remaining six at 100% RH and 73°F.	12 - 4 in x 4 in specimens	ASTM C 365-57
S4b	Same as S4a but with 1/2 inch cell honeycomb core.	12 - 3 in x 3 in specimens	ASTM C 365-57
S5a	NBS hail stone test reported in Reference 7		

Table 1.1c Test Program

Test No.

Test Description

Number of Tests

Test Arrangement

S5b

Indentation test on typical section of floor panel (0.05 inch thick aluminum skin) to conform to ASTM E72.

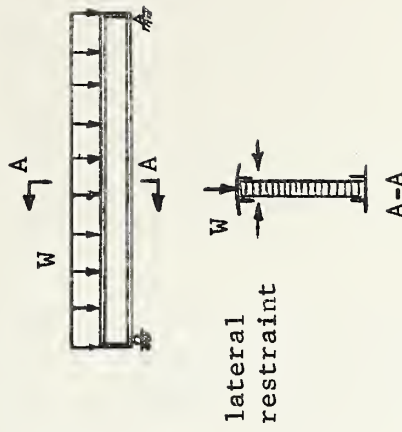
5

ASTM E72

S6

Uniform loading of full-size ridge beam on simply supported span with lateral bracing.

1



S7

Strength tests of extrusions, rivets, and other connecting hardware for expected loads. Tests procedure to be specified by NBS personnel.

None Performed

NBS Specified

S8

Flatwise tensile tests of 3 in x 3 in 3/4 inch honeycomb core at 50% RH - 73°F

12

ASTM C 297

Table 4.1 Test Series S1 Results

Specimen ^{1,2}	Maximum Load, psf	Maximum Moment, kip-ft	Percent of Computed Flexural Capacity	Failure
<u>Series S1a, 4' x 8' Panels Loaded by Air Bag</u>				
E	156	4.59	65.6	Wrinkling of compression face
F	158	4.65	66.4	Wrinkling of compression face
G	157	4.62	65.9	Wrinkling of compression face
<u>Series S1b, 3 - 4' x 14' Panels Loaded by Air Bag</u>				
1	86	16.1	114.8 ³	Cleat Split
2	90	16.8	76.6 ⁴ 120.1 ³ 80.1 ⁴	Cleat Split
<u>Series S1c, 4' x 8' Panels Loaded by Vacuum</u>				
H	117	3.44	49.2 ⁵	Shear failure at "dry" splice in core
I	116	3.41	48.7 ⁵	Shear failure
J	141	4.15	59.3	Wrinkling of Compression face

1. All panels conditioned at 50% RH - 73°F
2. All cell sizes are 3/4 in
3. Based on only two panels effective
4. Based on three panels equally effective
5. Shear failures

Table 4.2 Test Series S3 Results of
Midpoint Loading (8 in x 64 in Specimen)

Test Series, Cell Size, and Conditioning	Specimen	Total Failure Load, lb	Average Facing Stress ¹ , psi	Slope of Load-Deflection Curve ² in/100 lb
S3a, 3/4 in Cell, 50% RH - 73°F	A-1	445	11,400	0.1036
	A-2	477	12,300	0.0987
	B-1	545	14,000	0.1155
	Average	489	12,600	0.1059
S3a, 3/4 in Cell, 100% RH - 73°F	A-3	379	9,750	0.1372
	B-2	379	9,750	0.1426
	B-3	369	9,490	0.1522
	Average	376	9,660	0.1440
S3b, 1/2 in Cell, 50% RH - 73°F	C-1	615	15,800	0.1218
	C-2	605	15,600	0.1242
	D-3	463	11,900	0.1207
	Average	561	14,400	0.1222
S3b, 1/2 in Cell 100% RH - 73°F	C-3	523	13,500	0.1320
	D-1	501	12,900	0.1298
	D-2	569	14,600	0.1340
	Average	531	13,700	0.1319

Notes:

1. Computed by eq B.1 in Appendix B
2. Slope of the secant line drawn through the load-deflection curve at one-half the failure load.
3. All failures were by buckling of the compression facing near the load.
4. Span normal to paper core ribbon.

Table 4.3 Test Series S3, Results of
Quarter-Point Loading (8 in x 32 in Specimen)

Test Series, Cell Size, and Conditioning	Specimen	Total Failure Load, lb	Average Core Shear Stress, ¹ psi	Slope of Load-Deflection Curve, ² in/100 lb
S3a, 3/4 in Cell, 50% RH - 73°F	A-1	614	12.9	0.01792
	A-2	674	14.2	0.01528
	B-1	634	13.3	0.01956
	Average		13.5	0.01759
S3a, 3/4 in Cell, 100% RH - 73°F	A-3	414	8.7	0.02512
	B-2	378	7.9	0.02910
	B-3	406	8.5	0.03005
	Average		8.4	0.02809
S3b 1/2 in Cell, 50% RH - 73°F	C-1	926	19.5	0.02030
	C-2	818	17.2	0.02371
	D-3	854	17.9	0.02155
	Average		18.2	0.02185
S3b 1/2 in Cell, 100% RH - 73°F	C-3	652	13.7	0.02853
	D-1	740	15.5	0.02487
	D-2	698	14.7	0.02350
	Average		14.6	0.02363

Notes:

1. Computed by eq B.2 in Appendix B
2. Slope of the secant line drawn through the load-deflection curve at one-half the failure load.
3. All failures were by shear in the core in the shear span
4. Span normal to paper core ribbon.

Table 4.4 Flexural Rigidity and Shear Modulus

Test Series, Cell Size and Conditioning	Flexural Rigidity			Shear Modulus*		
	Experimental Eq. 8.7a lb - in ² /in	Calculated ** lb-in ² /in	Method 1 Eq. B.8a psi	Method 2 Eq. B.9a psi	Method 3 Eq. B.10a psi	Method 4 ASTM C-273 psi
S3a, 3/4 in. Cell 50%RH - 73°F	1,039,000	1,085,000	1208	1156	1189	1845
S3a, 3/4 in. Cell 100%RH - 73°F	1,167,000	1,085,000	652	678	661	--
S3b, 1/2 in. Cell 50%RH - 73°F	1,061,000	1,085,000	904	888	898	1690
S3b, 1/2 in. Cell 100%RH - 73°F	1,256,00	1,085,000	718	781	738	--

*Method 1 - Experimental using midpoint and quarterpoint loading tests

Method 2 - Experimental using midpoint loading test and calculated flexural rigidity

Method 3 - Experimental using quarter point loading test and calculated flexural rigidity

Method 4 - Experimental using plate shear test

**Calculated from properties of the aluminum skin and dimensions (core neglected)

TABLE 4.5 FLATWISE COMPRESSION TEST RESULTS

(ASTM C 365-57), 4in x 4in SPECIMENS

Cell Size	Conditioning Method			
	50%RH - 73°F		100%RH - 73°F	
	<u>Specimen</u>	<u>Strength, psi</u>	<u>Specimen</u>	<u>Strength, psi</u>
Test S4a 3/4" hex	A-a	41.2	A-i	16.9
	A-d	44.3	A-k	16.9
	A-h	42.0	A-l	16.9
	Average of A	42.5	Average of A	16.9
	B-e	58.0	B-b	24.7
	B-g	60.0	B-h	23.9
	B-l	57.0	B-k	22.0
	Average of B	58.3	Average of B	23.5
	Average of A & B	50.4	Average of A & B	20.2
	Test S4b 1/2" hex	C-a	85.0	C-k
C-c		86.2	C-m	48.0
C-d		82.0	C-p	62.4
Average of C		84.4	Average of C	56.6
D-d		90.5	D-b	59.1
D-i		84.0	D-f	58.0
D-m		95.3	D-g	67.0
Average of D		89.9	Average of D	61.4
Average of C & D		87.2	Average of C & D	59.0



Table 5.1 Properties of 3/4 in and 1/2 in Cell
Honeycomb Panels

Property	3/4 in Cell		1/2 in Cell	
	50%RH 73°F	100%RH 73°F	50% RH 73°F	100%RH 73°F
Flatwise Compressive Strength, psi	50.4	20.2	87.2	59.0
Flatwise Tensile Strength, psi	10.6	--	--	--
Shear Strength, psi	13.5	8.4	18.2	14.6
Shear Modulus, psi	1189	661	898	738
Flexural Rigidity, 10^3 lb-in ² /in	1,085	1,085	1,085	1,085



9. FIGURES

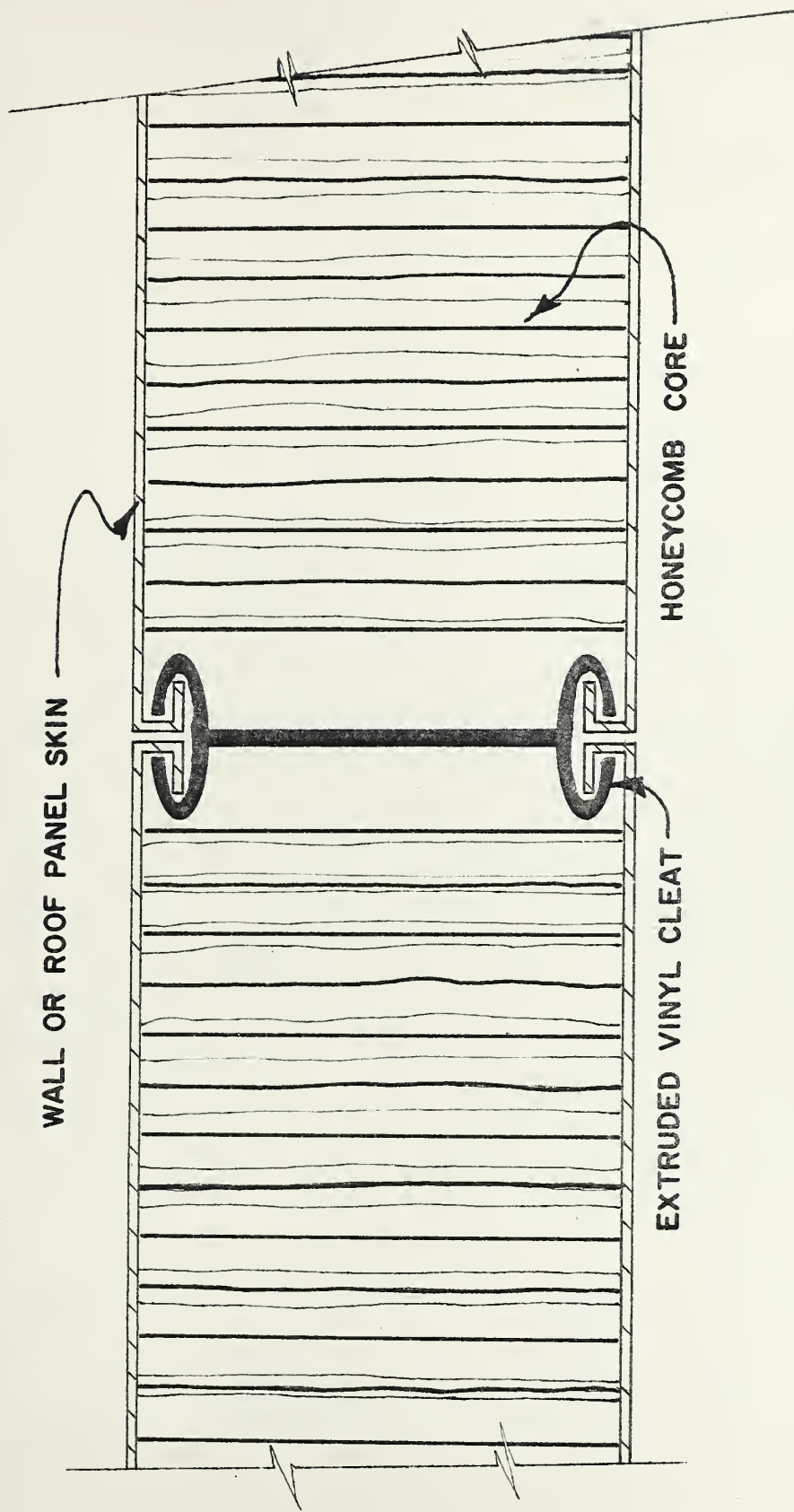
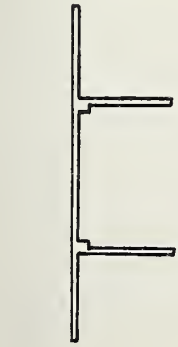


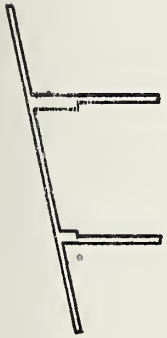
Figure 2.1 Method of Using Vinyl Cleat
to Connect Panels





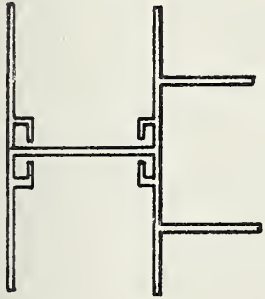
"A"

BEAM FLANGE



"B"

WALL TO ROOF



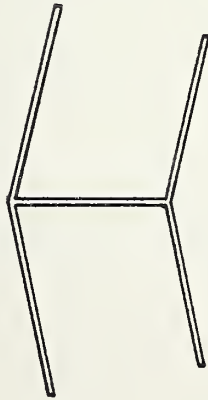
"C"

WALL TO TRANSVERSE BEAM



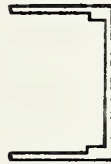
"D"

WALL TO FLOOR



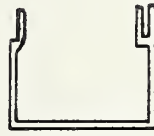
"E"

ROOF RIDGE



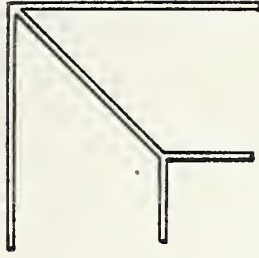
"F"

ROOF EDGE



"G"

FLOOR PANEL



"H"

WALL CORNER

Figure 2.2 Aluminum Extrusions (1/4 size)

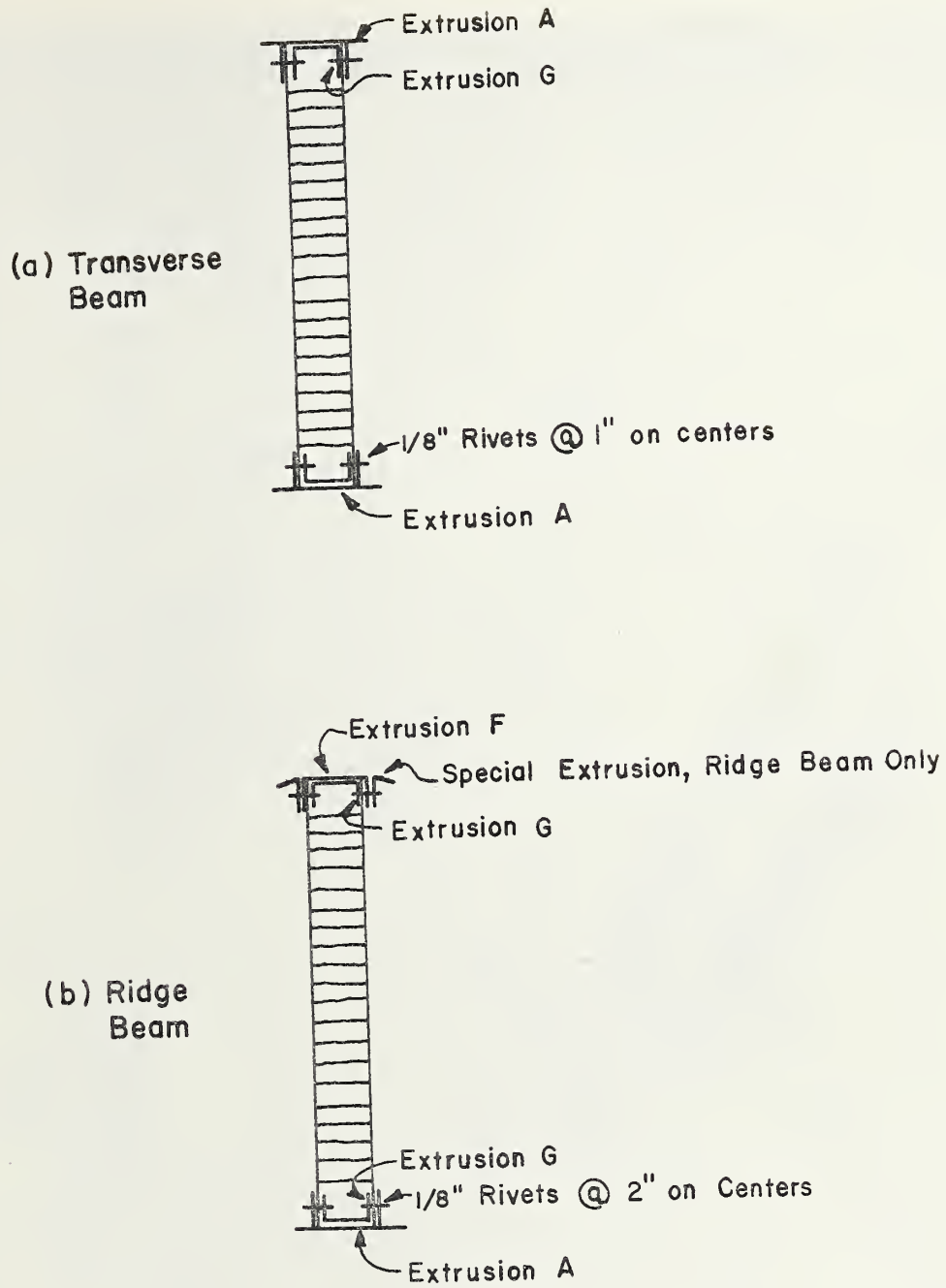


Figure 2.3 Ridge and Transverse Beam Cross Sections

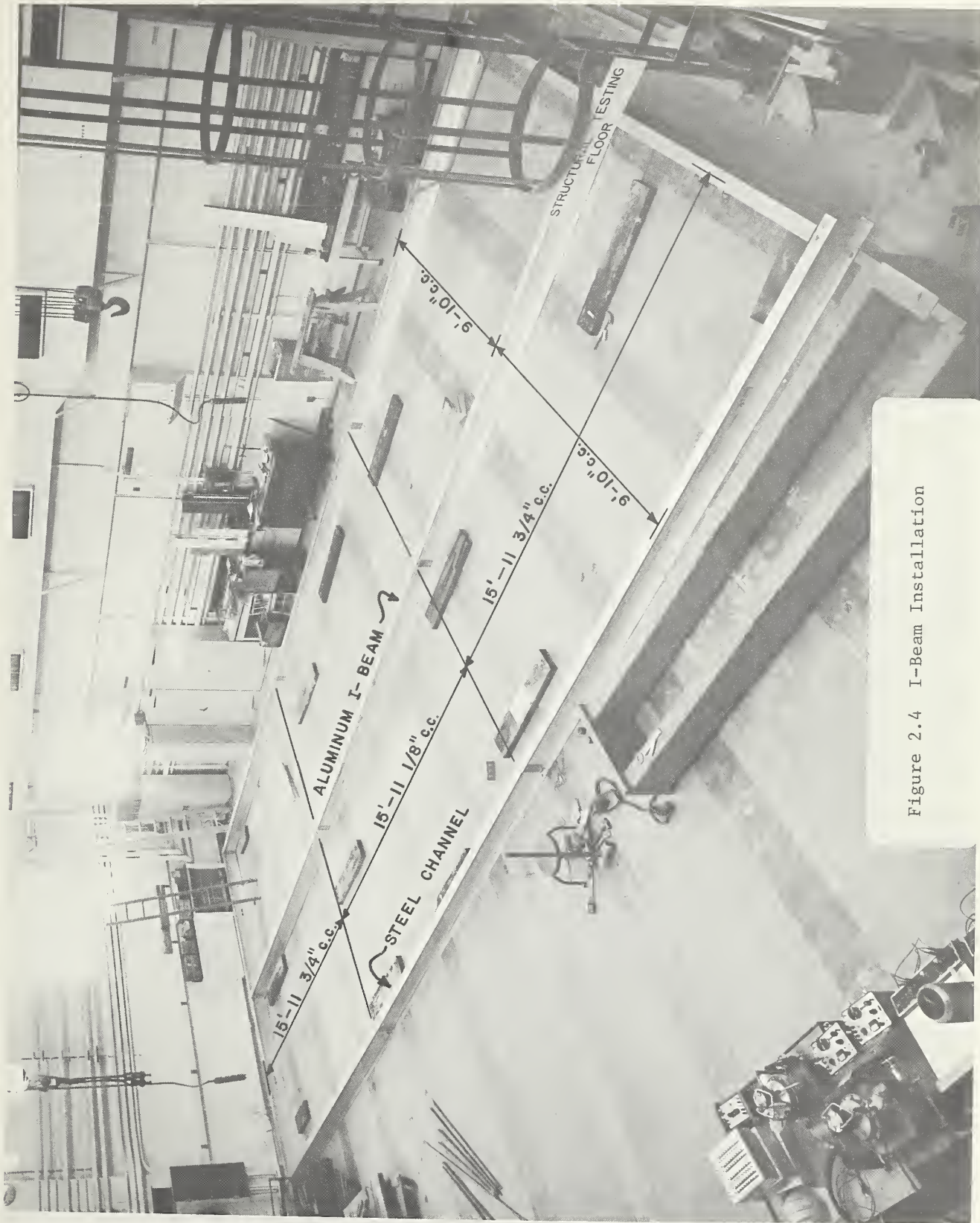


Figure 2.4 I-Beam Installation



Figure 2.5 I-Beams Installed and First Floor Panel in Place

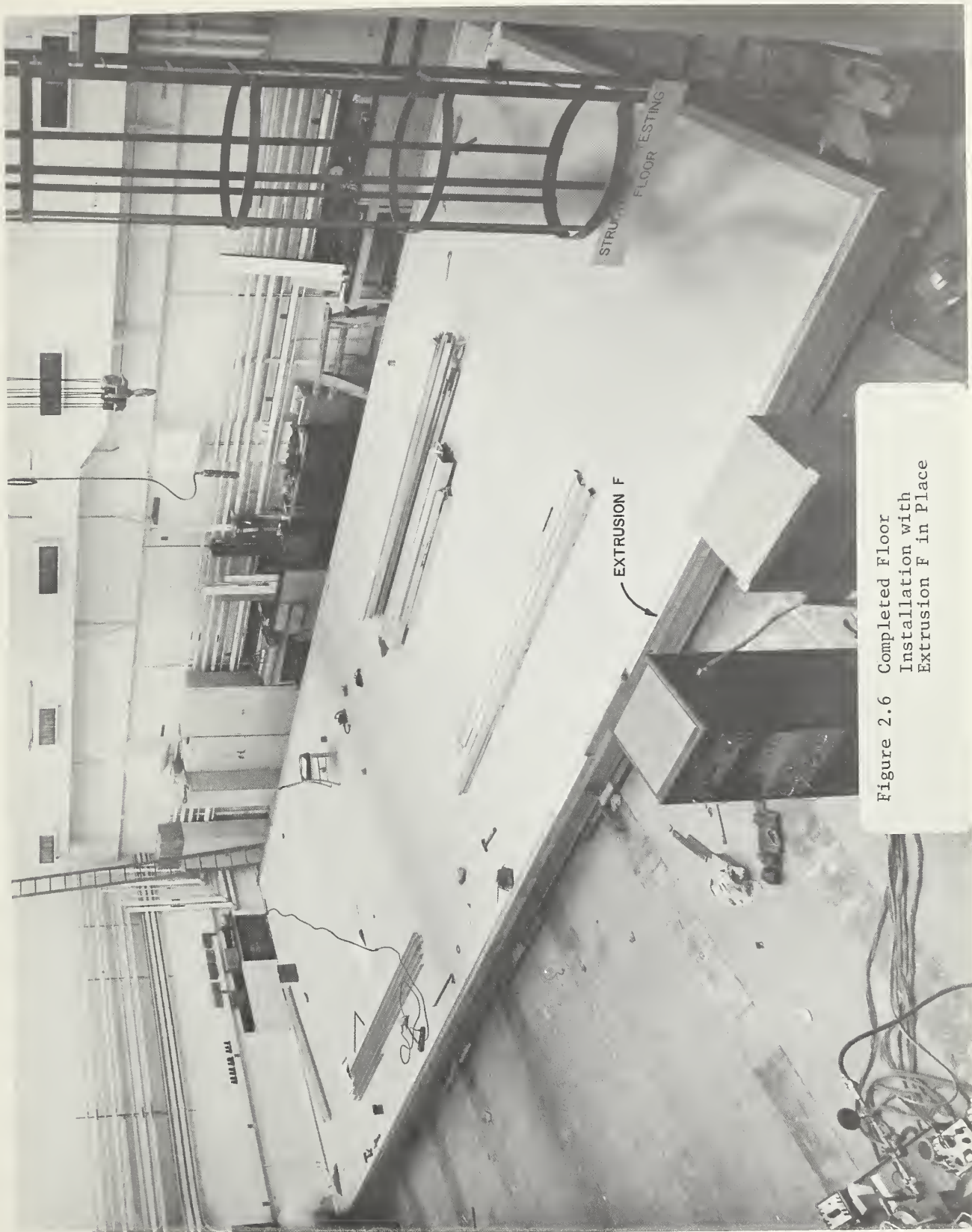


Figure 2.6 Completed Floor Installation with Extrusion F in Place



Figure 2.7 Wall Panel Installation

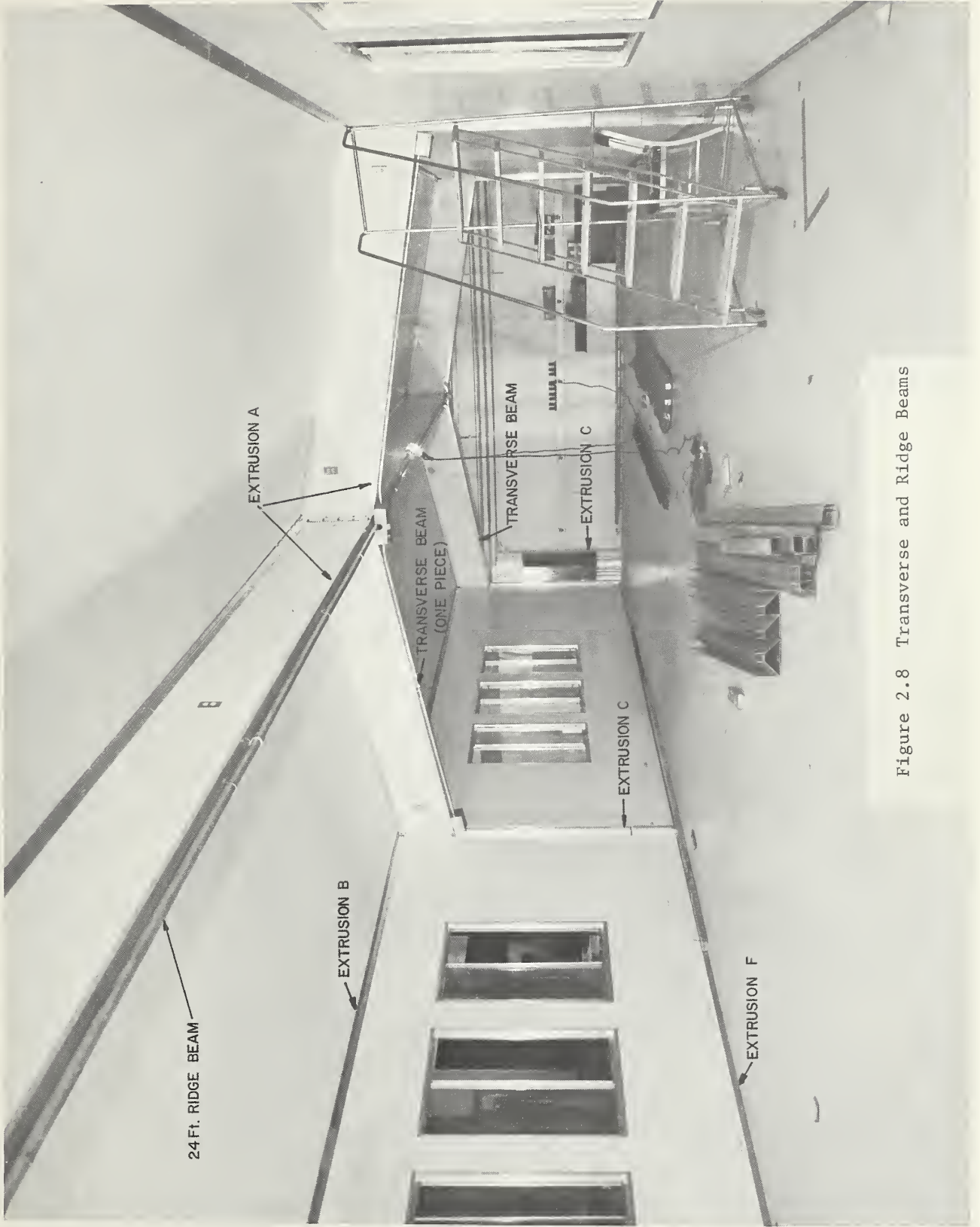


Figure 2.8 Transverse and Ridge Beams

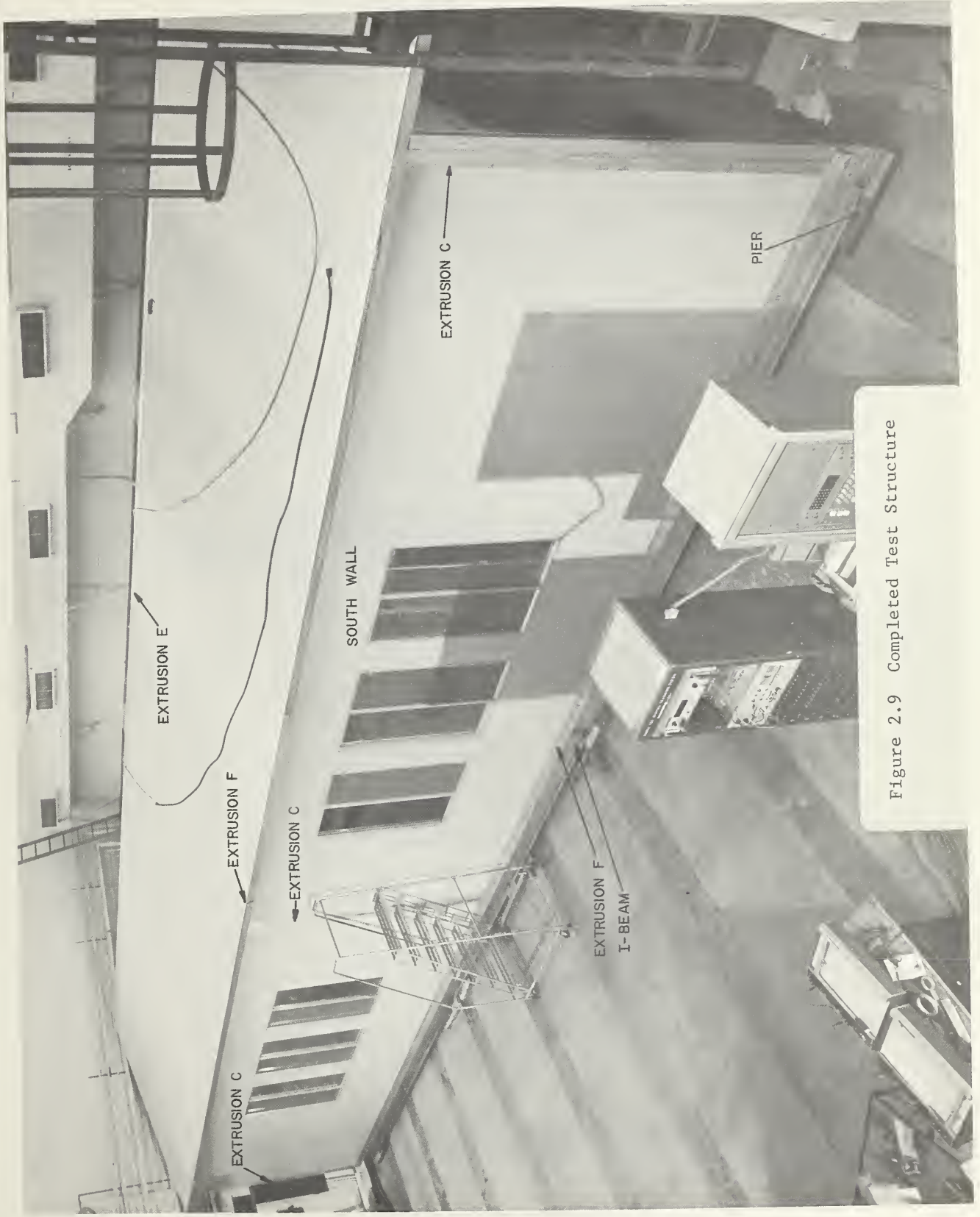
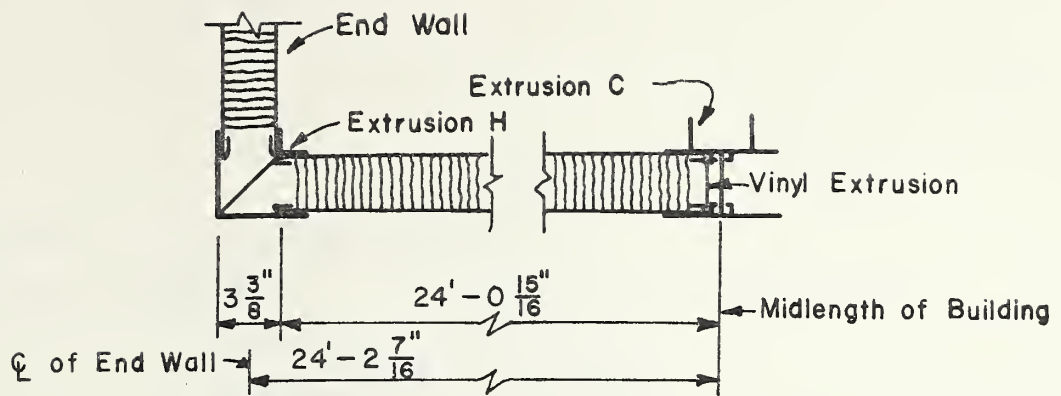
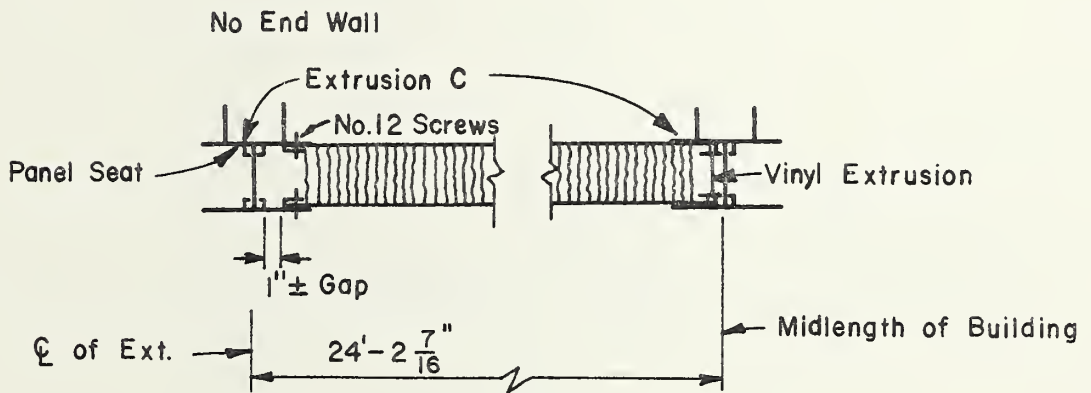


Figure 2.9 Completed Test Structure

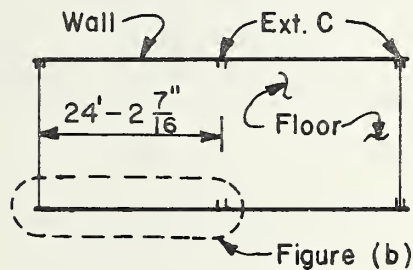




(a) Normal Installation



(b) Modified Installation



(c) Cross Section Through Building Plan

Figure 2.10 Building Modifications



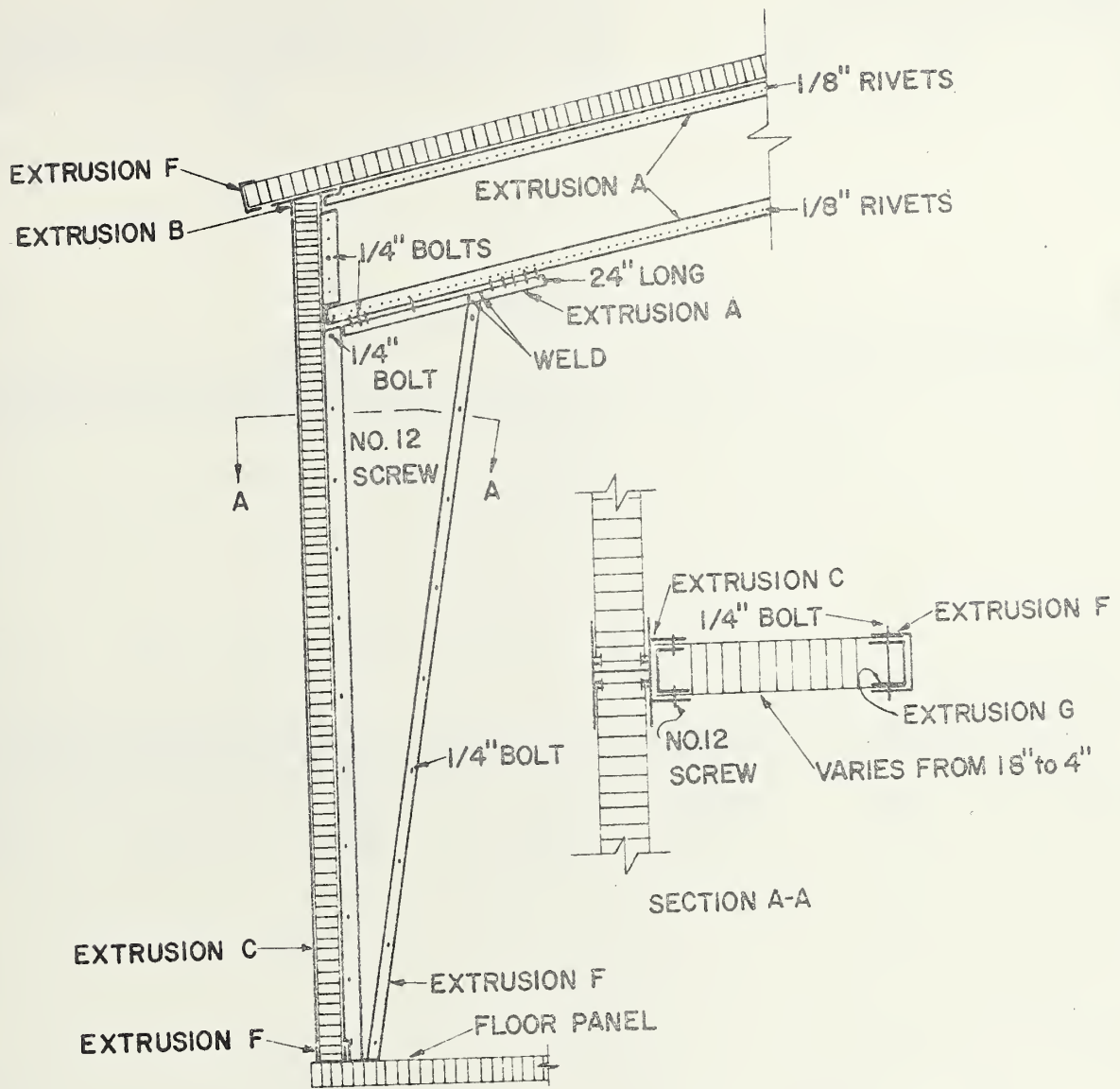
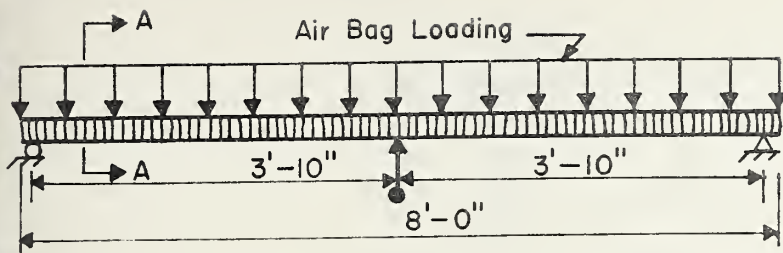
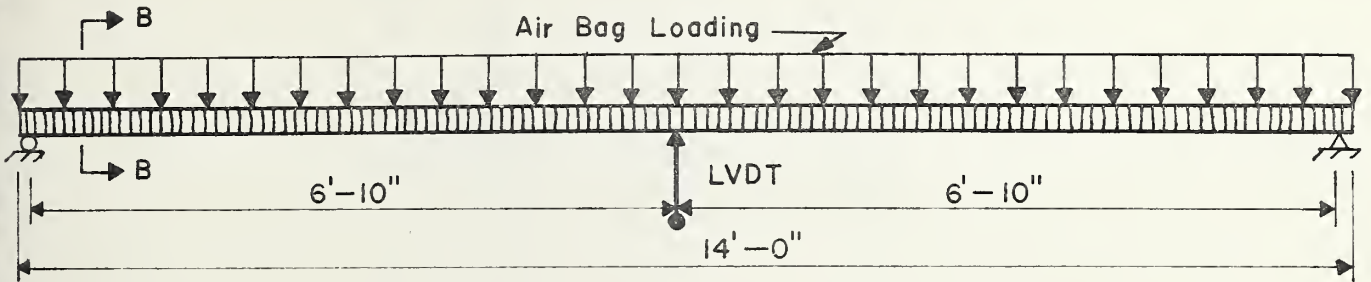
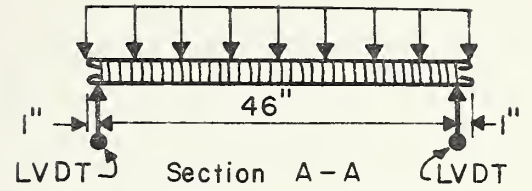


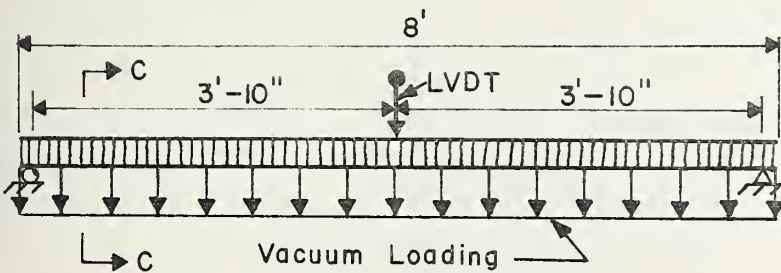
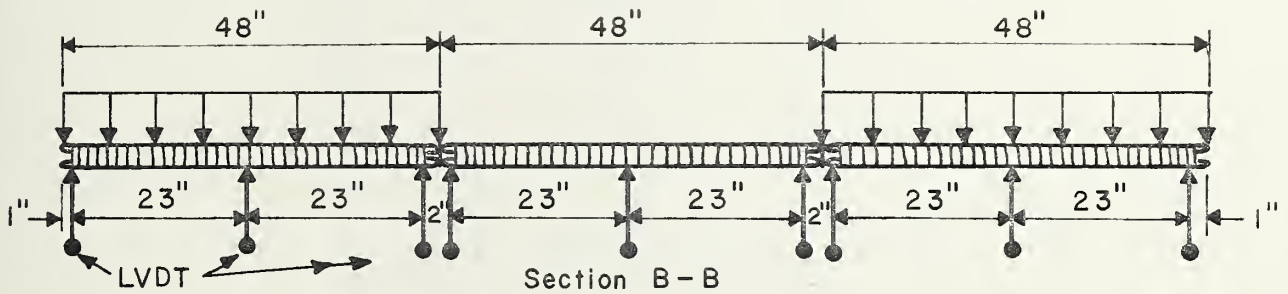
Figure 2.11 Optional Knee Brace Installation



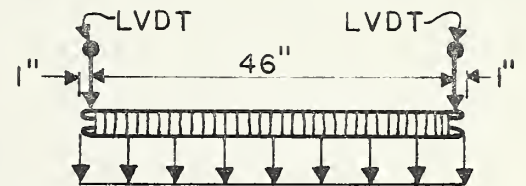
(a) Test Sl a



(b) Test Sl b



(c) Test Sl c



Section C-C

Figure 3.1 Test Series S1 (Panel Tests), Loading and Instrumentation

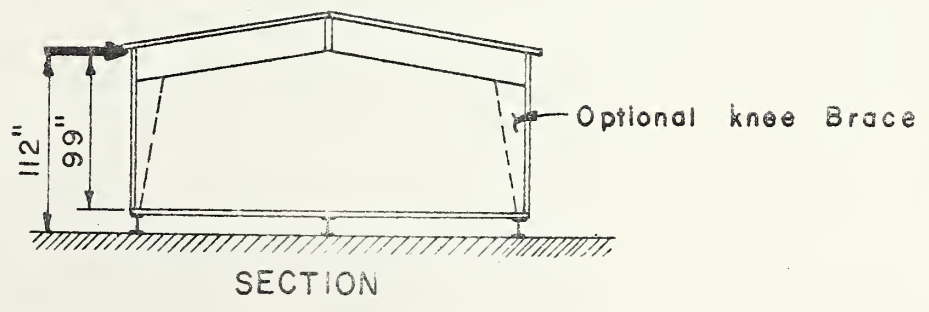
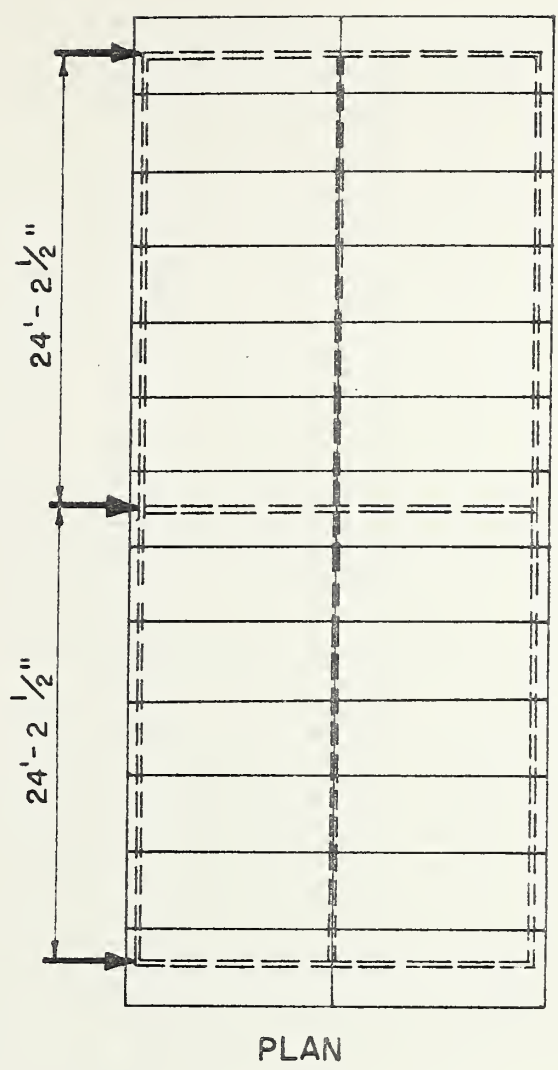


Figure 3.2 Loading for Tests S2a and S2c (Building Tests)

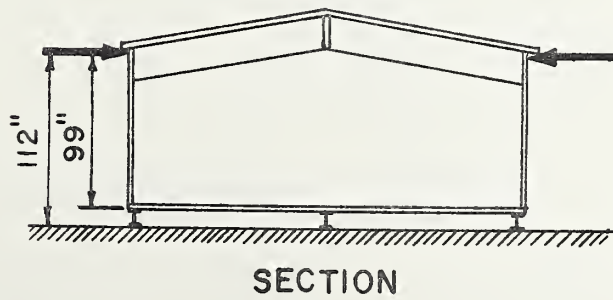
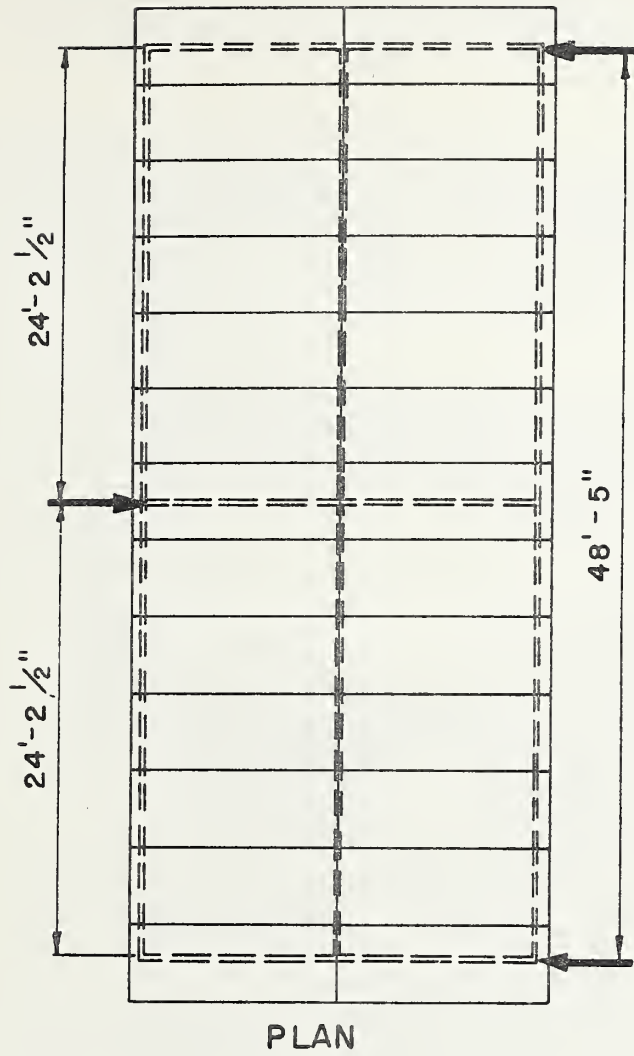
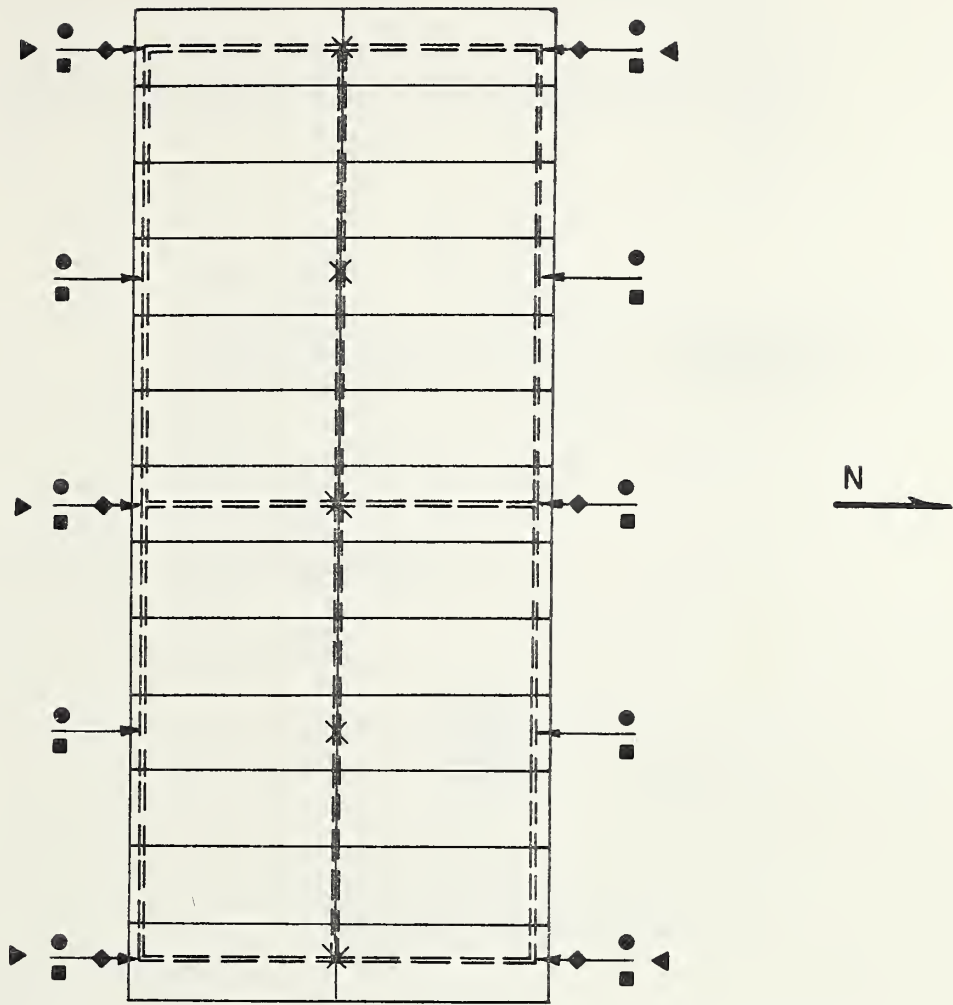


Figure 3.3 Loading for Test S2b (Building Test)



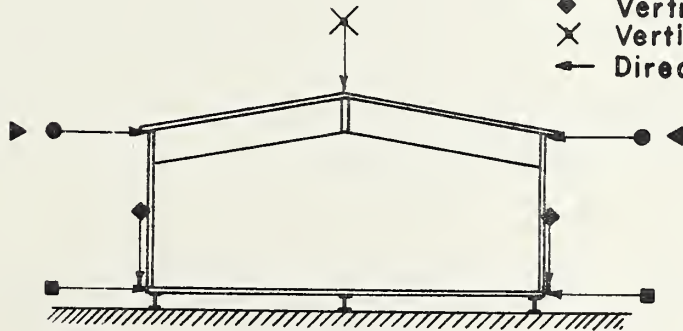
Figure 3.4 View of Mark III-A Ready for testing



PLAN

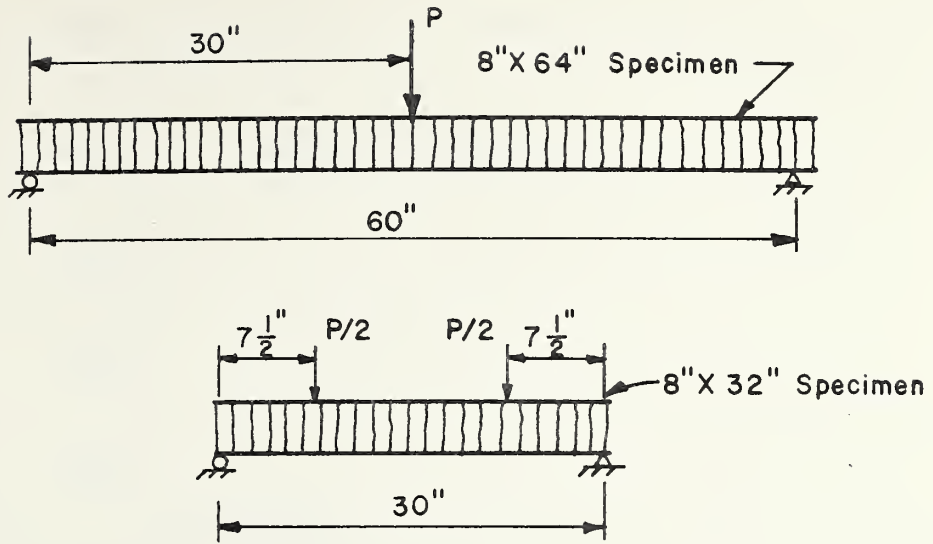
Symbols

- ▶ or ◀ Lateral Load
- Lateral Deflection at Eave
- Lateral Deflection at Floor
- ◆ Vertical Deflection at Floor
- × Vertical Deflection at Ridge
- ← Direction of Measurement

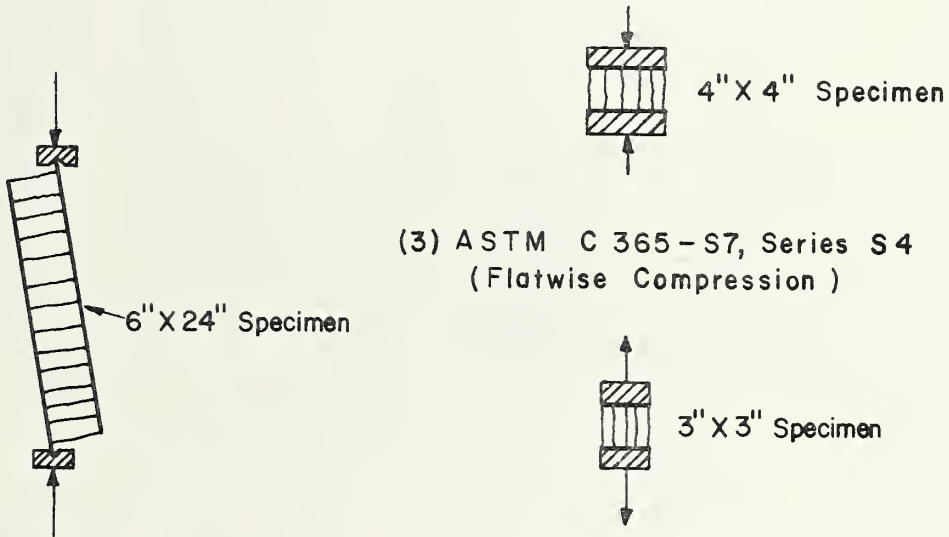


SECTION

Figure 3.5 Instrumentation for Test Series S2 (Building Tests)



(1) ASTM C 393 - 62, Series S3



(3) ASTM C 365 - S7, Series S4
(Flatwise Compression)

(2) ASTM C 273,
Series S3
(Plate Shear)

(4) ASTM C 297, Series S8
(Flatwise Tension)

Figure 3.6 Test Methods Used in Test Series S3, S4 and S8

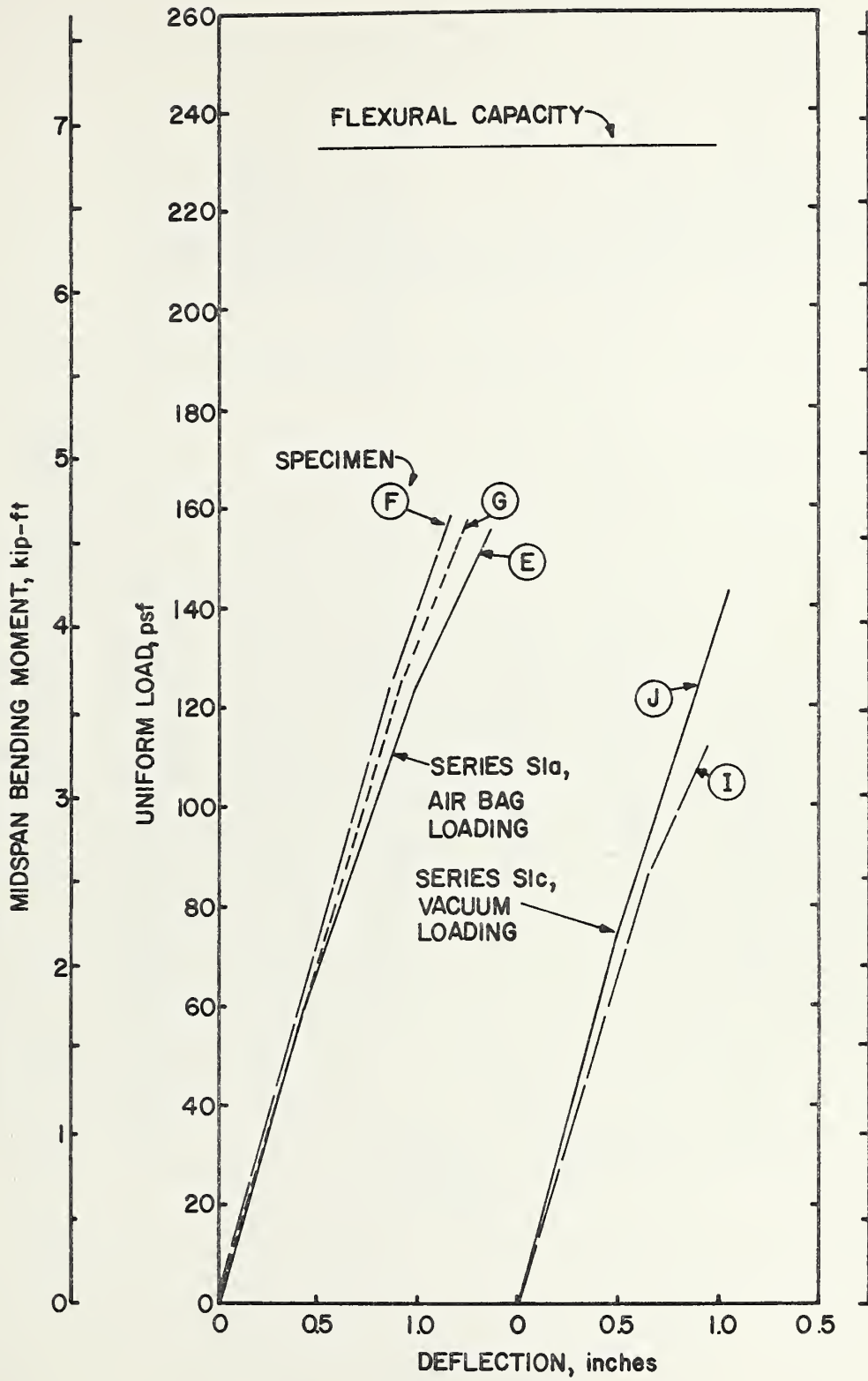


Figure 4.1 Load-Deflection Curves for Test Series Sla and Slc

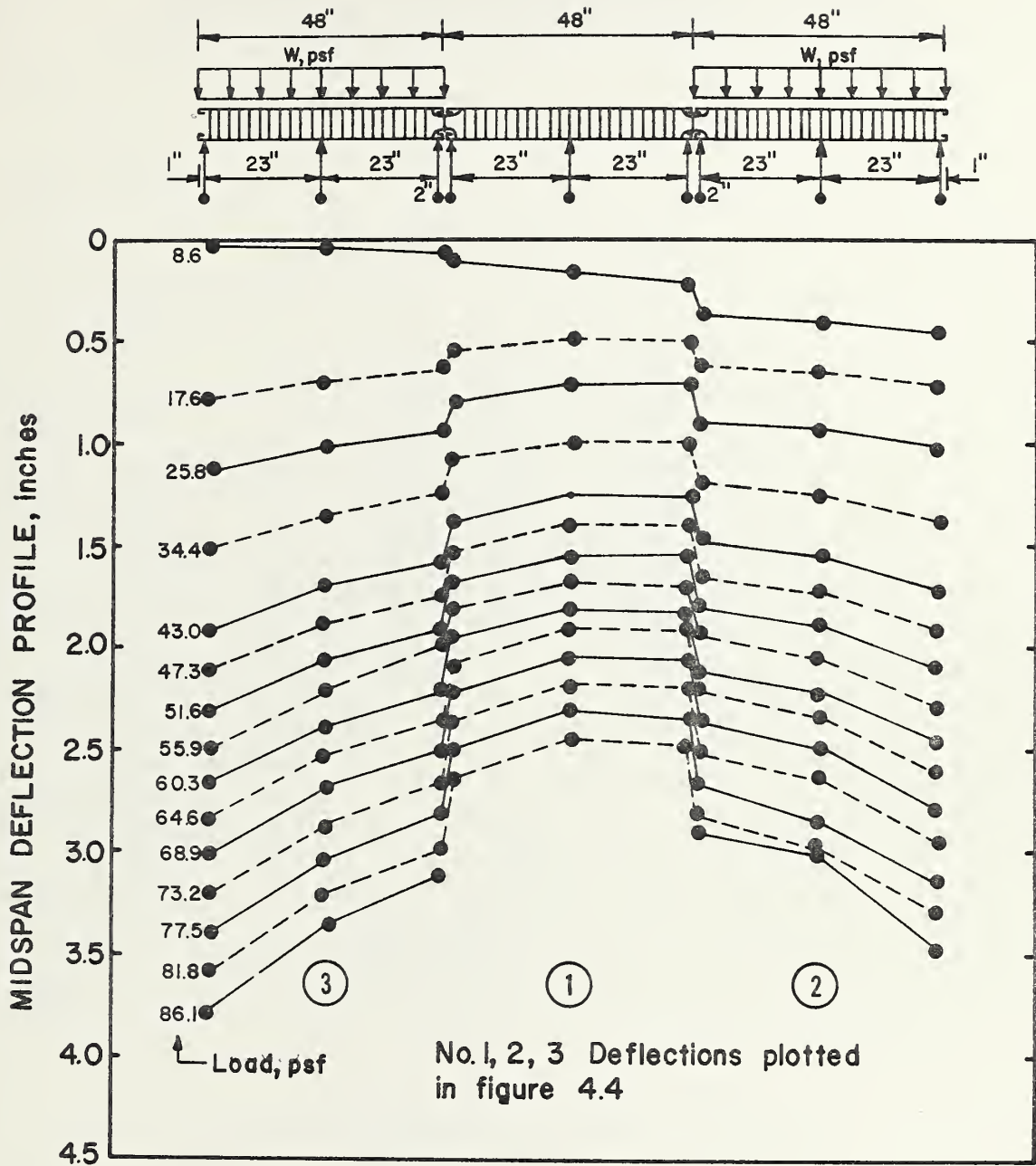


Figure 4.2 Deflection Profiles for Specimen S1b-1

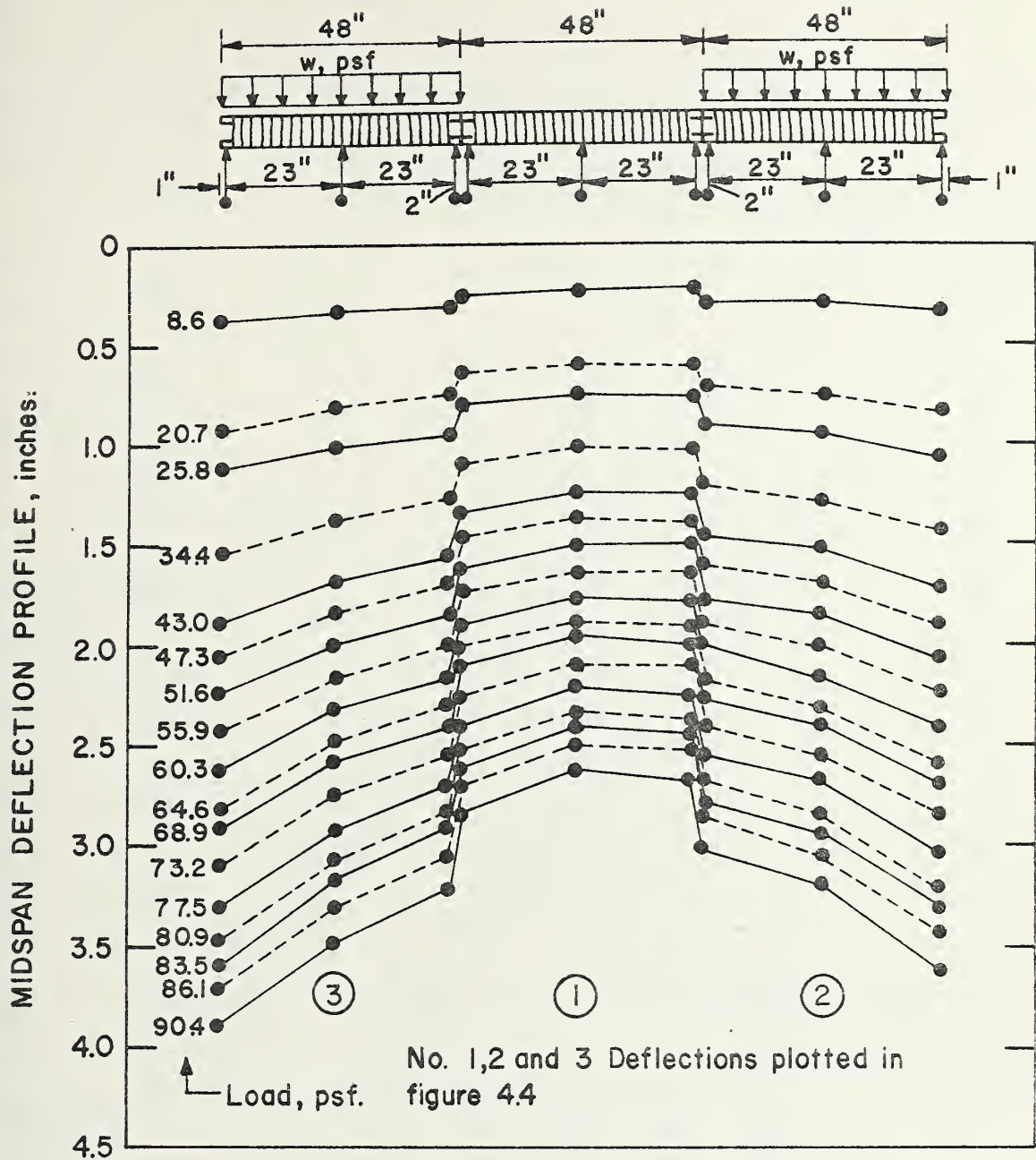


Figure 4.3 Deflection Profiles for Specimen S1b-2

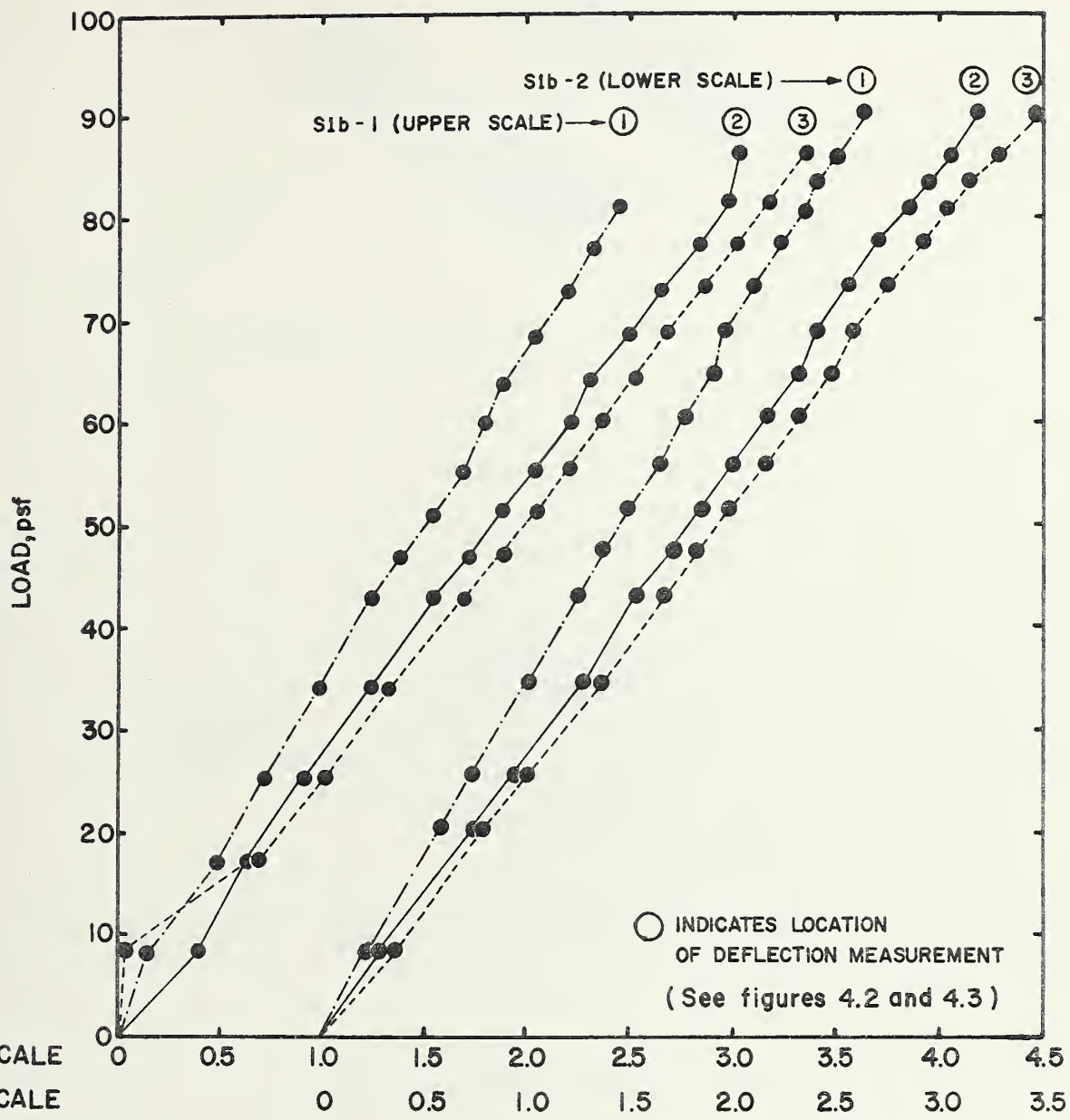
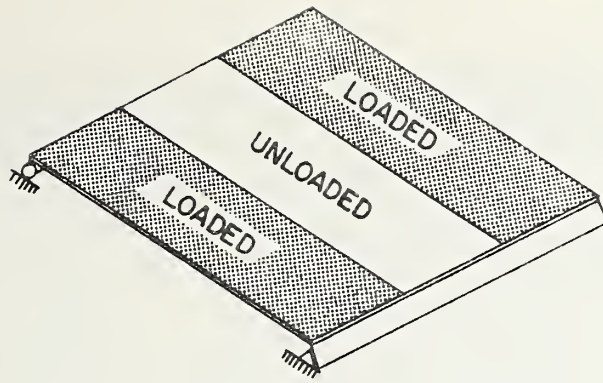
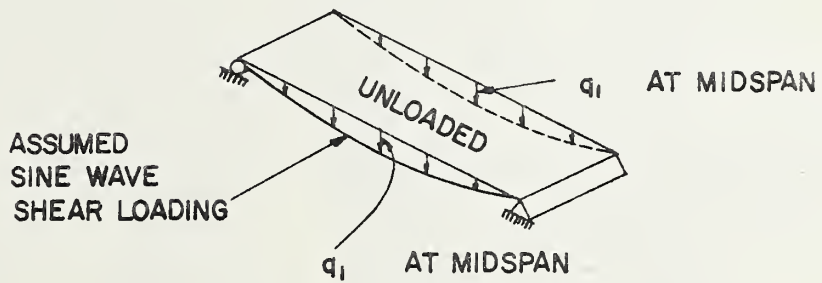


Figure 4.4 Load-Deflection Curves for Test Series S1b



a) LOADING CONDITION



b) ASSUMED SHEAR LOAD DISTRIBUTION ON CENTER PANEL

Figure 4.5 Forces on Unloaded Center Panel,
Test Series S1b

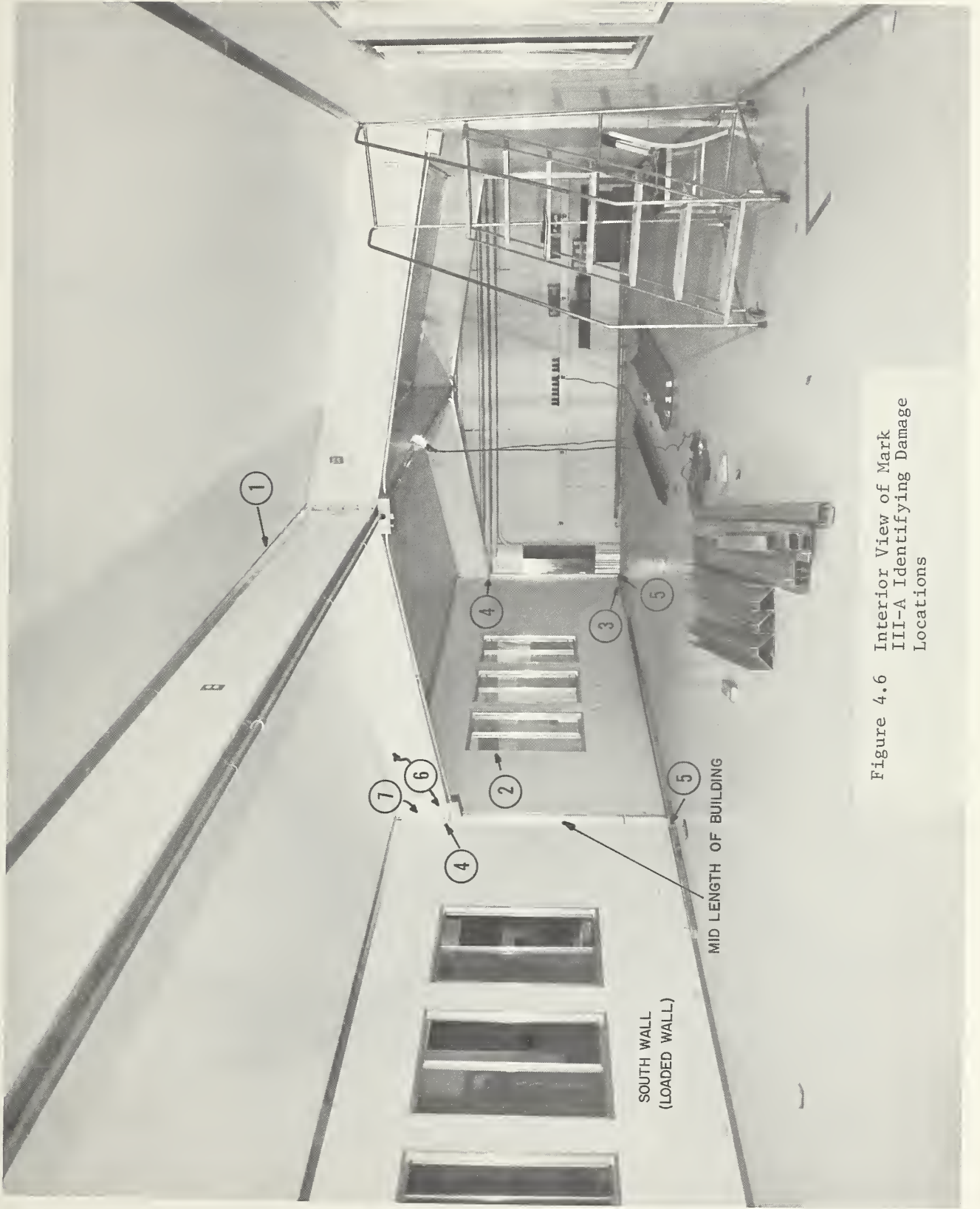
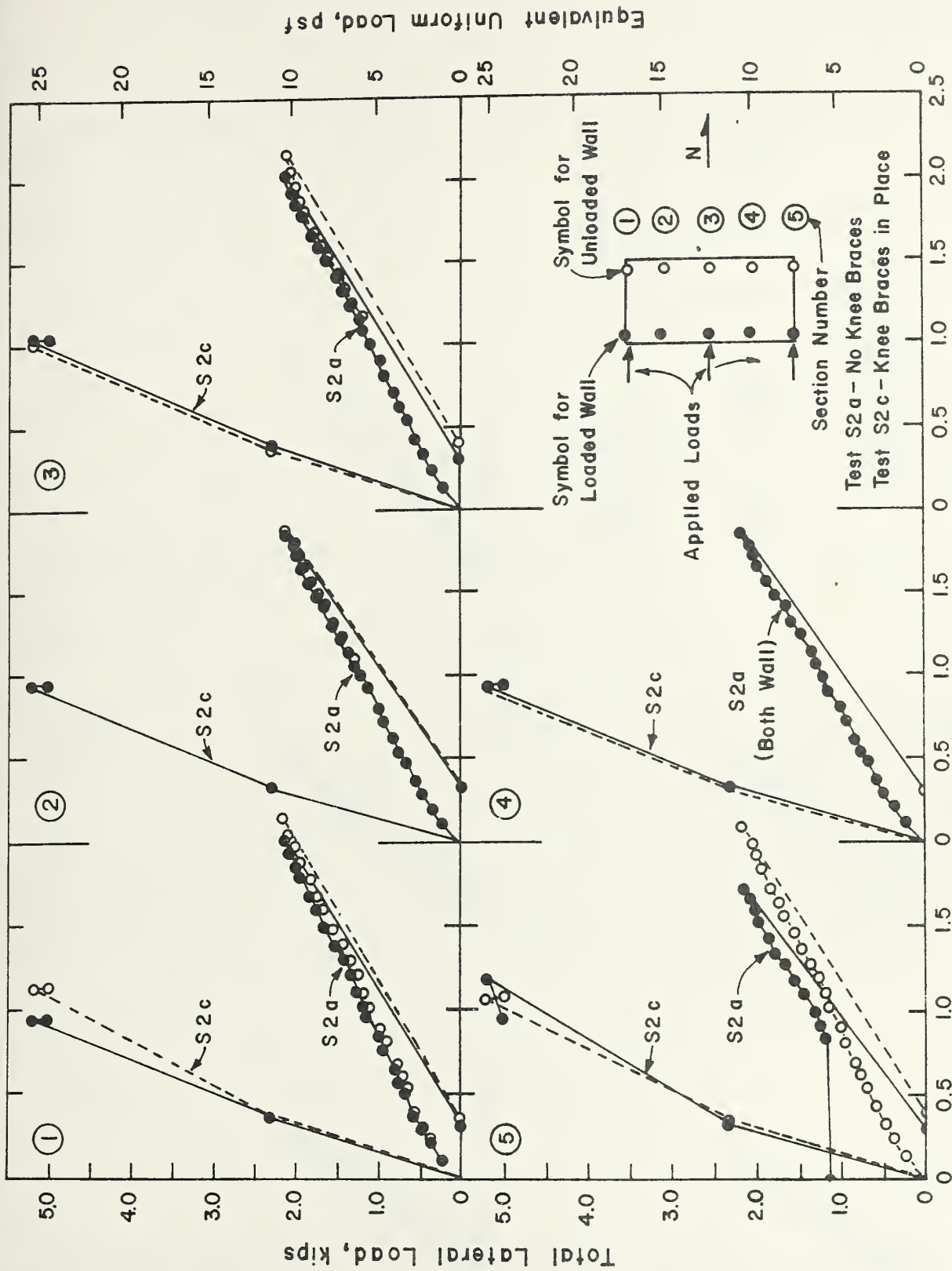


Figure 4.6 Interior View of Mark III-A Identifying Damage Locations



NET LATERAL DEFLECTION, inches

Figure 4.7 Load-Deflection Curves for Tests S2a and S2c

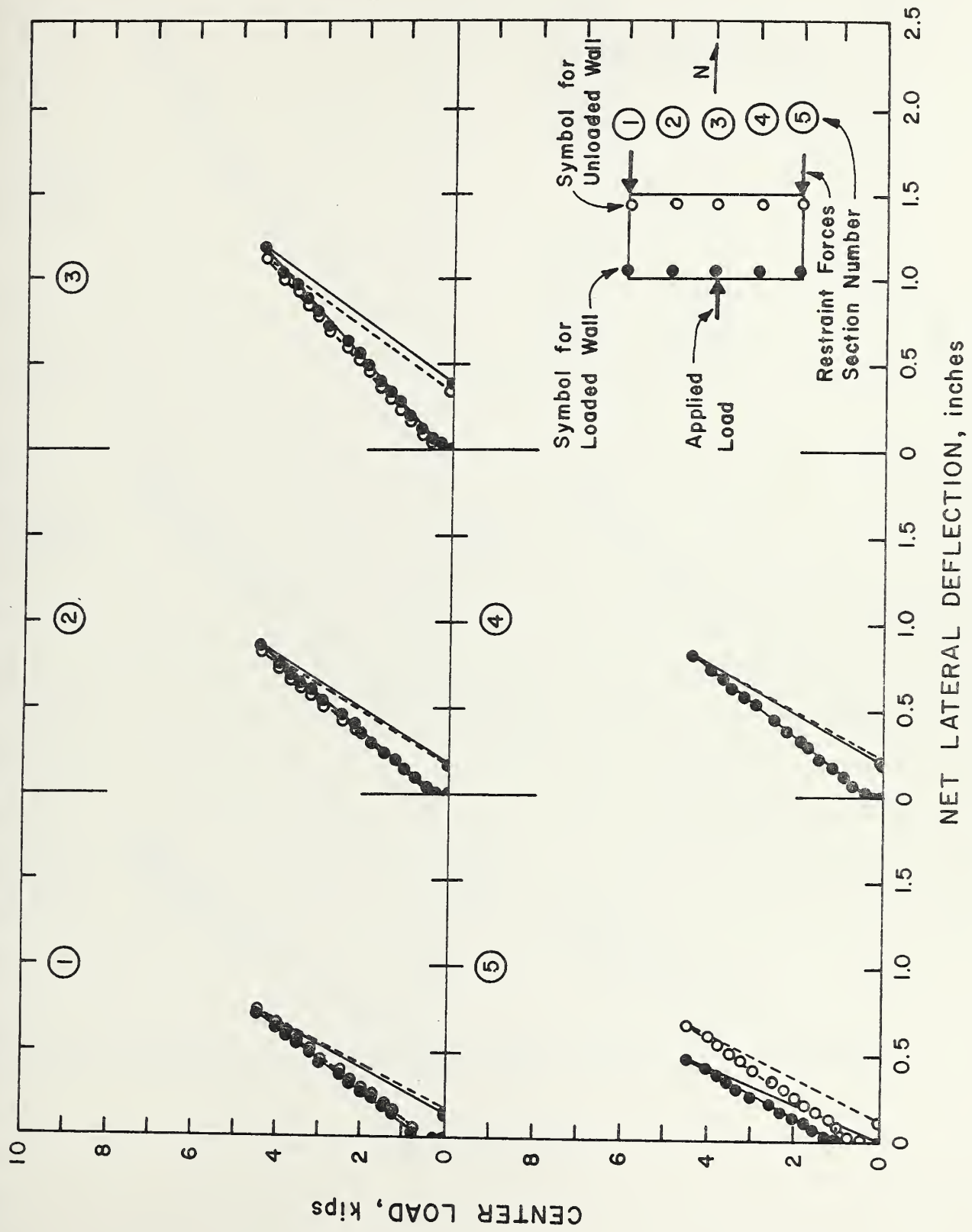


Figure 4.8 Load-Deflection Curves for Test S2b(1)

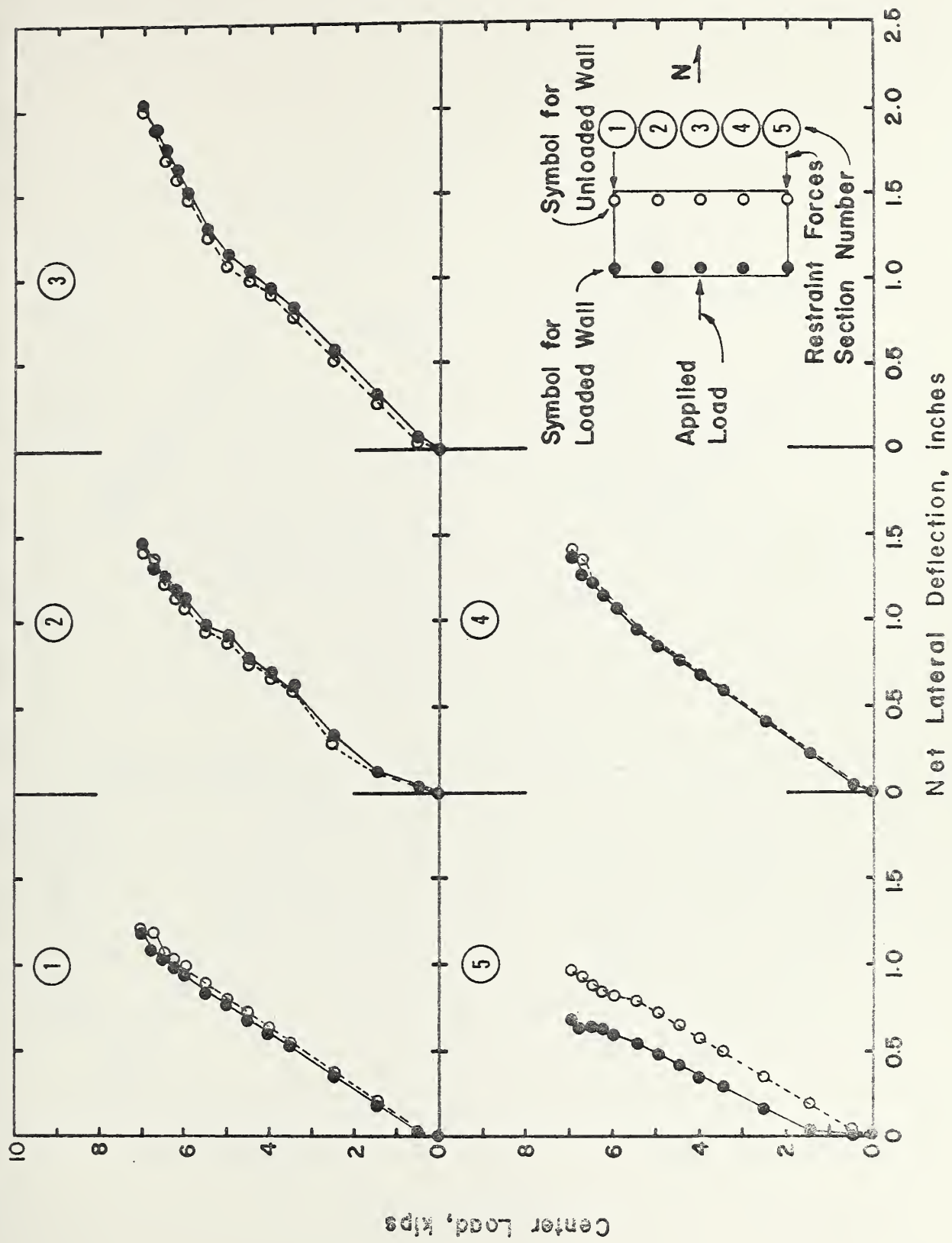
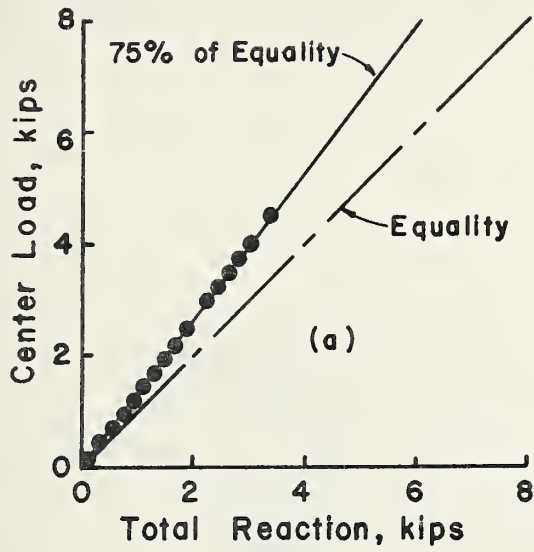
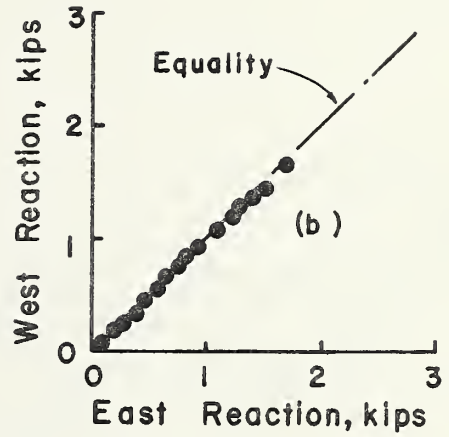


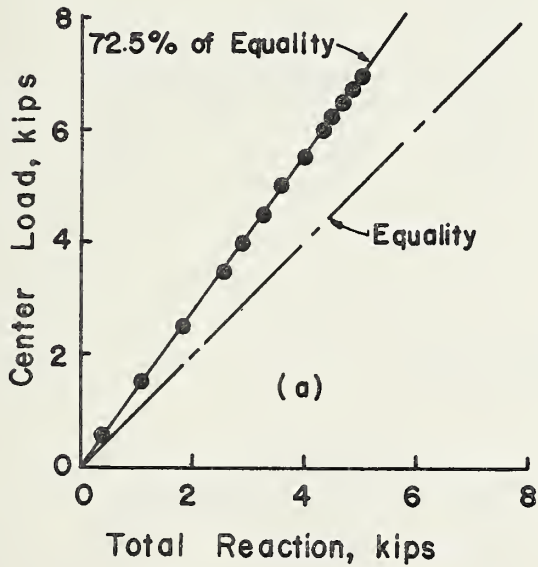
Figure 4.9 Load-Deflection Curves for Test S2b(2)



Test S2b(1)



3



Test S2b(2)

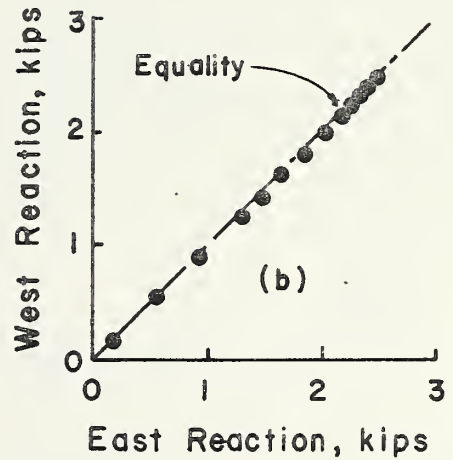
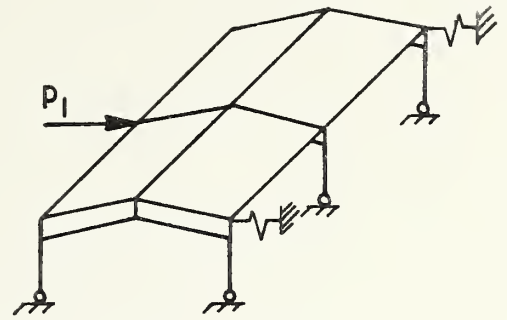
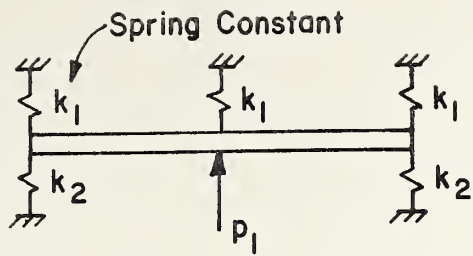
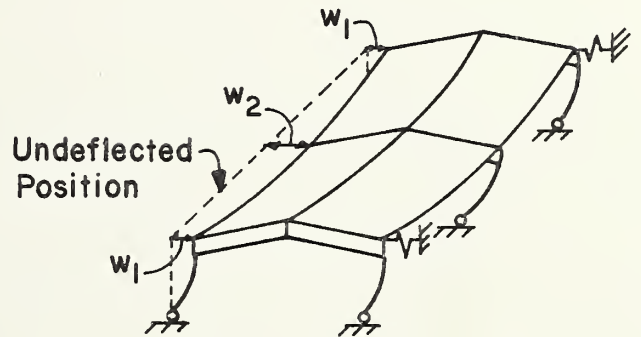
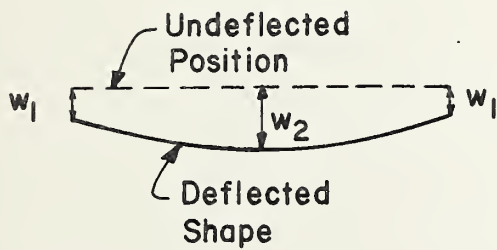


Figure 4.10 Center Load vs. Measured End Reactions for Tests S2b(1) and S2b(2)

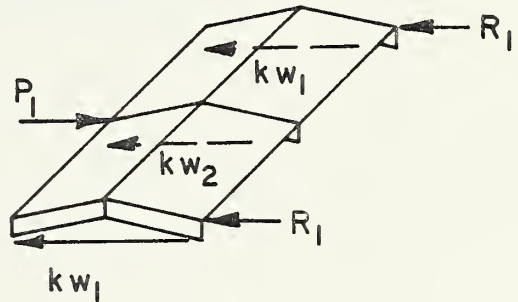
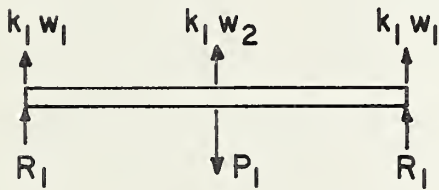




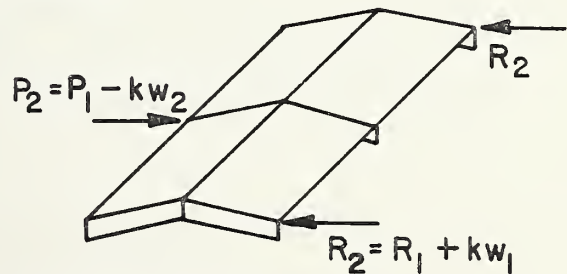
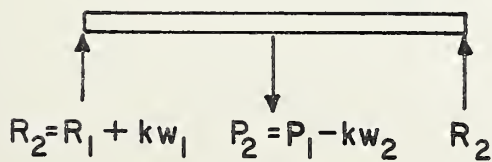
(a) Loading



(b) Deflected Shape



(c) Lateral Forces



(d) Equivalent Lateral Forces

Beam

Building

Figure 4.11 Elastic Support System



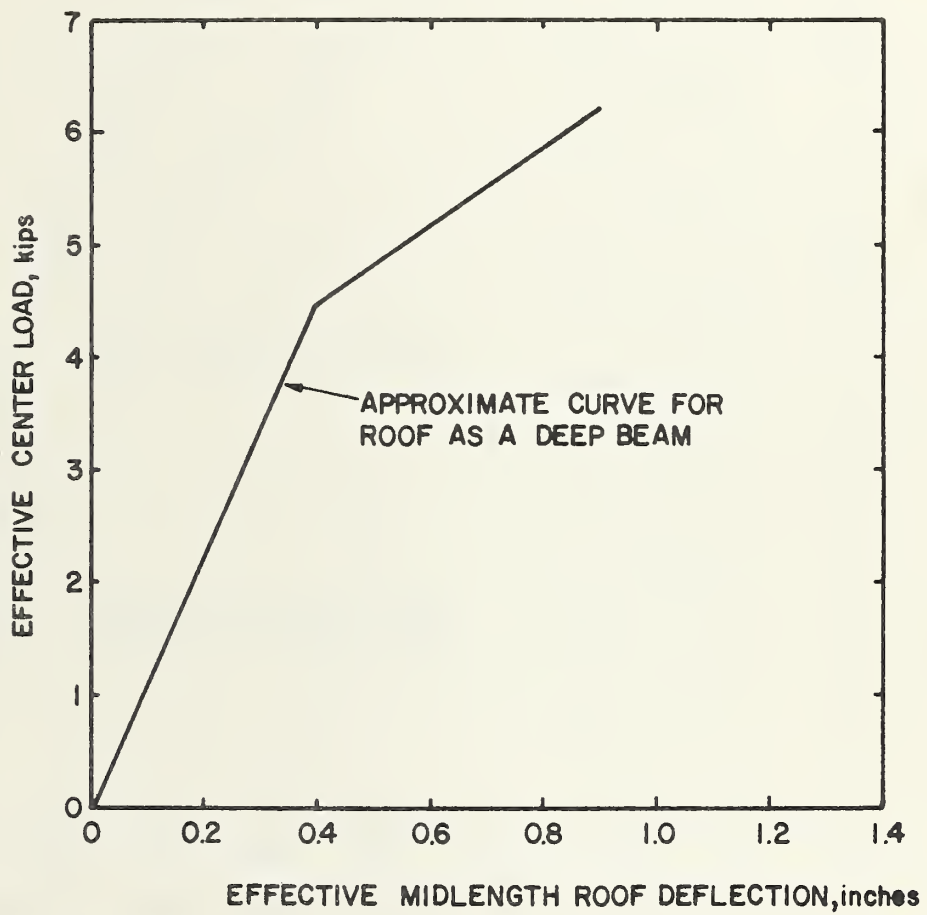
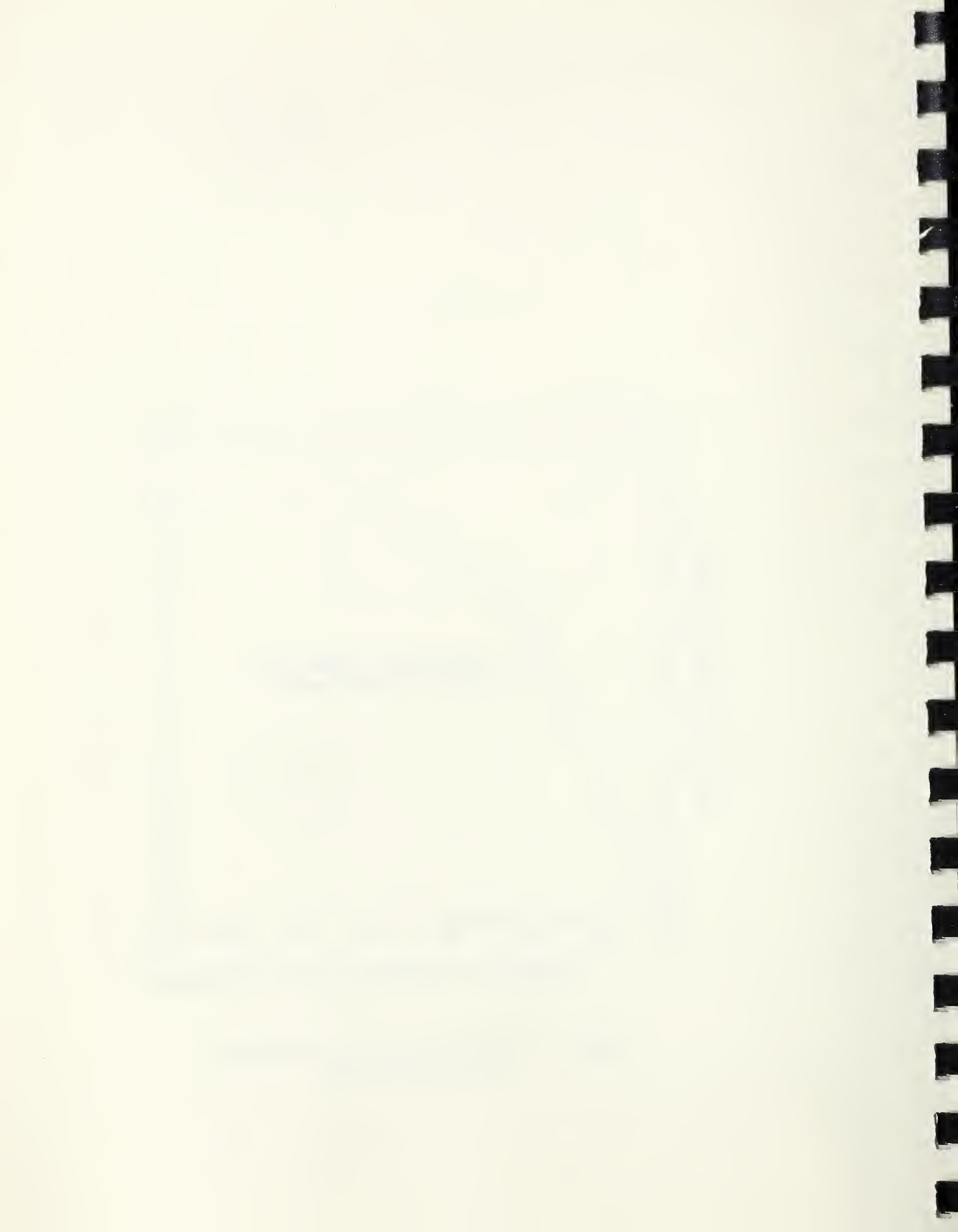


Figure 4.12 Effective Roof Load-Deflection Curve at Midlength



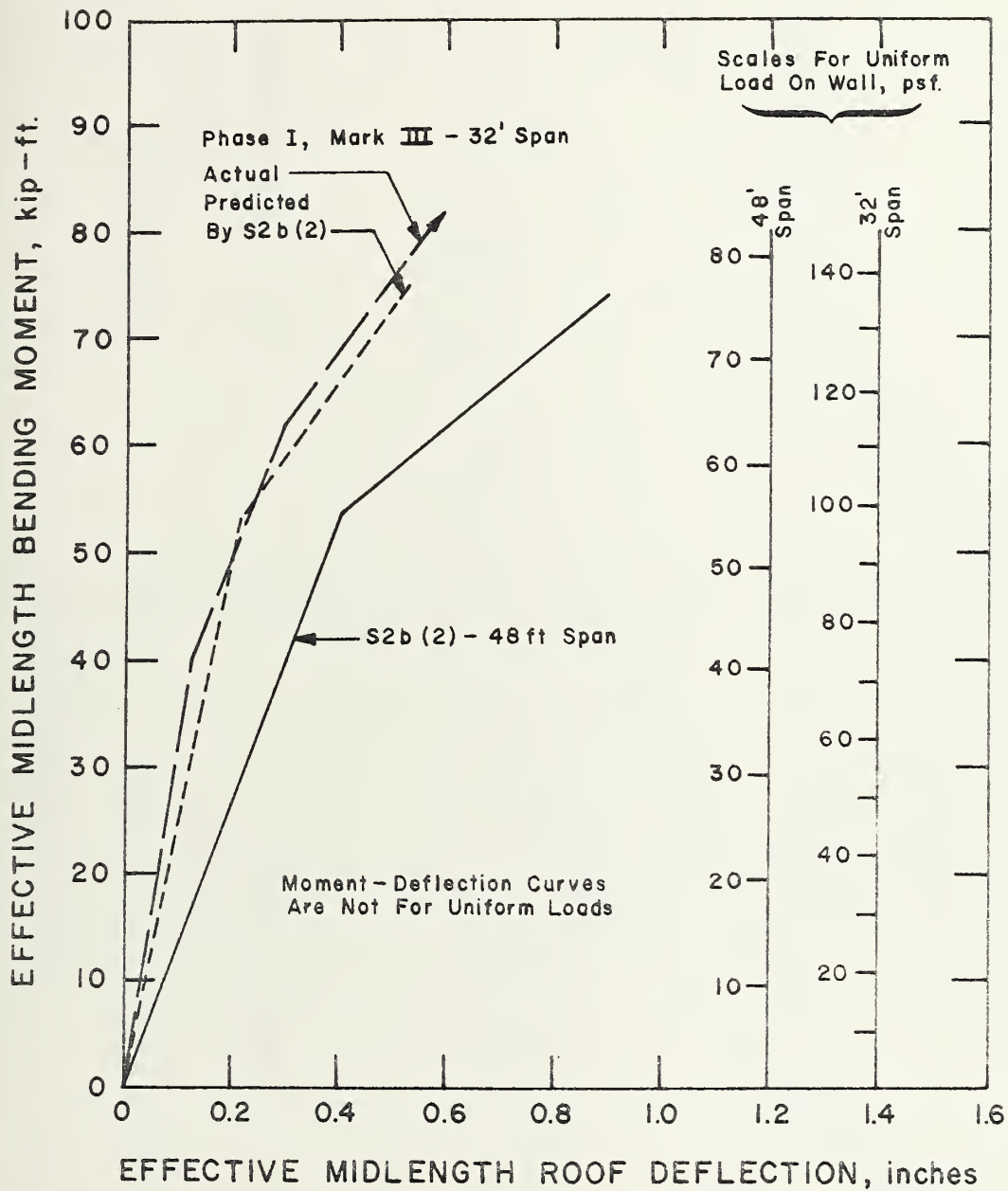


Figure 4.13 Comparison of 32 ft. and 48 ft. Roof Spans



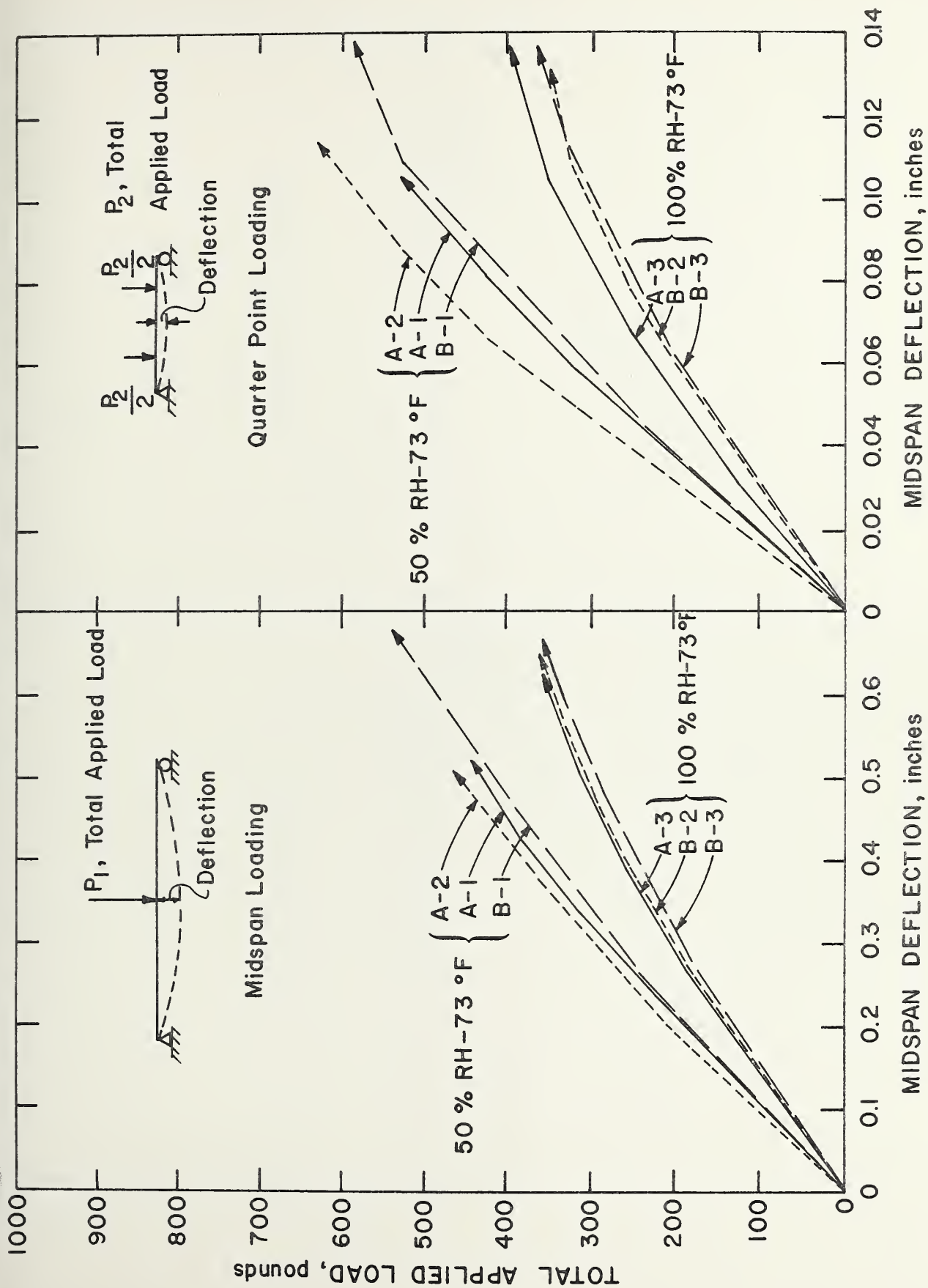


Figure 4.14 Load vs. Midspan Deflection for Test Series S3a

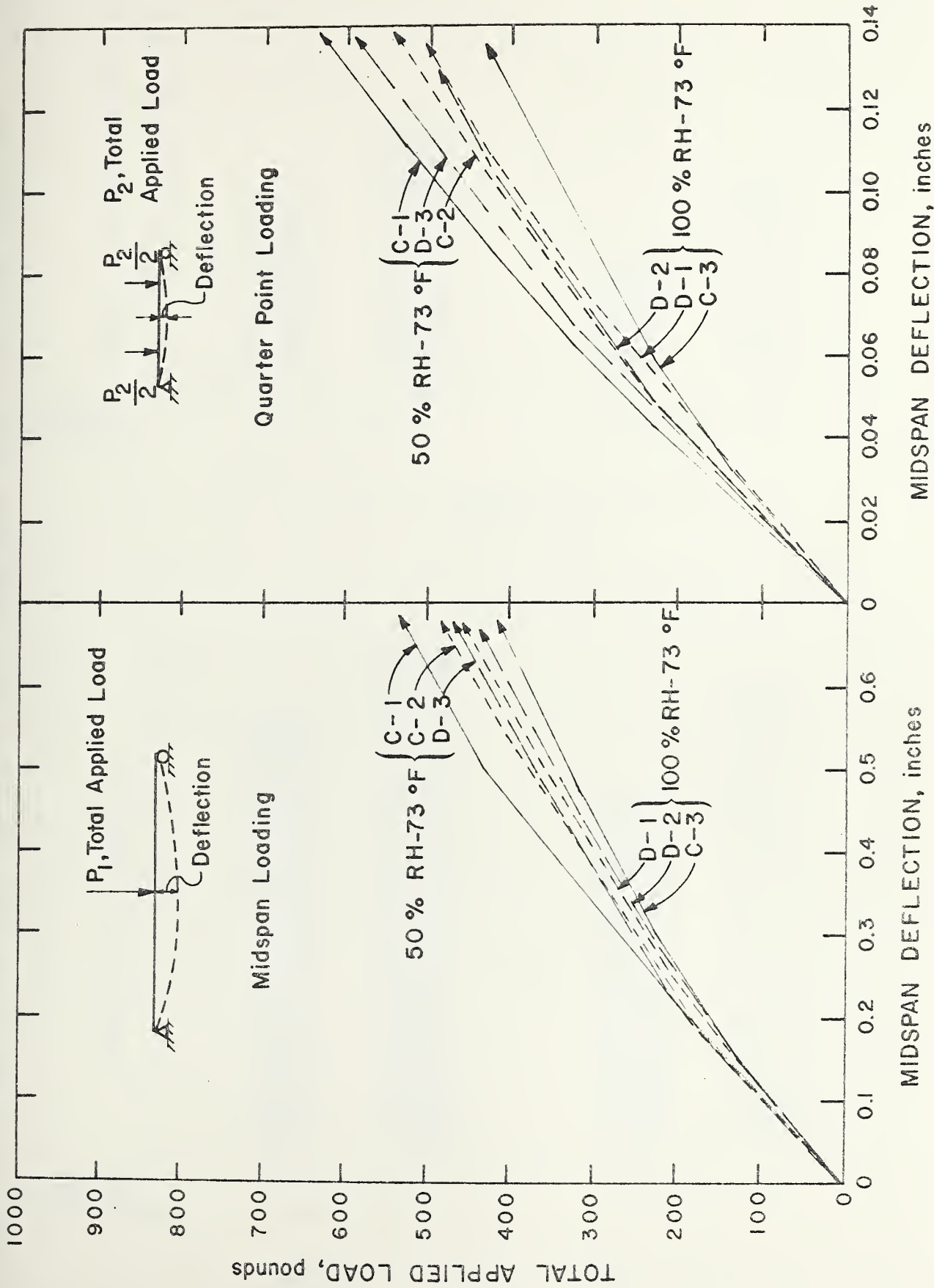


Figure 4.15 Load vs Midspan Deflection for Test Series S3b

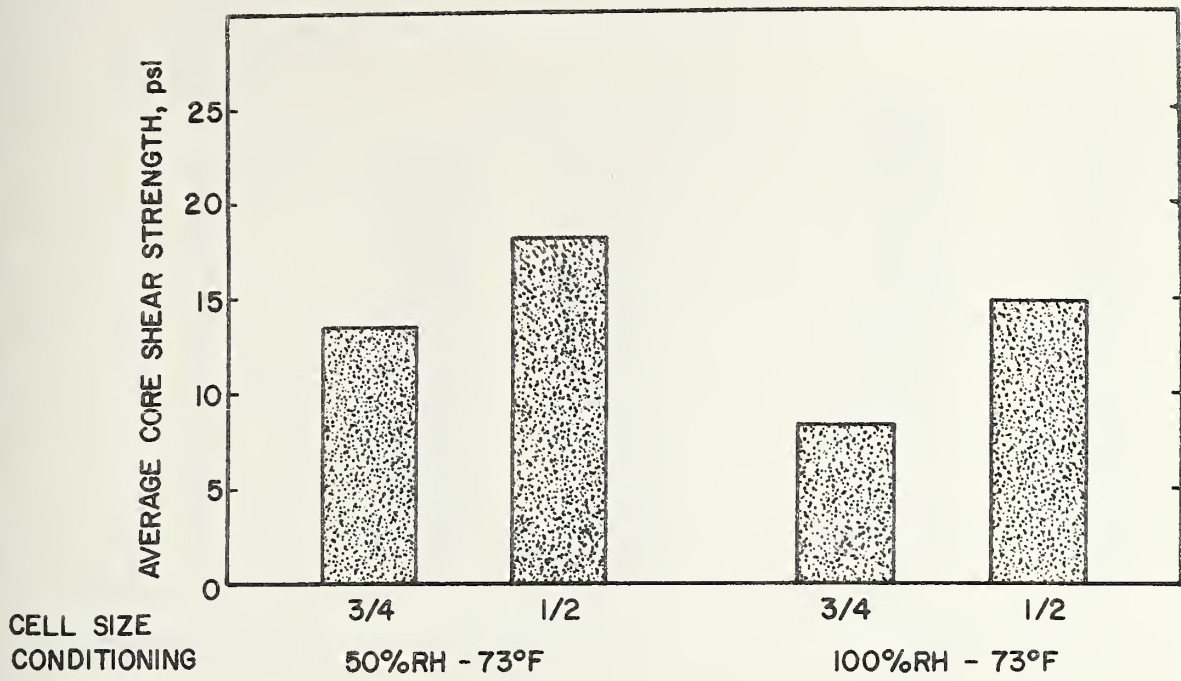


Figure 4.16 Comparison of Average Core Shear Strengths

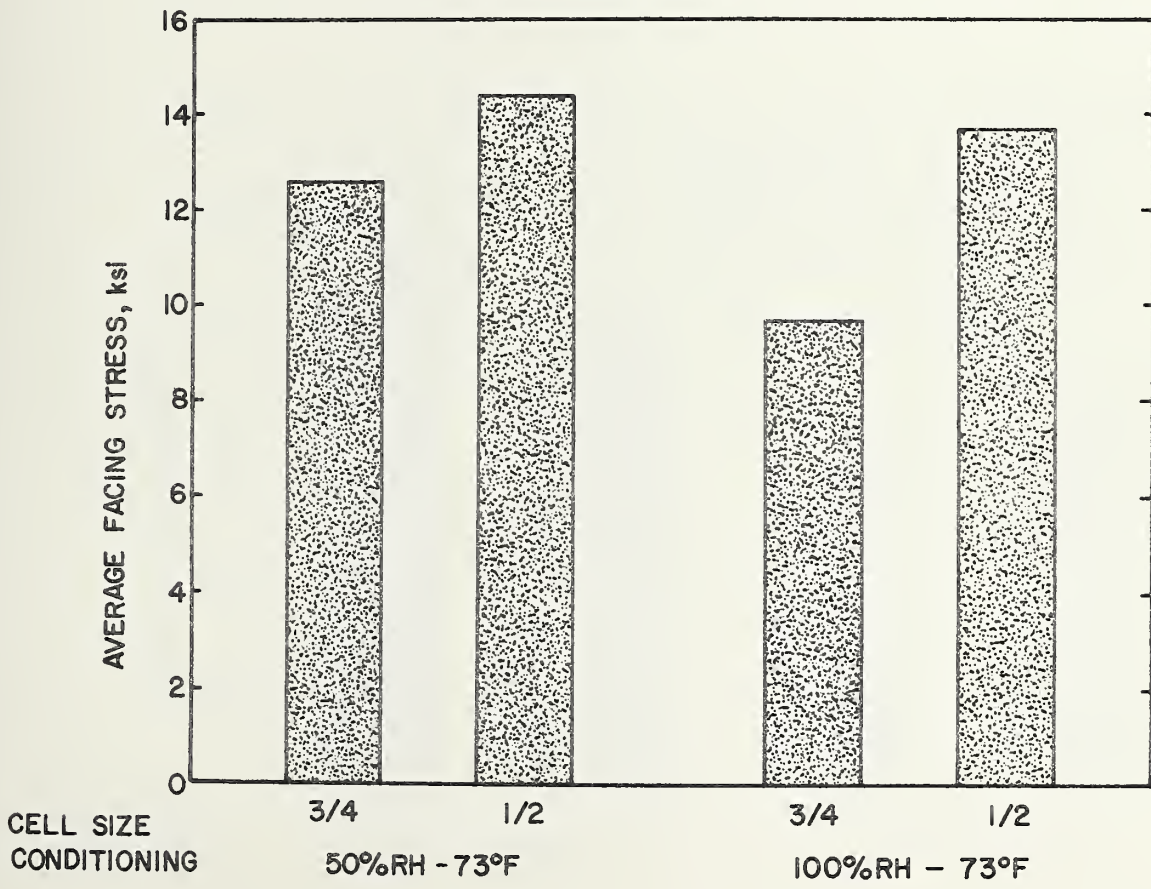


Figure 4.17 Comparison of Average Facing Stresses

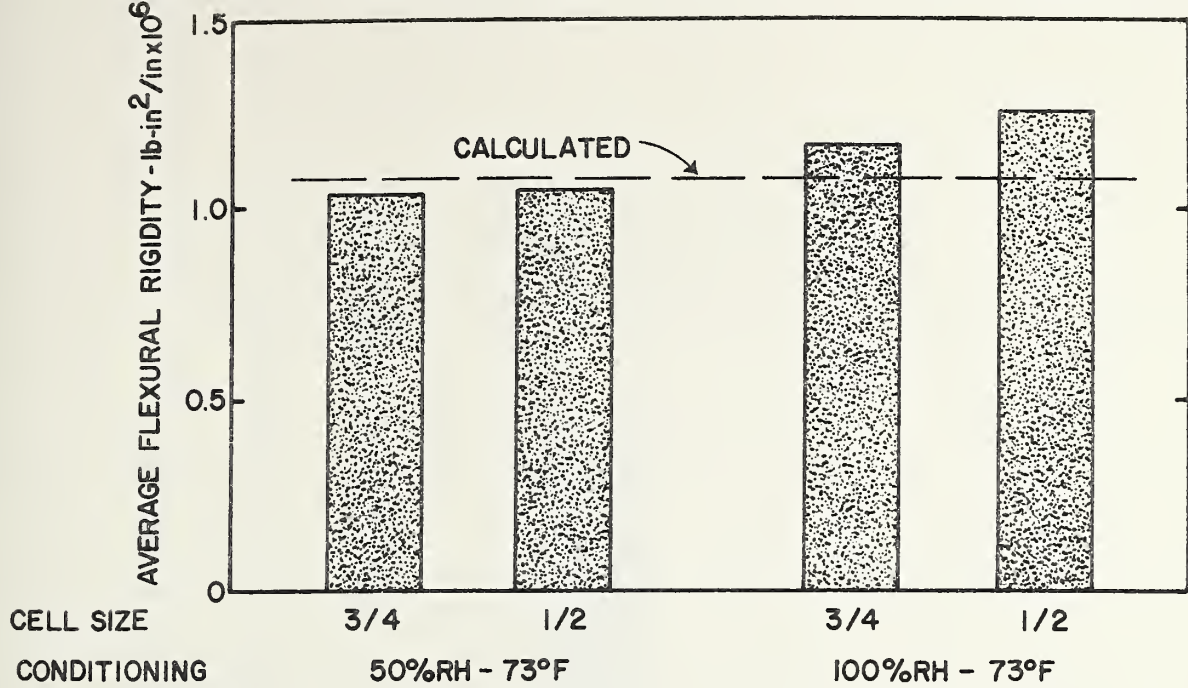


Figure 4.18 Comparison of Flexural Rigidities

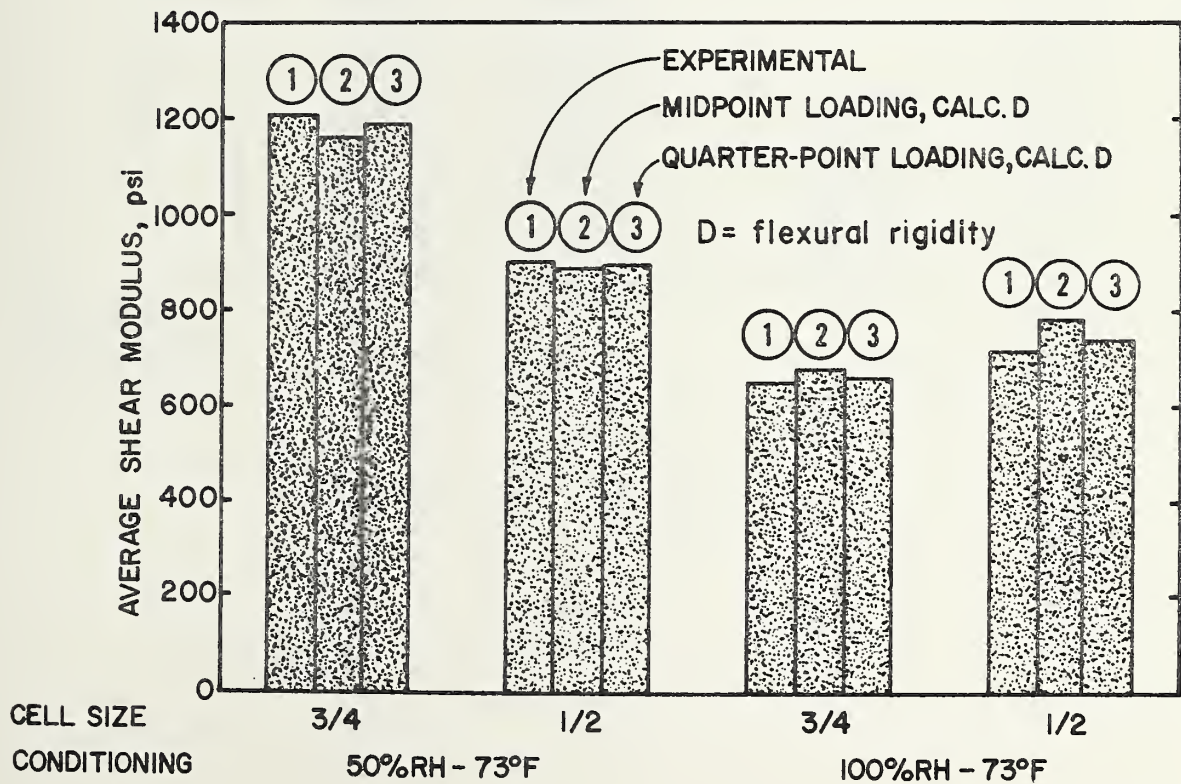


Figure 4.19 Comparison of Shear Moduli



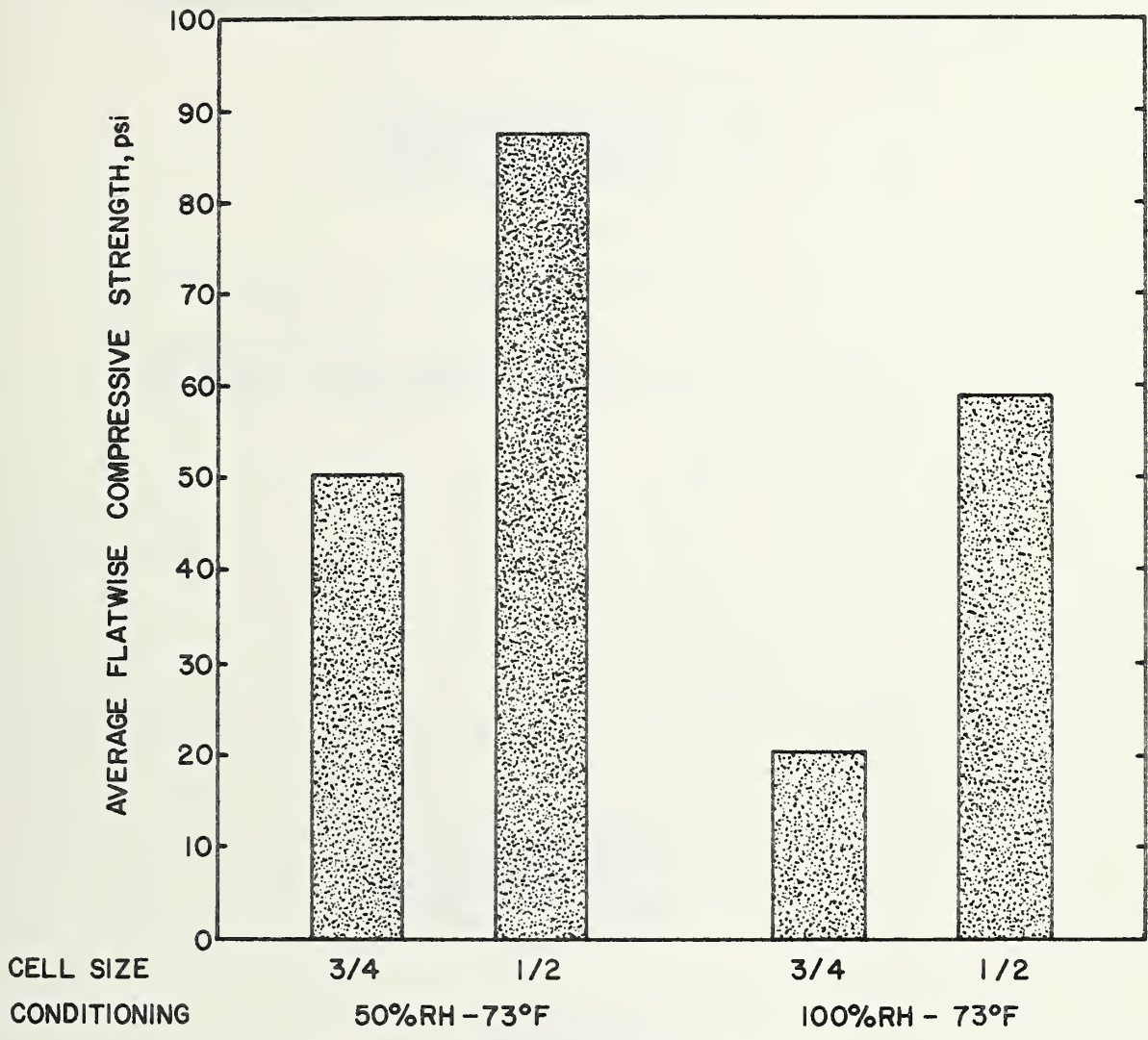
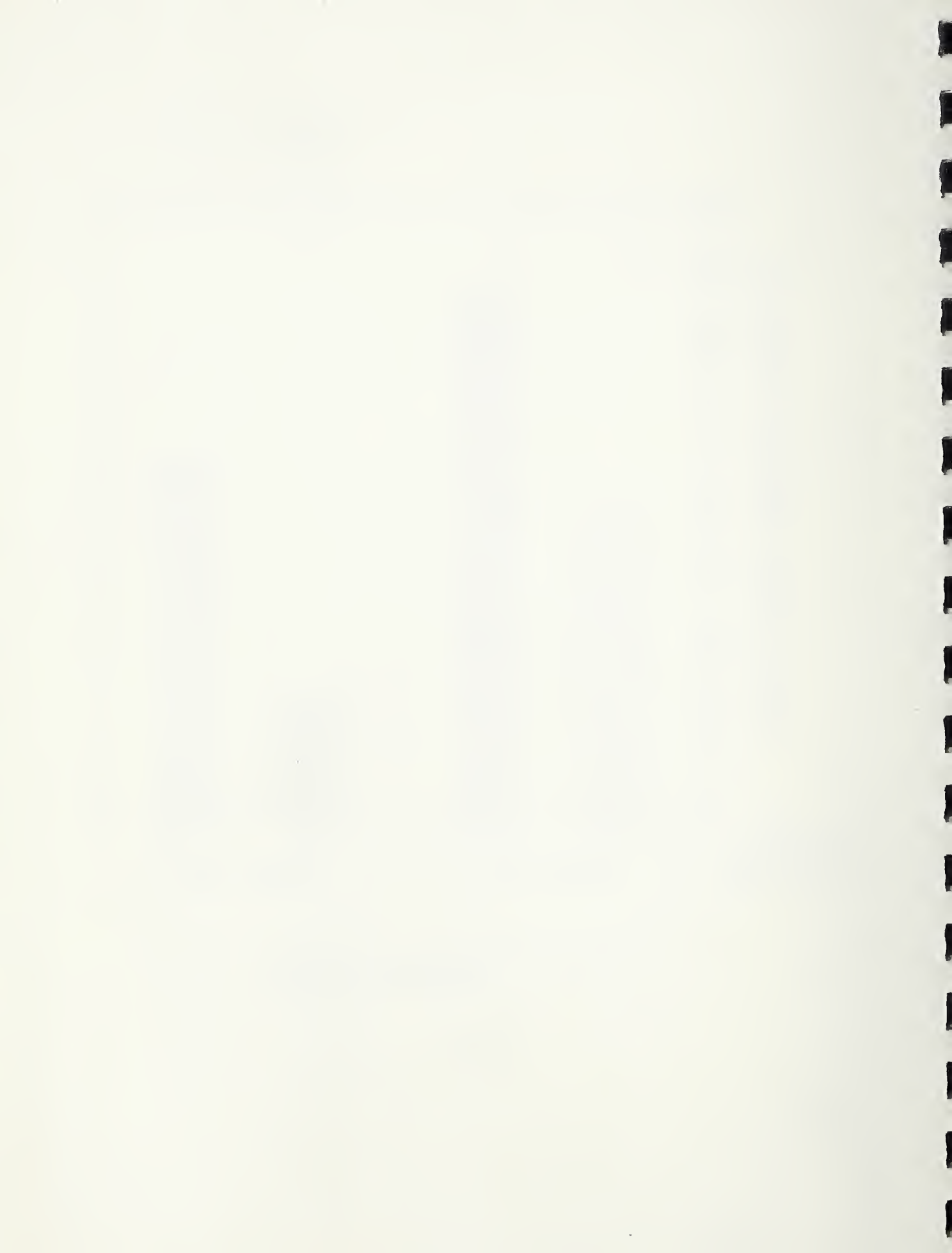


Figure 4.20 Comparison of Flatwise Compressive Strengths



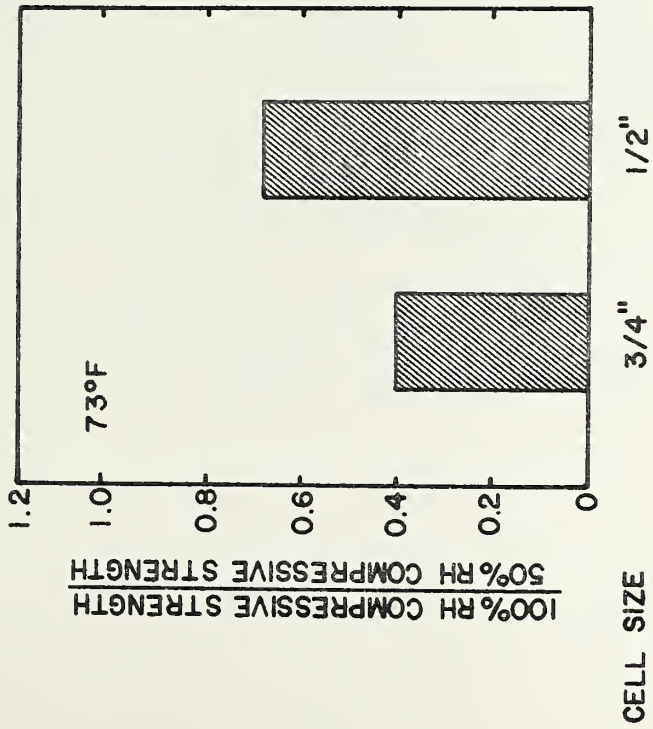


Figure 4.21 Effect of Curing Condition on Flatwise Compressive Strengths

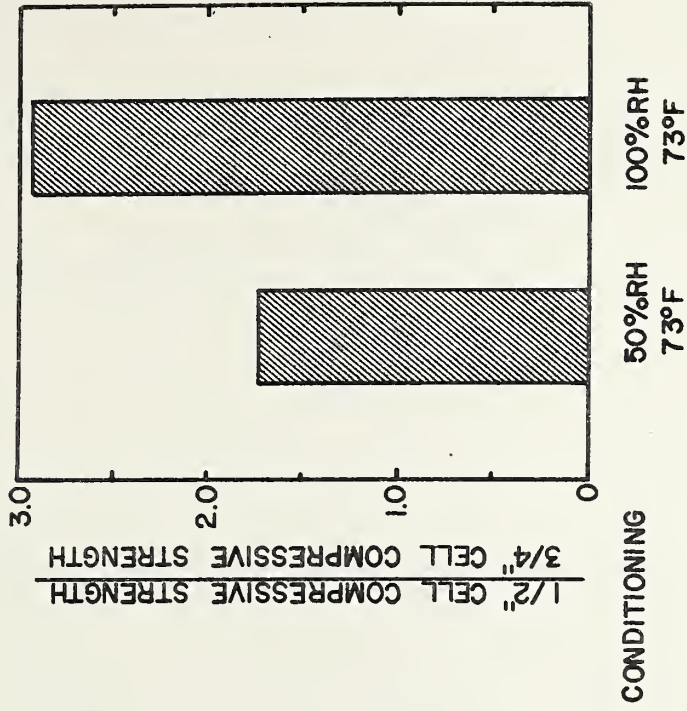
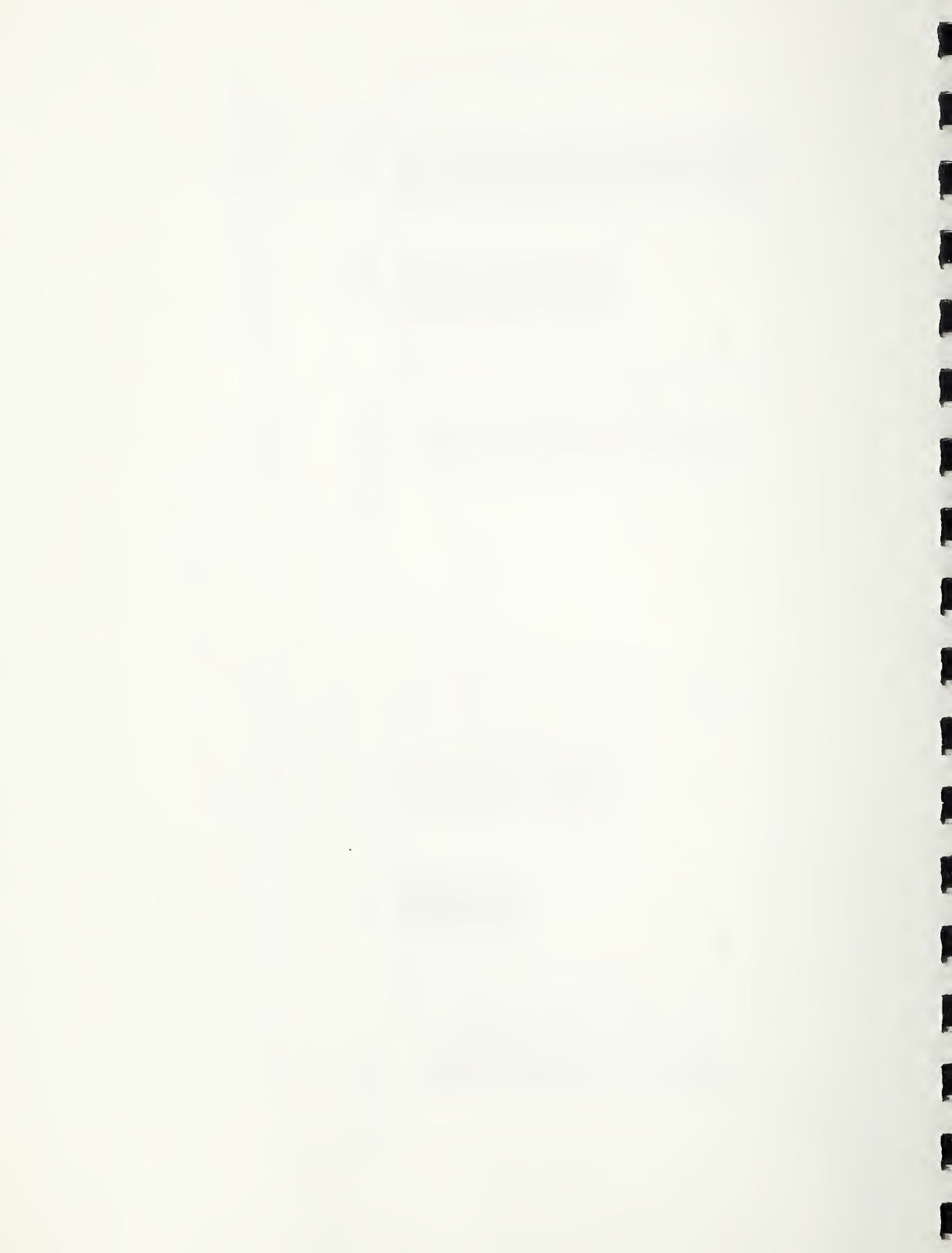


Figure 4.22 Effect of Cell Size on Flatwise Compressive Strength



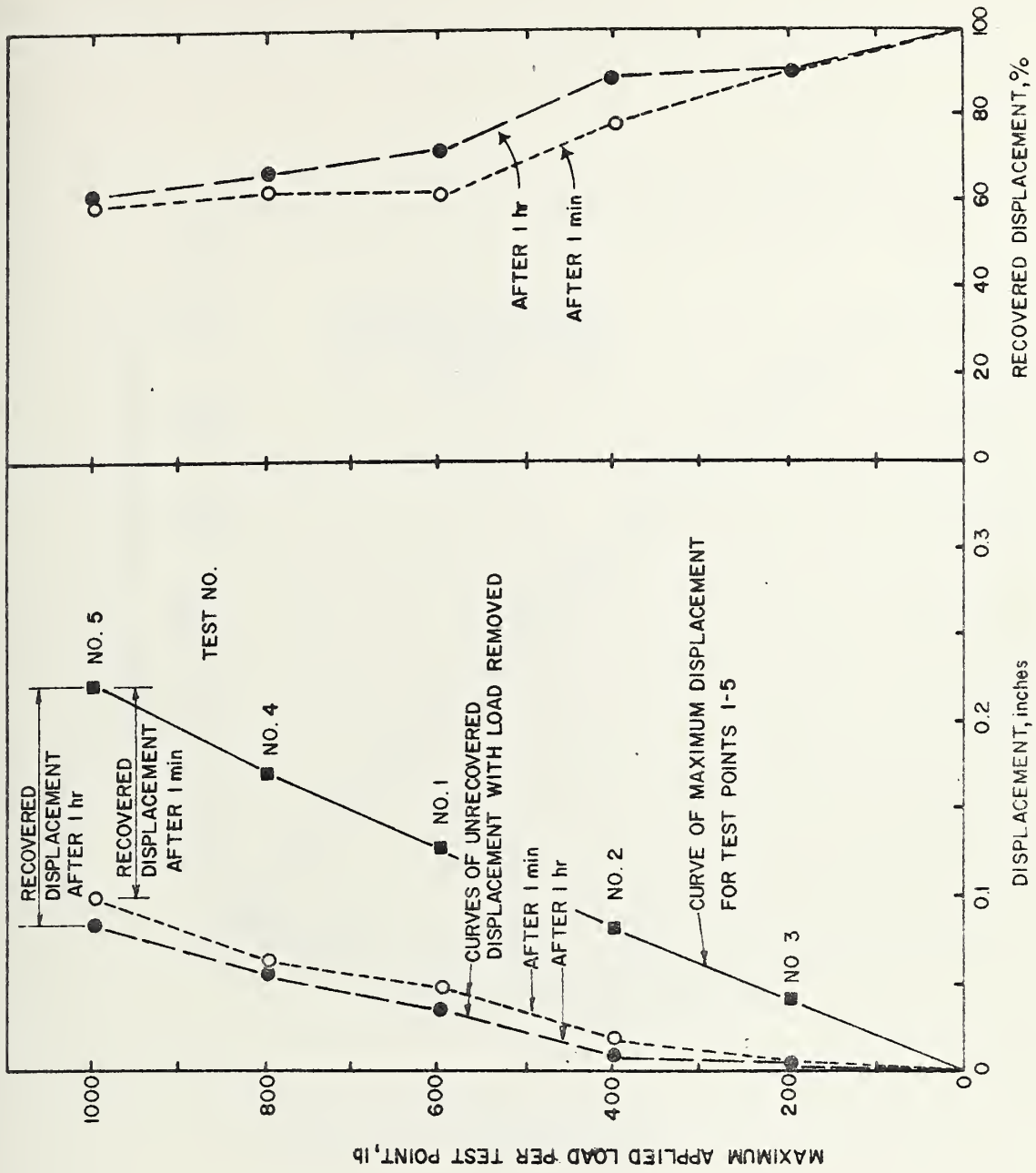


Figure 4.23 Displacement and Recovered Displacement Under Concentrated Loads with Tile in Place

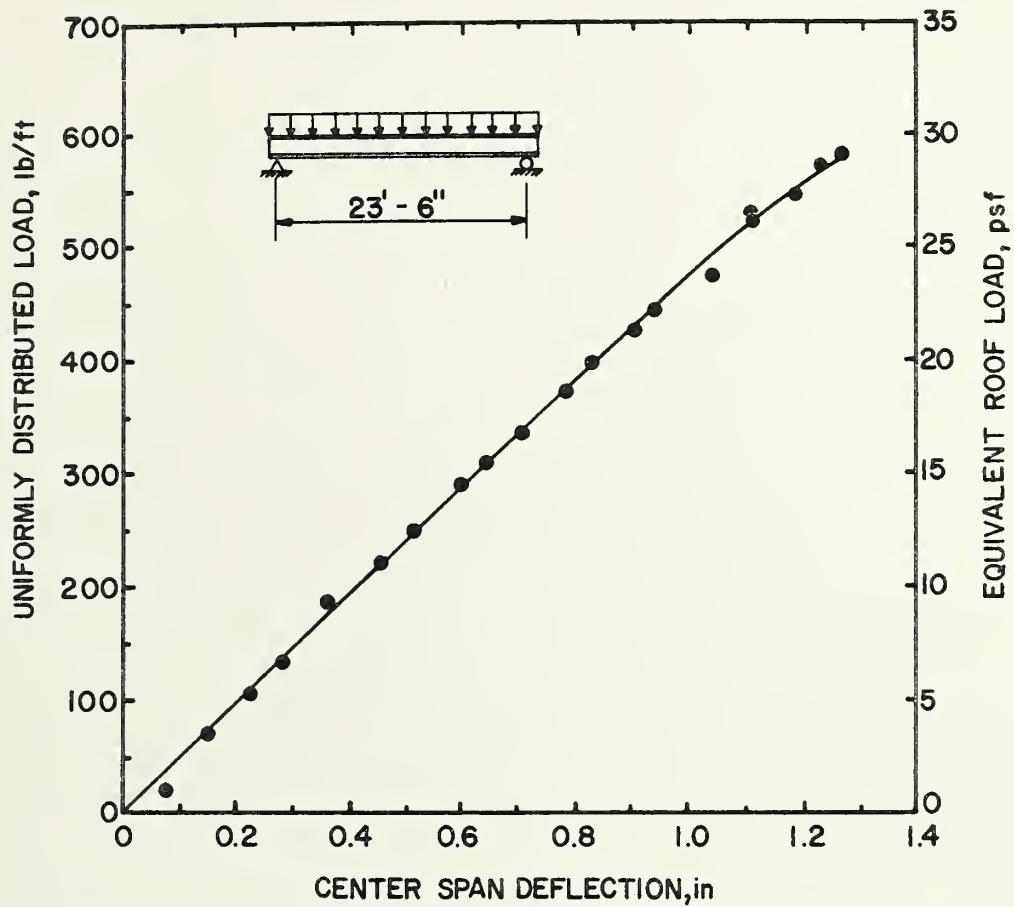


Figure 4.24 Load-Deflection Curve for Test S6 (Ridge Beam)

APPENDIX A
Packing List

PACKING LIST

CRATE NO. 1 OF 6

INSIDE DIMENSIONS: 16'-6" L x 2'-3" W x 2'-2" H

OUTSIDE DIMENSIONS: 16'-8 $\frac{1}{2}$ " L x 2'-5 $\frac{1}{4}$ " W x 2'-9" H

CUBIC FEET: 110

GROSS WEIGHT: 1325

CONTENTS

<u>ITEM NO.</u>	<u>NO. REQ'D</u>	<u>DESCRIPTION</u>
13.	24	15" x 3" x $\frac{1}{2}$ " Anchor bolts, nut & washer
14.	4	10" I Beams 9'-9"
15.	3	10" I Beams 15'-10 $\frac{7}{8}$ "
16a.	2	10" I Beams 16'-4 $\frac{3}{4}$ "
16b.	2	10" I Beams 16'-4 $\frac{3}{4}$ "
16c.	2	10" I Beams 16'-4 $\frac{3}{4}$ "
17a.	2	3" Base 5'-11 $\frac{13}{16}$ "
17b.	2	3" Base 5'-11 $\frac{13}{16}$ "
17c.	10	3" Base or Facia 12'-3"
17d.	2	3" Facia 12'-3"
17e.	2	3" Facia 3"-0 $\frac{3}{4}$ "
17f.	2	3" Facia 10'-11"
17g.	2	3" Facia 10'-11"
18a.	2	3" Facia 10'-3 $\frac{1}{2}$ "
18b.	2	3" Facia 10'-3 $\frac{1}{2}$ "
19a.	2	Corner post 8'-5 $\frac{3}{8}$ "

PACKING LIST

CRATE NO. 1 OF 6

(CONTINUED)

<u>ITEM NO.</u>	<u>NO. REQ'D.</u>	<u>DESCRIPTION</u>
19b.	2	Corner post 8'-5 3/8"
20.	22	Wall and column joint 8'-5 3/8"
21.	4	Ridge cap 11'-6"
21.	1	Ridge cap 5'-9 1/4"
22.	4	Flat top cap 10'-8"
23.	8	Slant top cap 11'-11 5/8"
28.	14	Silicone caulking
29.	3,300	#12 x 1" S.S. Hex head screws
30.	150	1/4" x 1" S.S. Hex head bolts with 2 S.S. flat washers and nut each
31.	150	1/4" x 4" S.S. Hex head bolts with 1 S.S. flat washer, 1 S.S. cap washer and 1 neoprene gasket each.

EXTRA MATERIALS

<u>ITEM NO.</u>	<u>NO. REQ'D.</u>	<u>NO. EXTRA</u>	<u>DESCRIPTION</u>
17c.	10	3	3" Base or Facia 12'-3"
13.	24	2	Anchor bolts, washer & nut
		3	Flat top cap 10'-10"
29.	3,300	3,300	#12 x 1" Screws
30.	150	150	1/4" x 1" Bolts, washer & nuts
31.	150	150	1/4" x 4" Bolts, washer, nuts & gaskets

PACKING LIST

CRATE NO. 2 OF 6

INSIDE DIMENSIONS: 10'-8" L x 4'-0 1/2" W x 5'-0" H

OUTSIDE DIMENSIONS: 10'-10 1/4" L x 4'-2 3/4" W x 5'-7" H

CUBIC FEET: 250

GROSS WEIGHT: 1500

CONTENTS

<u>ITEM NO.</u>	<u>NO. REQ'D</u>	<u>DESCRIPTION</u>
1.	8	Panel 8'-6"
2.	4	Window panel 8'-6"
3.	1	Panel 9'-4 5/8"
4.	1	Panel 10'-2 5/8"
5.	1	Panel 10'-7 5/8"
6.	1	Door panel 10'-2 5/8"
7.	1	Panel 9'-4 5/8"
24.	12	Drive cleats 8'-6"
25.	2	Drive cleats 9'-4"
26.	2	Drive cleats 10'-2"
33.	1	Door lock set
34.	1	Threshold
35.	1	Door closer chain

EXTRA MATERIALS

1 Panel 10'-7 5/8"

PACKING LIST

CRATE NO. 3 OF 6

INSIDE DIMENSIONS: 10'-8" L x 4'-0 1/2" W x 5'-0" H

OUTSIDE DIMENSIONS: 10'-10 1/4" L x 4'-2 3/4" W x 5'-7" H

CUBIC FEET: 250

GROSS WEIGHT: 1500

CONTENTS

<u>ITEM NO.</u>	<u>NO. REQ'D</u>	<u>DESCRIPTION</u>
1.	8	Panel 8'-6"
2.	4	Window Panel 8'-6"
3.	1	Panel 9'-4 5/8"
4.	1	Panel 10'-2 5/8"
5.	1	Panel 10'-7 5/8"
6.	1	Door panel 10'-2 5/8"
7.	1	Panel 9'-4 5/8"
24.	12	Drive cleat 8'-6"
25.	2	Drive cleat 9'-4"
26.	2	Drive cleat 10'-2"
33.	1	Door lock set
34.	1	Threshold
35.	1	Door closer chain

EXTRA MATERIALS

1 Panel 10'-7 5/8"



PACKING LIST
CRATE NO. 4 OF 6

INSIDE DIMENSIONS: 24'-0" L x 4'-2" W x 2'-2" H

OUTSIDE DIMENSIONS: 24'-2 1/4" L x 4'-4 1/4" W x 2'-9" H

CUBIC FEET: 295

GROSS WEIGHT: 1100

CONTENTS

<u>ITEM NO.</u>	<u>NO. REQ'D</u>	<u>DESCRIPTION</u>
8.	1	Truss 20'-0 3/8" x 3'-9 3/4"
9a.	1	Beams 23'-11 3/4" x 1'-11 7/16"
9b.	1	Beams 23'-11 3/4" x 1'-11 7/16"
23.	36	"Silicone caulking"
32a.	1	Circuit breaker panel assembly
32b.	1	Ground rod assembly
32c.	1	Incoming service assembly
32d.	1	Incoming service spool rack
32e.	24	Lighting fixtures
32f.	4	Wire mold assemblies



PACKING LIST
CRATE NO. 5 OF 6

INSIDE DIMENSIONS: 10'-11" L x 4'-0 1/2" W x 7'-0" H

OUTSIDE DIMENSIONS: 11-1 1/4" L x 4'-2 3/4" W x 7'-7" H

CUBIC FEET: 349

GROSS WEIGHT: 2200

CONTENTS

<u>ITEM NO.</u>	<u>NO. REQ'D</u>	<u>DESCRIPTION</u>
10.	26	Roof panels 10'-10"
27.	24	Drive cleats 10'-10"



PACKING LIST
CRATE NO. 6 OF 6

INSIDE DIMENSIONS: 20'-7 1/2" L x 4'-1 1/4" W x 3'-10" H

OUTSIDE DIMENSIONS: 20'-9 3/4" L x 4'-3 1/2" W x 4'-5" H

CUBIC FEET: 390

GROSS WEIGHT: 3625

CONTENTS

<u>ITEM NO.</u>	<u>NO. REQ'D</u>	<u>DESCRIPTION</u>
11.	12	Floor panels 4'-0" x 20'-7"
12.	1	Floor panel 0'-7" x 20'-7"



APPENDIX B
Mathematical Expressions



B.1 Average Facing Flexural Stress

Based on Case 1 - Midpoint Loading

Assumption: Neglect contribution of Core

$$f = \frac{P_1 a_1}{2tb(h+c)} = 25.72p_1 \quad (\text{B.1})$$

Where:

f = Average facing stress in psi when P_1 is pounds

P_1 , a_1 , t , b , h and c are defined in figure B.1

B.2 Average Core Shear Stress

Based on Case 2 - Quarter-point Loading

Assumption: Neglect contribution of facings

$$v = \frac{P_2}{(h+c)b} = \frac{P_a}{47.6}$$

Where:

v = Average core shear stress in psi when P_2 is in pounds

P_2 , b , h and c are defined in figure B.1



B.3

Deflection Calculations

Case 1

$$w_1 = \frac{P_1 a_1^3}{48Db} + \frac{P_1 a_1}{4N} \quad (\text{B.3})$$

Case 2

$$w_2 = \frac{11 P_2 a_2^3}{768Db} + \frac{P_2 a_2}{8N} \quad (\text{B.4})$$

Where:

D = Sandwich flexural stiffness per unit width calculated as follows:

$$D = \frac{E (h^3 - c^3)}{12} \quad (\text{B.5})$$

N = Sandwich shear stiffness, calculated as follows:

$$N = \frac{G (h + c)^2 b}{4c} \quad (\text{B.6})$$

E = Modulus of elasticity of facings

G = Effective core shear modulus

Other symbols are defined in figure B.1



B.4 Experimental Flexural Stiffness

Solving Case 1 and Case 2 deflection expressions:

$$D = \frac{P_1 a_1^3}{48 w_1 b} \frac{\left(1 - \frac{11 a_2^2}{8 a_1^2}\right)}{\left(1 - \frac{2 P_1 a_1 w_2}{P_2 a_2 w_1}\right)} \quad (B.7)$$

Where:

Symbols are as previously defined

For Test Series S3

$$D = \frac{36,914}{w_1' \left(1 - 4 \frac{w_2'}{w_1'}\right)} \quad (B.7a)$$

Where u_1' and w_2' are secant slopes of the load deflection curves at one-half the ultimate load in inches/100 lb.

B.5 Experimental Shear Modulus, Unknown D

Solving Case 1 and Case 2 deflection expressions:

$$G = \frac{P_1 a_1 c}{w_1 b (h+c)^2} \frac{\left(\frac{8 a_1^2}{11 a_2^2} - 1\right)}{\left(\frac{16 P_1 a_1^3 w_2}{11 P_2 a_2^3 w_1} - 1\right)} \quad (b.8)$$

where:

Symbols are as previously defined

For Test Series S3

$$G = \frac{119.31}{w_1' \left(11.636 \frac{w_2'}{w_1'} - 1 \right)} \quad (\text{B.8a})$$

Where w_1' and w_2' are as defined in B.4

B.6 Experimental Shear Modulus, known D

a) Case 1 - Midpoint Loading

$$G = \frac{4c}{(h+c)^2 b} \frac{P_1 a_1}{\left(4w_1' - \frac{P_1 a_1^3}{12Db} \right)} \quad (\text{B.9})$$

For Test Series S3

$$G = \frac{249.98}{4w_1' - 0.1887} \quad (\text{B.9a})$$

Where w_1' is defined in B.4

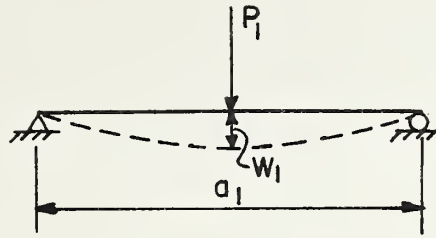
b) Case 2 - Quarter - Point Loading

$$G = \frac{4c}{(h+c)^2 b} \frac{P_2 a_2}{\left(8w_2' - \frac{11P_2 a_2^3}{96Db} \right)} \quad (\text{B.10})$$

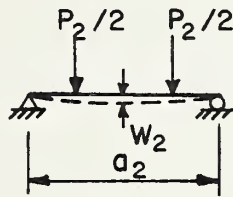
For Test Series S3

$$G = \frac{124.99}{(8w_2' - 0.03243)} \quad (\text{B.10a})$$

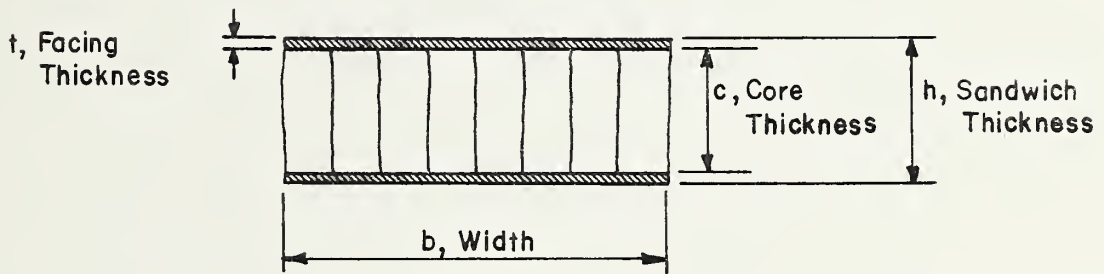
Where w_2' is defined in B.4



(a) Case 1 - Midpoint Loading



(b) Case 2 - Quarter Point Loading



(c) Cross Section

B.1 Loading Cases and Cross Section Notation

NATIONAL BUREAU OF STANDARDS REPORT

10 193

HAIL RESISTANCE TESTS OF ALUMINUM SKIN HONEYCOMB PANELS FOR THE RELOCATABLE LEWIS BUILDING, PHASE II

Report to
Commanding Officer
U. S. Navy Civil Engineering Laboratory
Port Hueneme, California



U.S. DEPARTMENT OF COMMERCE
NATIONAL BUREAU OF STANDARDS

NATIONAL BUREAU OF STANDARDS

The National Bureau of Standards¹ was established by an act of Congress March 3, 1901. Today, in addition to serving as the Nation's central measurement laboratory, the Bureau is a principal focal point in the Federal Government for assuring maximum application of the physical and engineering sciences to the advancement of technology in industry and commerce. To this end the Bureau conducts research and provides central national services in four broad program areas. These are: (1) basic measurements and standards, (2) materials measurements and standards, (3) technological measurements and standards, and (4) transfer of technology.

The Bureau comprises the Institute for Basic Standards, the Institute for Materials Research, the Institute for Applied Technology, the Center for Radiation Research, the Center for Computer Sciences and Technology, and the Office for Information Programs.

THE INSTITUTE FOR BASIC STANDARDS provides the central basis within the United States of a complete and consistent system of physical measurement; coordinates that system with measurement systems of other nations; and furnishes essential services leading to accurate and uniform physical measurements throughout the Nation's scientific community, industry, and commerce. The Institute consists of an Office of Measurement Services and the following technical divisions:

Applied Mathematics—Electricity—Metrology—Mechanics—Heat—Atomic and Molecular Physics—Radio Physics²—Radio Engineering²—Time and Frequency²—Astrophysics²—Cryogenics.²

THE INSTITUTE FOR MATERIALS RESEARCH conducts materials research leading to improved methods of measurement standards, and data on the properties of well-characterized materials needed by industry, commerce, educational institutions, and Government; develops, produces, and distributes standard reference materials; relates the physical and chemical properties of materials to their behavior and their interaction with their environments; and provides advisory and research services to other Government agencies. The Institute consists of an Office of Standard Reference Materials and the following divisions:

Analytical Chemistry—Polymers—Metallurgy—Inorganic Materials—Physical Chemistry.

THE INSTITUTE FOR APPLIED TECHNOLOGY provides technical services to promote the use of available technology and to facilitate technological innovation in industry and Government; cooperates with public and private organizations in the development of technological standards, and test methodologies; and provides advisory and research services for Federal, state, and local government agencies. The Institute consists of the following technical divisions and offices:

Engineering Standards—Weights and Measures—Invention and Innovation—Vehicle Systems Research—Product Evaluation—Building Research—Instrument Shops—Measurement Engineering—Electronic Technology—Technical Analysis.

THE CENTER FOR RADIATION RESEARCH engages in research, measurement, and application of radiation to the solution of Bureau mission problems and the problems of other agencies and institutions. The Center consists of the following divisions:

Reactor Radiation—Linac Radiation—Nuclear Radiation—Applied Radiation.

THE CENTER FOR COMPUTER SCIENCES AND TECHNOLOGY conducts research and provides technical services designed to aid Government agencies in the selection, acquisition, and effective use of automatic data processing equipment; and serves as the principal focus for the development of Federal standards for automatic data processing equipment, techniques, and computer languages. The Center consists of the following offices and divisions:

Information Processing Standards—Computer Information—Computer Services—Systems Development—Information Processing Technology.

THE OFFICE FOR INFORMATION PROGRAMS promotes optimum dissemination and accessibility of scientific information generated within NBS and other agencies of the Federal government; promotes the development of the National Standard Reference Data System and a system of information analysis centers dealing with the broader aspects of the National Measurement System, and provides appropriate services to ensure that the NBS staff has optimum accessibility to the scientific information of the world. The Office consists of the following organizational units:

Office of Standard Reference Data—Clearinghouse for Federal Scientific and Technical Information³—Office of Technical Information and Publications—Library—Office of Public Information—Office of International Relations.

¹ Headquarters and Laboratories at Gaithersburg, Maryland, unless otherwise noted; mailing address Washington, D.C. 20234.

² Located at Boulder, Colorado 80302.

³ Located at 5285 Port Royal Road, Springfield, Virginia 22151.

NATIONAL BUREAU OF STANDARDS REPORT

NBS PROJECT

4215421

April 10, 1970

NBS REPORT

10 193

HAIL RESISTANCE TESTS OF ALUMINUM SKIN HONEYCOMB PANELS FOR THE RELOCATABLE LEWIS BUILDING, PHASE II

by

Robert G. Mathey

Report to
Commanding Officer
U. S. Navy Civil Engineering Laboratory
Port Hueneme, California

IMPORTANT NOTICE

NATIONAL BUREAU OF STANDARDS REPORTS are usually preliminary or progress accounting documents intended for use within the Government. Before material in the reports is formally published it is subjected to additional evaluation and review. For this reason, the publication, reprinting, reproduction, or open-literature listing of this Report, either in whole or in part, is not authorized unless permission is obtained in writing from the Office of the Director, National Bureau of Standards, Washington, D.C. 20234. Such permission is not needed, however, by the Government agency for which the Report has been specifically prepared if that agency wishes to reproduce additional copies for its own use.



U.S. DEPARTMENT OF COMMERCE
NATIONAL BUREAU OF STANDARDS

T A B L E O F C O N T E N T S

	<u>Page</u>
1. Introduction.	1
2. Nature and Formation of Large Size Hail	3
3. Hail Occurrence and Intensity.	5
4. Description of Test Specimens	9
5. Test Procedure.	10
6. Test Results.	15
7. Conclusions	20
8. Acknowledgements.	21
9. References.	22

HAIL RESISTANCE TESTS OF ALUMINUM
SKIN HONEYCOMB PANELS FOR
THE RELOCATABLE LEWIS BUILDING, PHASE II

by
Robert G. Mathey

Ice spheres simulating hailstones were impacted on the surface of aluminum skin honeycomb panels in order to determine their resistance to hail. Various sizes of hailstones were projected at their terminal velocities and at velocities corresponding to wind driven hail. Damage caused by various sizes of hailstones on supported and unsupported areas of the panels are reported.

A brief discussion is given on the occurrence and intensity of hailstones and the probability of the size of hailstones when a hail day occurs.

1. INTRODUCTION

Hail resistance tests were carried out as part of the test and evaluation of the relocatable Lewis building, phase II. Structural tests on a full scale structural system of the relocatable Lewis building, phase II, were conducted in the Structural Laboratory at the National Bureau of Standards. A photograph of the building set up in the laboratory prior to the structural tests is presented in Figure 1. The building consists primarily of aluminum skin honeycomb panels having 3/4-inch cores.

The project leader of the full scale structural test, Mr. Thomas W. Recichard, requested on February 23, 1970 that hail resistance tests be conducted on typical aluminum skin honeycomb panels that are used or are proposed for use in the Lewis relocatable building. The hail impact tests were carried out in the Materials Durability and Analysis Section.

At the present time there are no standard methods of testing the hail resistance of materials nor are there standards for the evaluation of hail damage. Furthermore, there are no criteria for the



FIGURE I PROTOTYPE OF THE RELOCATABLE LEWIS BUILDING, PHASE II, SET UP IN THE LABORATORY FOR STRUCTURAL TESTS.





design of structures to resist hail. Because of the lack of standard test, evaluation, and design methods regarding hail resistance, the hail tests were planned to cover a range of sizes of ice spheres and impact energies. Although the density of hailstones is generally less than that for pure ice, ice was selected for the simulated hailstones for two reasons. First in some cases hail has been reported to have the same density as ice, thus providing more potential for structural damage, and secondly if some other material were used to simulate hailstones the damage evaluation may not correlate with that resulting from hail. Other investigators [1, 2, 3, 4]* used ice spheres in evaluating damage to structures that may be caused by hail.

2. NATURE AND FORMATION OF LARGE SIZE HAIL

Hailstorms are generally the outgrowth of thunderstorms and usually contain relatively small hailstones. However, large size hailstones, 1-inch in diameter or larger, have been reported to frequently fall in the United States and many other parts of the world. A review of the literature on hail formation [5, 6, 7, 8, 9] indicated that the mechanism of hail formation is not completely understood. However, in the United States it is generally accepted that the majority of the hailstorms result from warm moist tropical air from the Gulf area as it moves into the Middle Western States. Storms resulting in the fall of large size hail mostly occur in the States located between the Appalachian and Rocky Mountains. The surface temperatures are generally above freezing when hail occurs. Hail occurrence in Texas for example, is in the spring, early part of summer, and late fall.

The conditions needed to produce thunderstorms with sufficient intensity to develop damaging hail are (1) the air aloft is cooler than normal, (2) the air near the surface of the earth is warm and moist, (3) strong winds aloft to assist in developing vertical motion, (4) means of lifting the warm air to cause updrafts such as frontal lifting and

*Numbers in brackets indicate literature references given at the end of this report.



orographic lifting, and (5) air temperature not too warm below cloud formation so that the hail does not melt before reaching the earth. These conditions cause a rising column of air or updraft chimney that is roughly cylindrical in shape and topped by a half spherical cap. The updraft velocities in thunderstorms have exceeded 100 ft/sec and the distance these updrafts travel or the height of the storm effects the size of the hail that is discharged. This means that the longer the path length available for the growth of hailstones the larger they may grow.

The air in the upper portion of a thunderstorm is super cooled, with temperatures ranging from 0 to -40°C . The rising moist warm air is cooled below the freezing point and remains subcooled until it encounters a nucleus on which to freeze. As more water comes in contact with the ice particle it grows in size. At the higher levels of the storm cloud the very low temperatures cause rapid freezing of moisture and entrainment of air bubbles in the ice. Thus, an opaque low density layer of ice is formed. Falling of the hailstones into warmer regions results in accumulation of moisture in the form of water. When the ice particle encounters an updraft it is pushed up where it is cooled and the water freezes and forms a layer of dense clear ice. The ice particle again subcools and goes through the process of rising and falling, subcooling and freezing over and over until the updraft no longer is able to lift it. The hailstone then falls to earth at a constant velocity depending on its mass and the drag encountered. The hailstone in its cycling process of rising and falling developed alternate layers of opaque and clear ice. Hailstones with as many as 22 layers of ice have been reported [9].

It is also interesting to note that large size hailstones have been reported that have been of clear high density ice. The growth of large size hailstones can be compared to the accretion of ice on aircraft which is formed in layers. The hailstones move downward through the subcooled water drops at their terminal velocities. The updraft encountered serves primarily to increase the length of time and path

the hailstone travels through the cloud and thus to increase its collection of ice.

There are in general two types of hailstorms, the frontal storm which has been described and the orographic storm. In the latter, lifting of moist air occurs as it moves up the slopes of mountains. In the western-Midwestern States, orographic storms result from the lifting of air as it moves up the eastern slopes of the Rocky Mountains. The frontal storms occur in northern Texas and in the midwestern states extending northward. The duration of these hailstorms generally range between 1 and 15 minutes with the median length of hail duration being 5 minutes. The size of a representative hailstorm covers an area of 20 square miles.

Hail is defined as being composed of ice balls or stones ranging in diameter from that of medium size raindrops to about 5-inches in diameter. Hailstones 5-inches in diameter are theoretically the limiting size and hail this size was reported falling in Potter, Nebraska in November 1928. Hailstones of many different sizes fall at the same time. The size range was estimated to be about 3 to 1, or in most cases the largest size stone is about three times the size of the minimum stone. The large stones which are discharged by the heaviest storms are in general spherical in shape. In a study to determine the hail intensity in Northeastern Colorado and Western Nebraska in the summer of 1959 it was found that more than 75 percent of the hailstones that fell in this area approximated spheres [10]. Furthermore, the density of the hailstones were found to be 0.9 gm per cm^3 .

3. HAIL OCCURENCE AND INTENSITY

Rational methods for predicting hail occurrence have been developed by Thom [11]. A method for predicting the frequency and probability of size of hail for the Midwestern States was developed by Friedman [12]. It is important to the engineer to have criteria to be able to design structures that will perform satisfactorily. Information presented by Friedman [12] will enable a more rational design of



structures in the Midwest to resist hail damage.

In the Midwestern States the occurrence of hail large enough to cause property damage is relatively rare for any given location. Some locations in this area of the United States are more likely than others to have hailstorms containing large size hail. The average number of days per year that hail storms have occurred in the Midwestern States over a period of 57 years has been reported [12]. These data were derived from U. S. Weather Bureau reports that include only the annual number of days with hail and did not mention hail size. It is noted that the Weather Bureau does not normally report hail size. The annual frequency patterns of the number of days with hail reported by Friedman [12] is shown in Figure 2.

Using several sources of data Friedman [12] also estimated the probability that hail will be of a given size on a day when hail occurs. Over 3,000 reports from the U. S. Weather Bureau monthly bulletin Storm Data covering a 17 year period (1950-1966) were tabulated and studied in order to validate the estimated probability of hail size on a hail day. Many of the damage reports for which hail was a factor, hail size was estimated. The probability of a given size of hail with regard to the annual average number of days with hail is given in Table 1. By using Figure 2, the average annual number of days with hail in the Midwestern States, and Table 1, the hail size occurrence could be estimated on a geographical basis. An example of hail size probability, areas having 4 average annual number of days with hail, the probability of hailstones exceeding 1-inch in diameter on a day with hail is about 13 out of 100.

Most of the property damage due to hail has been to roofing. A hailstorm struck Billings, Montana on July 6, 1955 and caused over 5 million dollars in property damage [13]. Damage to roofs accounted for nearly 80 percent of the building losses. The storm lasted 15 minutes and hailstones the size of baseballs (2 3/4-in. in diameter) were found embedded in the lawn of a homeowner after the storm.



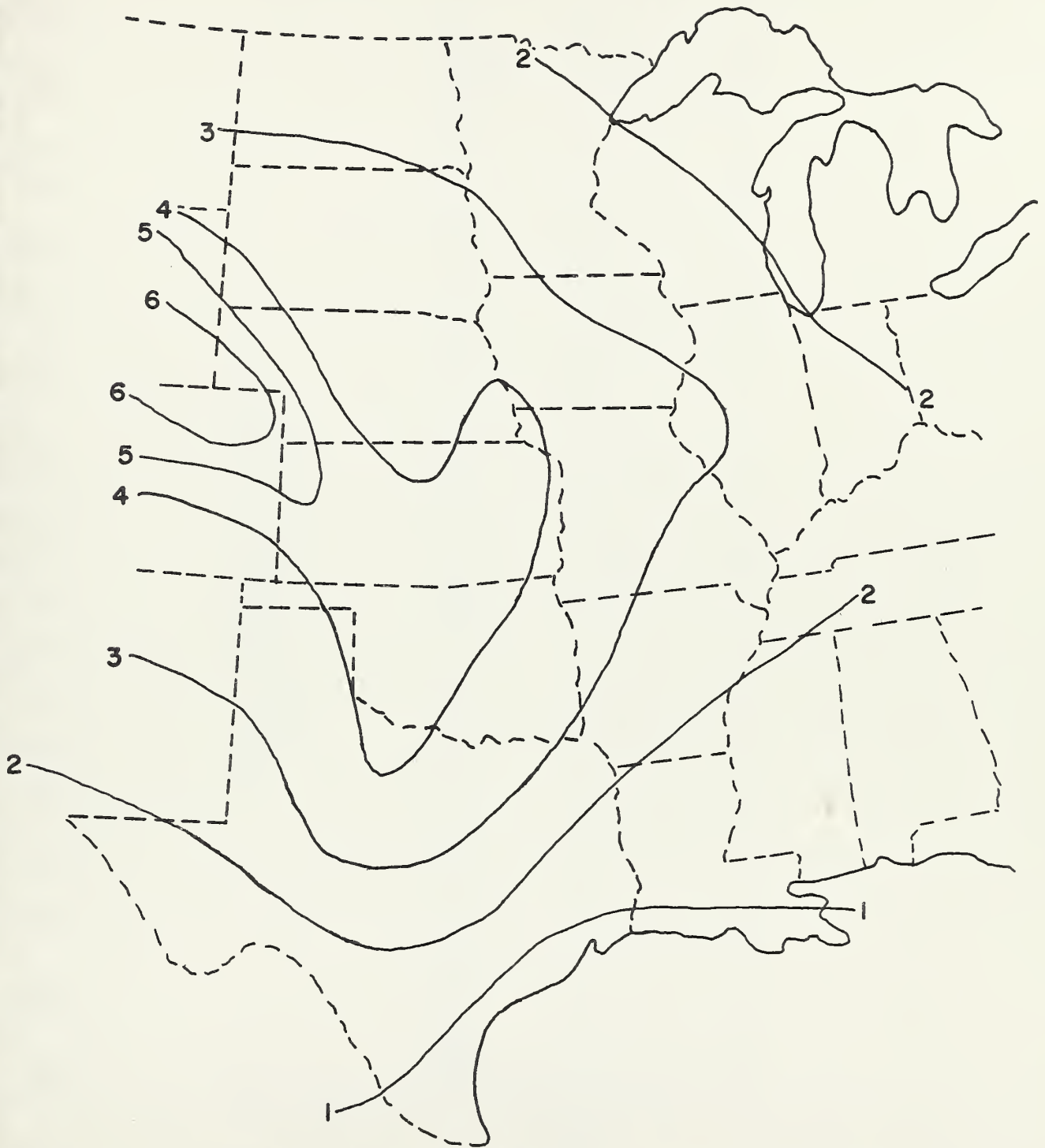


FIGURE 2. AVERAGE ANNUAL NUMBER OF DAYS WITH HAIL IN THE MIDWESTERN STATES [12]



TABLE 1. Probability of A Given Hail
 Size as A Function of Annual
 Average Days with Hail [12].

Average Annual Number of Days with Hail	P R O B A B I L I T Y O F H A I L S I Z E W H E N A H A I L D A Y O C C U R S										
	Less Than 0.5-in.	0.5-in.	1.0-in.	1.5-in.	2.0-in.	2.5-in.	3.0-in.	3.5-in.	4.0-in.	More Than 4.0-in.	Total
2	0.613	0.284	0.035	0.031	0.016	0.005	0.002	0.002	0.002	0.002	1.000
4	0.435	0.433	0.044	0.039	0.023	0.006	0.004	0.004	0.004	0.004	1.000
6	0.254	0.580	0.053	0.047	0.030	0.008	0.008	0.004	0.004	0.007	1.000



In South Africa the more common hail storms are those where the hail size is 0.5-inches in diameter or less, damage due to this size hail by impact is negligible. Property losses from these storms results from the accumulation of hail that dams rainwater which penetrates the laps in roofing materials. The severe hailstorms in South Africa occur in the summer rainfall area and hailstones up to 3-inches in diameter have occurred over most of this area. Pretoria has experienced a number of severe hailstorms within the last forty years [1]. A hailstorm in 1958 in the Woomera area of Australia damaged roofs and other property. It is estimated that hail was approximately 1 1/2-inch in diameter [4]. Hailstones were also reported falling in California that had diameters up to 1 3/4-inches.

4. DESCRIPTION OF TEST SPECIMENS

The test specimens were cut from two types of full size honeycomb sandwich panels having aluminum skins and paper cores. The skins were 3105-H264 aluminum 0.024-in. in thickness that were stucco embossed and prefinished by the aluminum producer. The only difference in the two types of 3-in. thick panels were the paper cores. In one type of panel the cores were 3/4-in. and were made with No. 99 paper. The paper number indicates its weight per 3,000 ft². The second type of panel had 1/2-in. cores made with No. 70 paper. Both types of paper were impregnated with 11 percent phenolic resin. The adhesive used to attach the aluminum skin to the cores was a neoprene phenolic resin, a contact adhesive applied with 25 to 30 percent solids. The solvent was evaporated out of the adhesive in a flash oven.

The full scale relocatable Lewis building, Phase II, shown in Figure 1 was fabricated with 4 x 8-ft. panels having 3/4-inch cores. Panels having 1/2-inch cores were not included in the prototype building. However, it was desirable to also determine the hail resistance of these panels since they may be used in future buildings.

Two 2 x 3-ft. test specimens were cut from both the 1/2-inch and 3/4-inch core panels. Strips of wood nominally 2 x 2-inches in cross section and 2-ft. long were attached using an adhesive along a line



3-inches from the ends of the specimens. The strips were oriented along the 2-ft. length of the specimen. By attaching strips of wood to the specimens it provided supported and unsupported areas that were impacted with simulated hailstones. Photographs of damaged specimens are shown in Figures 3 and 4.

5. TEST PROCEDURE

Simulated hailstones, ice spheres, were fired at the test specimens from a compressed air gun. The method used in these tests for shooting hailstones was a modification of the method developed by Greenfeld [2]. The test system for shooting and measuring the velocity of hailstones is shown in Figure 5. The inside diameter of the 40-inch long barrel on the gun was 3 1/16-in. Hail carriers made from 3-inch diameter polyethylene cylinders 6-inches long were used to carry the ice spheres out of the barrel of the gun. The polyethylene cylinders were cut in half longitudinally. The hemicylinders had hemispheres cut in them 2 1/4-inches from one end and were truncated at the other end at an angle of 45 degrees to a plane passing through the longitudinal axis. Therefore, various sizes of ice spheres could be fired from the same gun barrel. A different carrier for each size of ice sphere was used. The truncated portions of the carrier allowed the two hemicylinders to separate after leaving the barrel of the gun while the ice sphere continued toward the target area.

The pressure in the chamber of the gun was determined by a pressure gage. The desired velocity of the hailstone was calibrated with gun chamber pressure. However, the velocity was determined by using two 5-inch wide beams of light and a pair of photo electric cells. The beams of light were spaced 2-ft. apart with the second beam that the ice spheres passed through being 3-inches in front of the test specimen. The light source and the photo electric cells were supported on a steel frame. A digital timer powered by 100,000 cycles standard frequency recorded the time that the hailstone traveled between light beams. This time was measured with an accuracy of 1/2 percent.



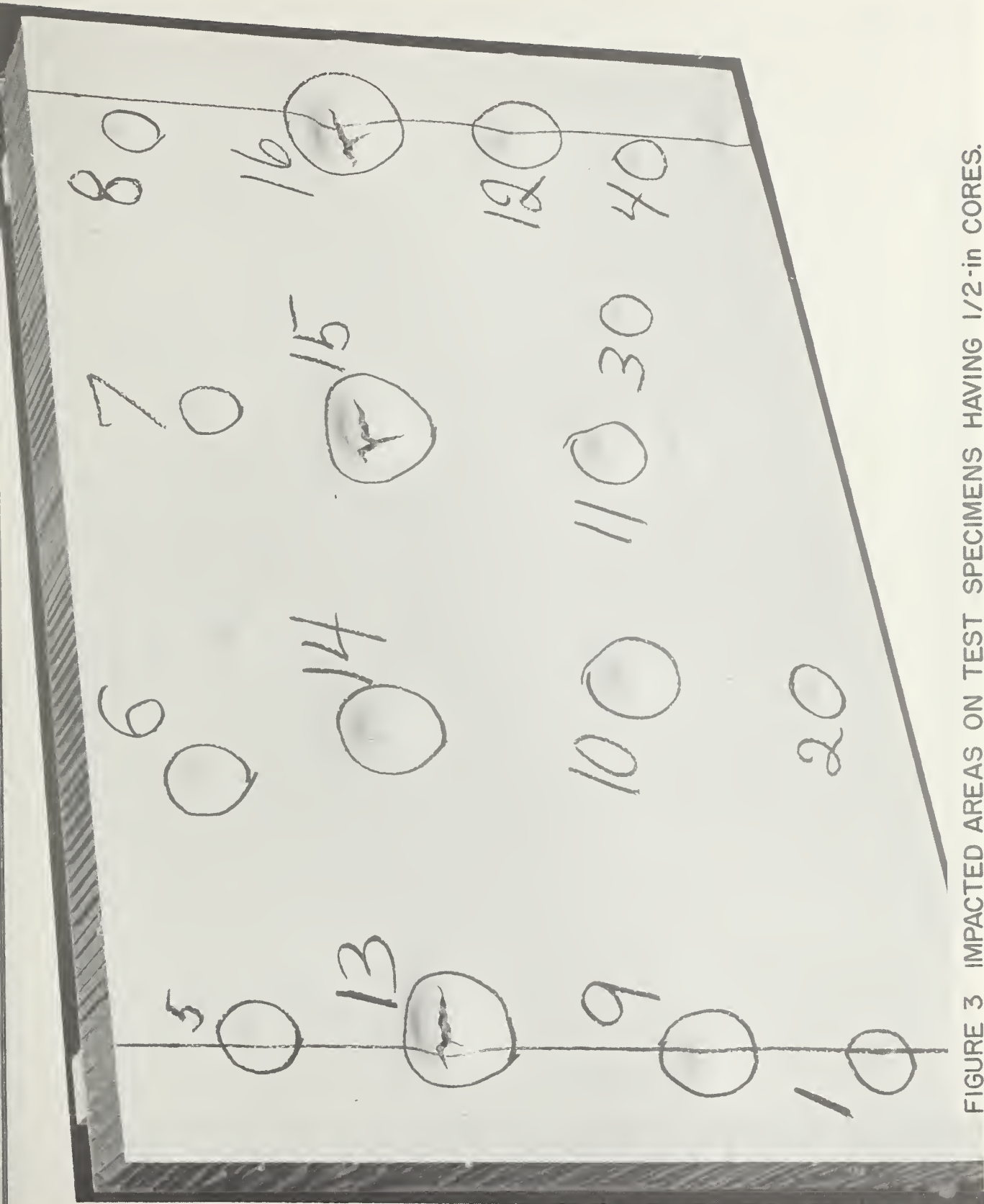


FIGURE 3 IMPACTED AREAS ON TEST SPECIMENS HAVING 1/2-in CORES.

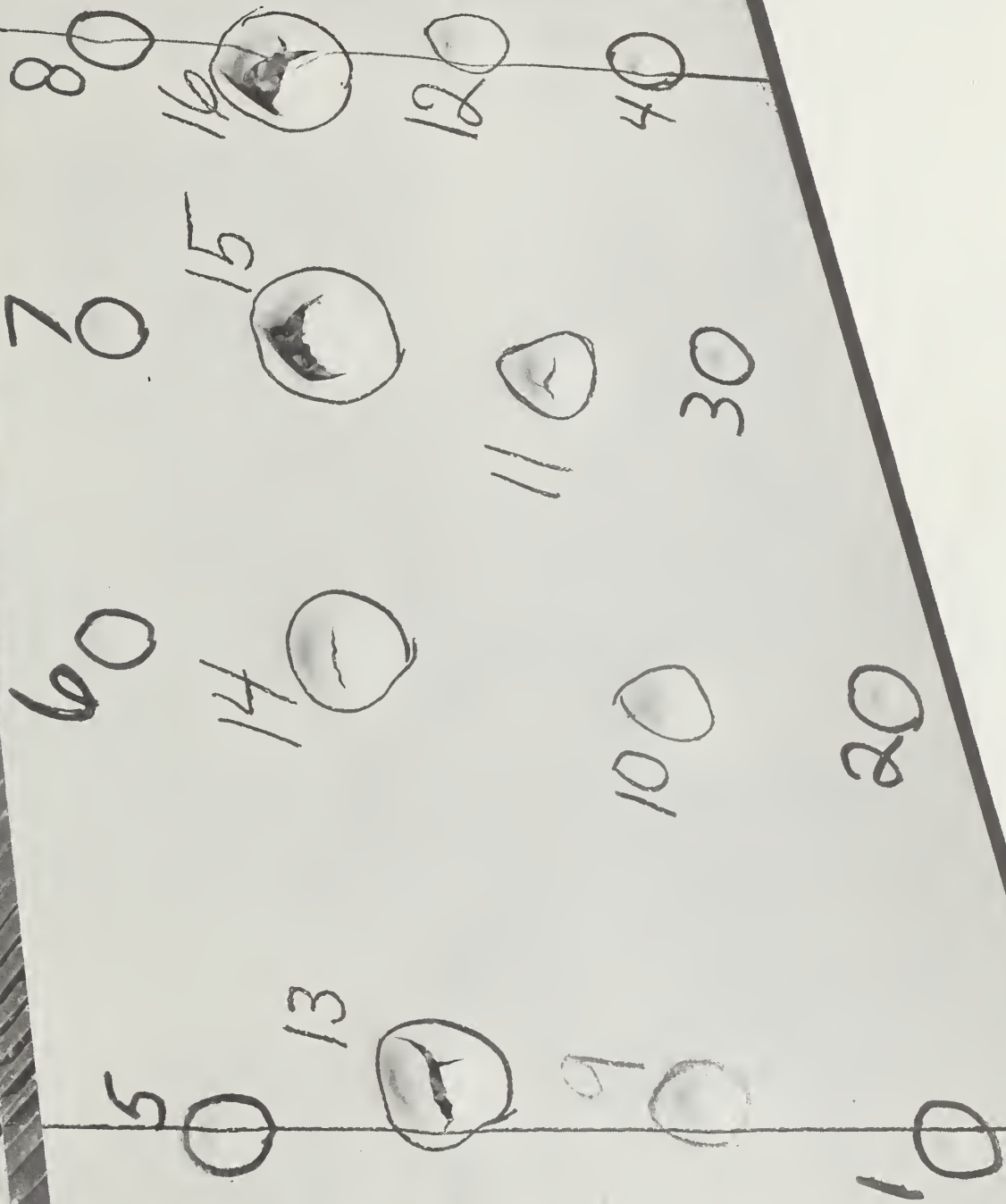
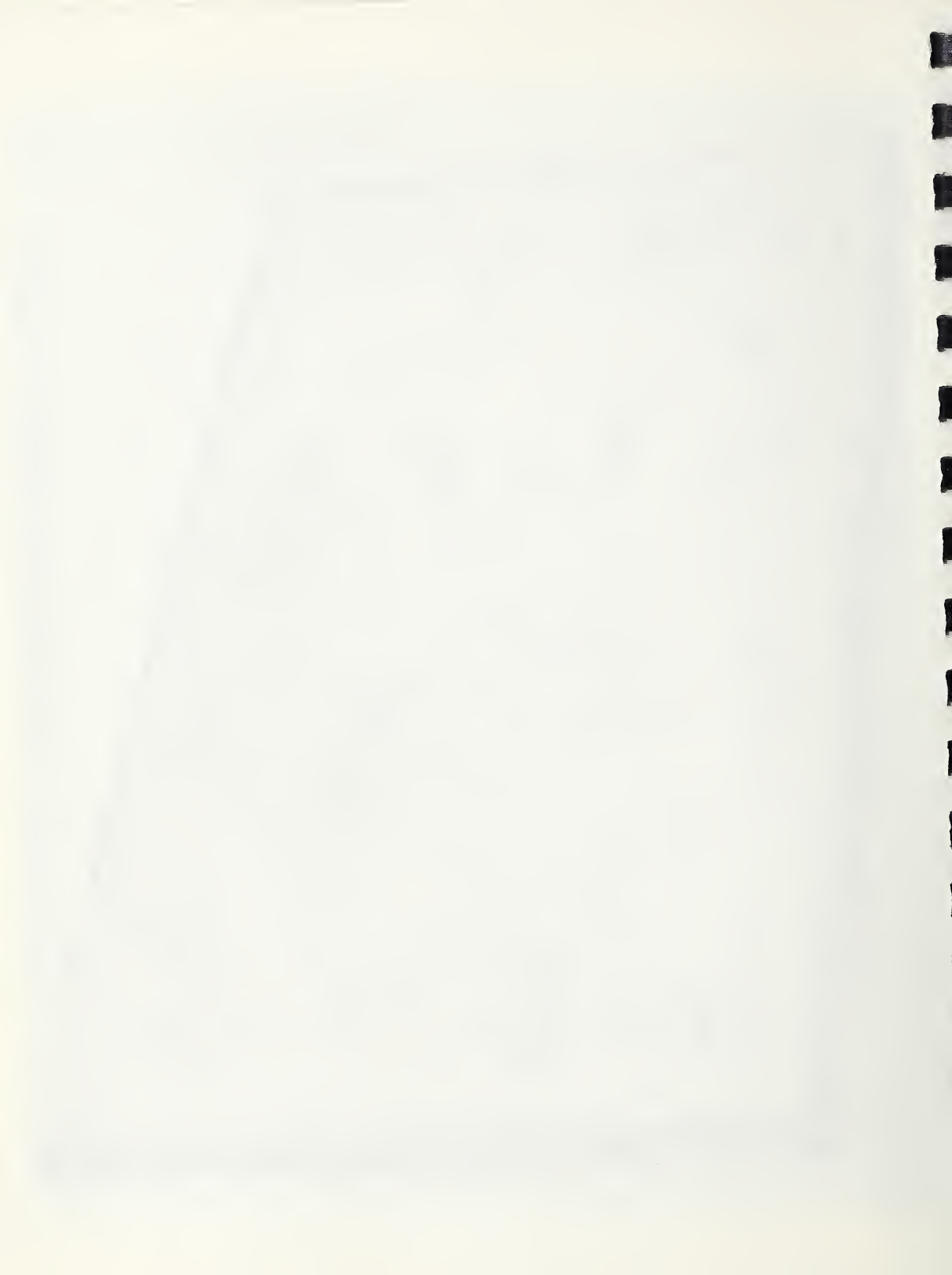


FIGURE 4 IMPACTED AREAS ON TEST SPECIMENS HAVING 3/4-IN CORES.



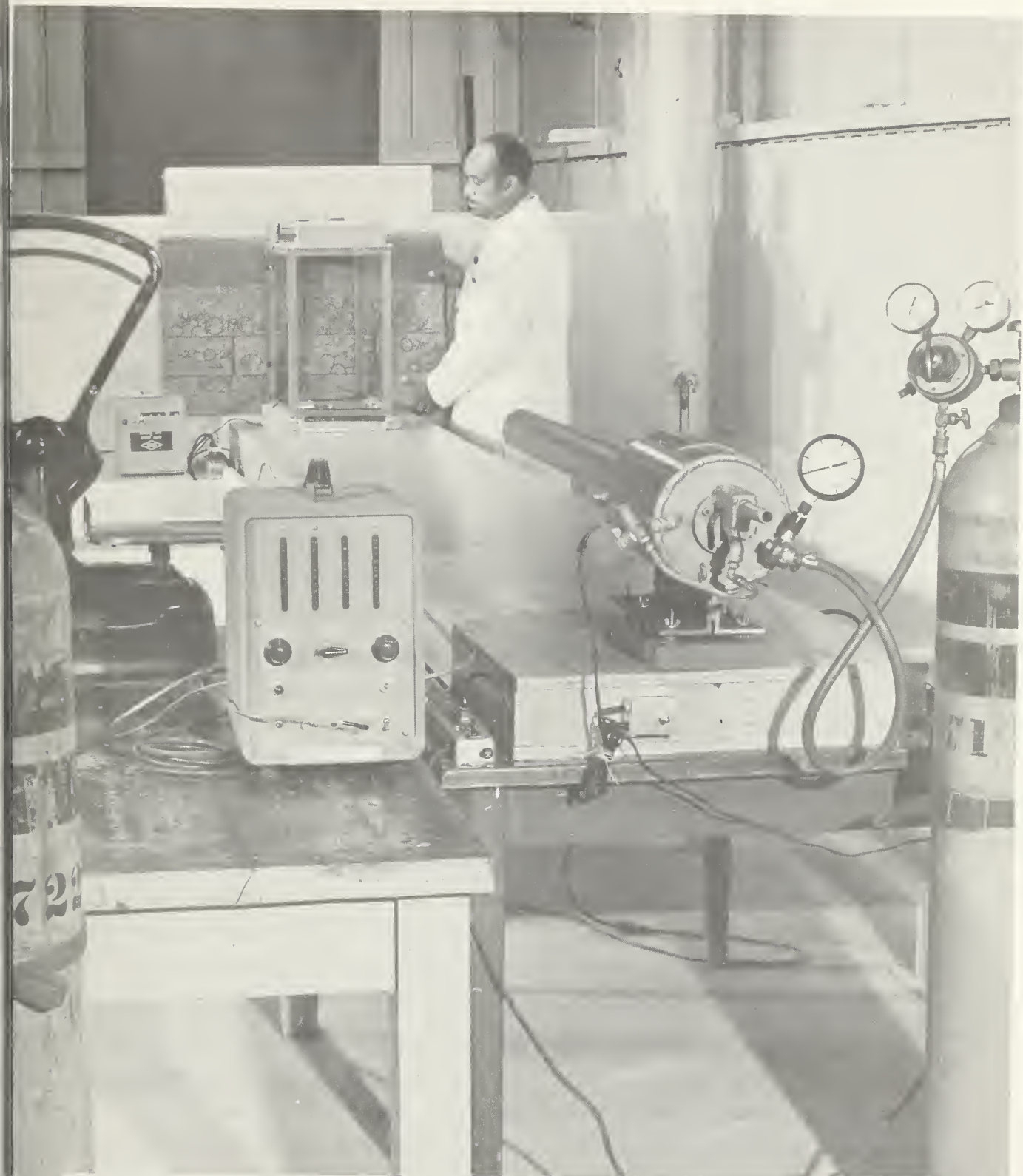
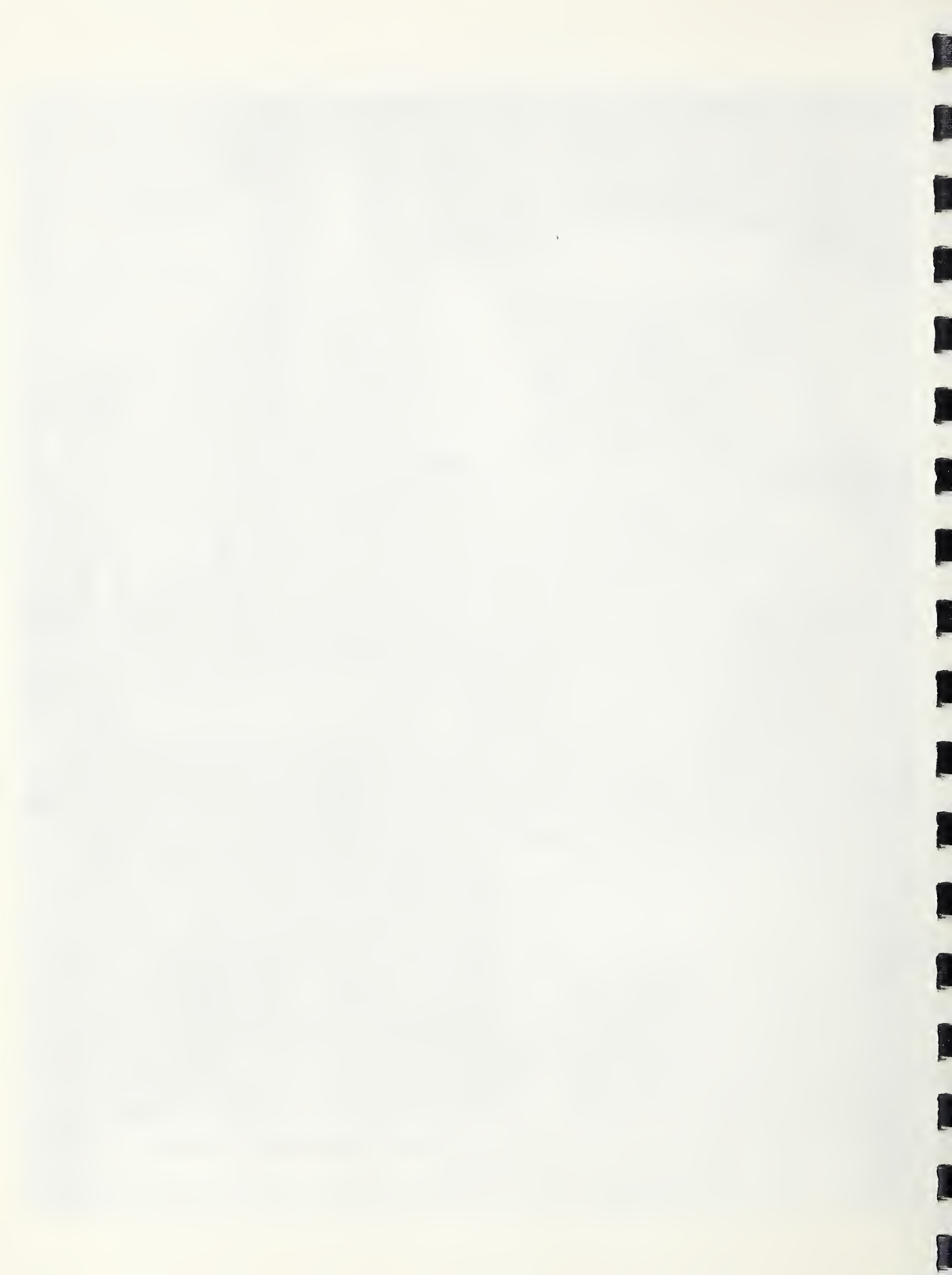


FIGURE 5 TEST SYSTEM FOR SHOOTING AND MEASURING THE VELOCITY OF HAILSTONES.



The test specimen was placed against the backstop shown in Figure 5 and held firmly in place with a C clamp. Ice spheres 1 1/4, 1 1/2, 2, and 2 1/2-inches in diameter were impacted on the specimen at velocities corresponding to the terminal velocity and a velocity which took into account a 45 mph wind acting on a free falling hailstone.

The hailstones were made in the laboratory in silicone rubber molds. They were cast in two stages in order to permit the expansion of water during freezing without causing cracking or shattering of the ice spheres. The density of the artificial hailstones was 0.9 gm/cm³. Density of hail has been reported to range between 0.7 and 0.91 gm/cm³, the latter value being the density of pure ice.

The ice spheres were stored in a freezer at about -19°C until ready for use. At the time of firing, an ice sphere was removed from the freezer cleaned of any burrs or projecting pieces of ice, weighed, placed in the hailstone carrier which was then slid into the barrel of the gun as far as possible. Air or nitrogen was then allowed to enter the chamber of the gun to the desired pressure and the gun was fired. The elapsed time between taking the ice sphere out of the freezer and it being fired from the gun was about 1 minute. When the carrier with the ice sphere was propelled from the gun, the air resistance forced the carrier to separate the two halves, thus allowing the hailstone to travel alone toward the target. Prior to hitting the target the ice sphere passed through two beams of light, the first starting the counter and the second stopping the counter. This enabled accurate determination of velocity and combined with the weight of the hailstone, values of kinetic energy were computed.

Test specimens were tested in duplicate with 16 shots fired at each specimen. Each of the four sizes of hailstones were fired at two different velocities at points on the specimen that were supported and unsupported.

The diameter and depth of indentation on the specimen was measured and the condition of the specimen after firing was recorded. Photographs of test specimens showing impacted areas are presented in Figures 3 and 4. The depth of the indentations were measured with a 0.001-inch micrometer dial gage that was supported on a steel frame. The stem of



the dial gage was at the center of two 1/4-inch diameter posts on the frame that were 3-inches apart. The position of the posts on the test specimen determined the plane of reference in making the depth measurements.

6. TEST RESULTS

Hailstones fall of different sizes, shapes and at different velocities depending on their mass and atmospheric conditions. Extensive studies [10] have shown that approximately over 75 percent of large size hail is spherical or nearly spherical in shape. Other experimental studies [14] have provided values of drag applicable to hail falling through the atmosphere. Coefficients of drag of ice spheres traveling through air were obtained in one investigation from observations on ice spheres towed by airplanes.

When a hailstone falls to earth, its velocity becomes a constant value when the drag forces equal its mass. Therefore, under conditions of no wind this constant velocity can be reasonably predicted. It has been pointed out that thunderstorms are generally accompanied by a strong wind. The value of wind speed varies considerably, however, reported values of range from 30 to 60 mph for the more frequently occurring winds during a hailstorm. Therefore, for the tests reported herein a value of 45 mph was taken as a representative value of the wind velocity for wind driven hail. Table 2 gives values of terminal velocity, resultant velocity (assuming a 45 mph wind), weight, and the kinetic energy for smooth ice spheres having diameters ranging from 1/2 to 4-inches. In computing these values the specific gravity of ice was taken as 0.915 gm/cm³. The terminal velocity was computed from an equation derived by Bilham and Relf [14]. Values for the density and kinematic viscosity of the air were taken as 0.0758 lb/ft³ and 0.000159 respectively.

Damage to property by hail generally starts with hail having a diameter between 1 and 1 1/2-inches and having kinetic energy from about 1.5 to 7.5 ft. lb. Roofing damage was defined [2] as severe or super-

TABLE 2. Values of Weight, Terminal Velocity, Resultant Velocity, and Kinetic Energy Computed for Smooth Ice Spheres.

Diameter in	Weight		Terminal Velocity ft/sec	Resultant Velocity ft/sec	Kinetic Energy ^{1/}	
	gm	lb			ft-lb	
1/2	0.98	0.002	51	83	0.09	0.24
3/4	3.30	0.007	62	91	0.44	0.94
1	7.85	0.017	73	98	1.43	2.58
1 1/4	15.33	0.034	82	105	3.53	5.79
1 1/2	26.50	0.058	90	112	7.35	11.38
1 3/4	42.08	0.093	97	117	13.56	19.73
2	62.81	0.138	105	124	23.71	33.07
2 1/4	89.43	0.197	111	129	37.73	50.96
2 1/2	122.67	0.270	117	134	57.48	75.39
2 3/4	163.28	0.360	124	140	85.95	109.57
3	211.98	0.467	130	146	122.66	154.71
3 1/4	269.51	0.594	137	152	173.21	213.21
3 1/2	336.61	0.742	143	157	235.67	284.08
3 3/4	414.02	0.913	149	163	314.71	376.63
4	502.46	1.108	155	168	413.31	485.55

^{1/} First value corresponds to the terminal velocity and the second value corresponds to the resultant velocity.



TABLE 3. Diameter and Depth of Impacted areas and Properties of Hailstones causing Indentations in Test Specimens

Indentation Number	Ice Sphere Diameter	Average Weight of Ice Spheres	Average Velocity	Kinetic Energy	Impact Location	Panels with 1/2-in. Cores			Panels with 3/4-in. Cores		
						Average Diameter	Average Indentation	Average Overall Indentation	Average Diameter	Average Indentation	Average Overall Indentation
	in.	gm	ft/sec	ft-lb	in.	in.	in.	in.	in.	in.	in.
1	1 1/4	14.5	85	3.6	1/4 span	0.82	0.11	1.48	0.72	1.51	0.12
2	1 1/4	14.5	85	3.6	support	0.81	0.12	1.48	0.80	1.55	0.11
3	1 1/4	14.5	105	5.5	1/4 span	0.79	0.17	1.64	0.75	1.65	0.14
4	1 1/4	14.5	105	5.5	support	0.68	0.16	1.49	0.80	1.62	0.15
5	1 1/2	25.8	93	7.6	1/4 span	0.81	0.20	2.04	0.75	1.86	0.17
6	1 1/2	25.8	93	7.6	support	0.95	0.20	1.86	0.91	2.08	0.20
7	1 1/2	25.8	115	11.7	1/4 span	0.88	0.24	1.98	0.86	2.12	0.24
8	1 1/2	25.8	115	11.7	support	0.95	0.25	2.11	0.95	2.21	0.25
9	2	60.2	109	24.5	1/4 span	1.45	0.36 ^{1/}	2.98	1.34	2.85	0.34
10	2	60.2	109	24.5	support	1.52	0.36	3.00	1.36	3.02	0.34 ^{2/}
11	2	60.2	123	31.2	1/4 span	1.46	0.39 ^{1/}	2.95	1.52	3.00	0.45 ^{2/}
12	2	60.2	123	31.2	support	1.48	0.40	3.41	1.25	3.28	0.35 ^{1/}
13	2 1/2	121.5	115	55.0	1/4 span	1.65	0.47 ^{1/}	3.61	2.01	3.90	0.51 ^{3/}
14	2 1/2	121.5	115	55.0	support	1.90	0.56 ^{2/}	3.86	2.30	3.82	0.70 ^{4/}
15	2 1/2	121.5	135	75.8	1/4 span	2.50	0.80 ^{4/}	4.12	2.98	3.98	1.0 ^{4/}
16	2 1/2	121.5	135	75.8	support	2.59	0.84 ^{4/}	4.18	2.91	4.22	1.0 ^{4/}

1/ Crack in indentation in one of the panels

2/ Large Y-shaped crack in indentation in one of the panels

3/ Crack in indentation of one panel and large Y-shaped crack in indentation in other panel

4/ Large Y-shaped cracks in indentations in both panels

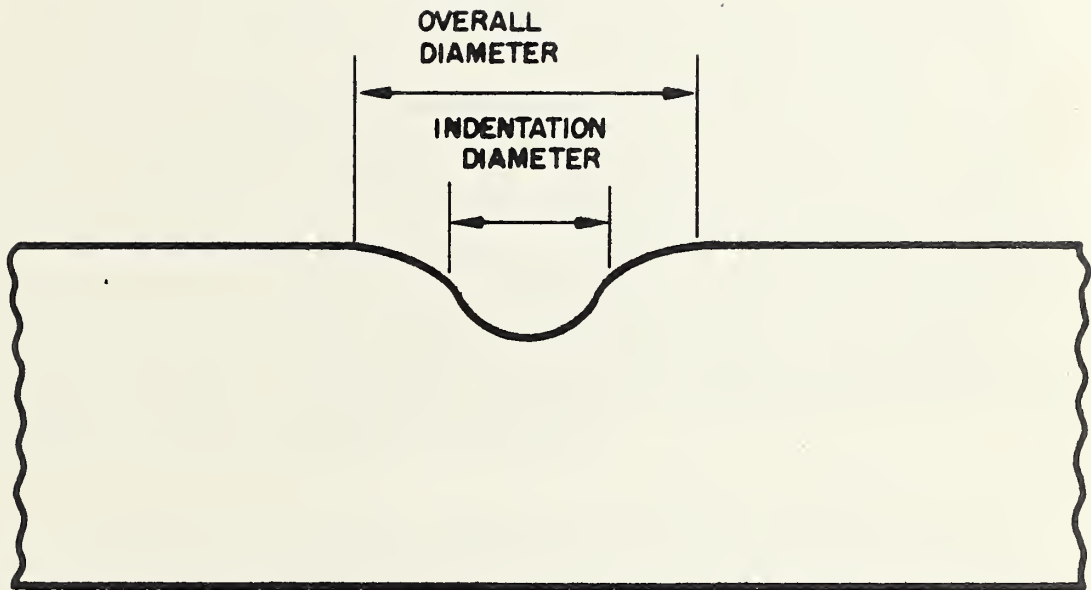


FIGURE 6 CROSS SECTION VIEW OF TYPICAL
INDENTATION IN ALUMINUM SKIN
HONEYCOMB PANEL TEST SPECIMENS

ficial. Severe damage leads to penetration of the structure by the elements. Some obvious indications of severe damage are cracks, punctures, tears or openings in the surface of the material protecting the structure. Superficial damage effects the appearance of the structure but does not interfere with its performance. Both types of damage lead to insurance claims; however, severe damage may result in losses far in excess of the replacement cost of the damaged area. The indentations in the test specimens are reported along with the fractures in the aluminum skin. These fractures in the material are considered as failure in this report.

The diameter and depth of the indentation in the test specimens shown in Figures 3 and 4 along with the weight, velocity, impact location, and kinetic energy of the hailstones are given in Table 3. This table also includes information on cracking in the test specimen due to impact of hailstones. The values in this table are average values for two test specimens. It is noted in Table 3 that there are two values given for the diameter of indentation. The sketch in Figure 6 depicts the typical cross section of an impacted area of the skin of the honeycomb panel. The overall diameter and indentation diameter of the impacted area are shown on the sketch.

In comparing the average indentation diameter, average overall indentation diameter, and the average depth of indentation given in Table 3 for panels having 1/2 and 3/4-inch cores, it can be seen that there was little difference in the hail resistance of the two panels. Only in the case of the indentation caused by the 2 1/2-inch diameter ice spheres was there a noticeable difference in performance of the panels to resist large size hail. The panels with the 1/2-inch cores developed smaller indentations, however, damage was very extensive for both types of panels. The location of impact with regard to supported or unsupported areas on the test specimens also had no appreciable effect on the hail resistance.

Both types of panels with the 1/2 and 3/4-inch cores resisted the 1 1/2-inch diameter hailstones without developing cracks or breaks in the aluminum skin. The kinetic energy of the 1 1/2-inch diameter hailstones traveling at the resultant velocity (terminal velocity combined with a 45 mph wind) was 11.7 ft-lb. The average depths of indentations caused by the 1 1/2-inch diameter ice spheres ranged from 0.17 to 0.25 inches for the terminal and resultant velocity respectively. These indentations at both supported and unsupported areas after affect the appearance but not the performance to resist penetration of moisture or water.

Values of kinetic energy for various sizes of hailstones ranging in diameter from 1/2 to 4-inches and traveling at the terminal velocity and resultant velocity are given in Table 2. These values differ slightly from those given in Table 3 since the values in Table 2 were determined from computed velocities of smooth ice spheres. The values in Table 3 were determined from the measured velocity and weight of the hailstone. The density of the ice balls used in the test was about 0.9 gm/cm³. In an investigation [3] to establish a quantitative method of evaluating hail damage to roofing products. The kinetic energy at impact was taken as a suitable criterion because the work required to stop a moving object is equal to its kinetic energy. The kinetic energy at impact of a hailstone which cracks or causes breaks in the roofing products was considered as a measure of hail resistance of the material..

Tests were carried out by hitting one area with a hailstone of a given size. Tests did not include multiple hits in one specific area because of the difficulty of evaluating damage.

In hail tests reported by Rigby [3] of plain corrugated aluminum roofing 0.025-inches in thickness and supported by 2 X 3-inch purlins at 2 1/2-ft. on centers on rafters at 4 1/2 ft-lb on centers the impact energy to cause failure was 56 ft-lb. This material was more severely damaged near the purlins. Once the material was punctured it was weakened considerably and subsequent shots easily extneded the damage.

7. CONCLUSIONS

1. The two types of aluminum smin honeycomb panels having 1/2 and 3/4-inch cores resisted hailstones up to 1 1/2-inches in diameter

without causing cracks or breaks in the aluminum skin. The kinetic energy of the 1 1/2-inch diameter hailstones at impact ranged from 7.6 to 11.7 ft-lb.

2. Kinetic energy is a suitable criterion for establishing a quantitative means for evaluating the hail resistance of building materials.

3. There was appreciably no difference in the hail resistance of the panels having 1/2 and 3/4-inch cores.

4. The location of the point of impact of the hailstone with regard to supported or unsupported areas on the test panels did not effect the hail resistance.

5. Data are presented [12] that gives the estimated probability of a given hail size when a hail day occurs for the Midwestern States of the U. S.

8. ACKNOWLEDGEMENT

Acknowledgement is made to Jessie C. Hairston for preparing the specimens for test, assisting in carrying out the tests and measurement of indentations.

USCOMM-NBS-DC

REFERENCES

1. Laurie, J. A. P., Hail and its Effects on Buildings, C. S. I. R. Research Report No. 176, Bull. 21, 1-12, National Building Research Institute, Pretoria, South Africa, August, 1960.
2. Greenfeld, Sidney H., Hail Resistance of Roofing Products, National Bureau of Standards (U. S.), Building Science Series 23, August 1969.
3. Rigby, Charles A., The Hail Resistance of South African Roofing Materials, South African Architectural Record, Vol. 37, No. 4, June 1952.
4. Simulated Hailstone Fabrication and Use in Testing Weatherability of Structures, Technical Support Package for NASA Tech Brief 68-10552, NASA Technology Utilization Office, Pasadena, California.
5. Friedman, D. G., Texas Hailstorms, Research Department Report, The Travleers Insurance Companies, May 1965.
6. Beckwith, W. Boynton, Hail Observations in the Denver Area, United Air Lines Meteorology Circular No. 40, April 1, 1956.
7. Weickmann, Helmut K., The Language of Hailstorms and Hailstones, USASRDL Technical Report 2277, U. S. Army Signal Research and Development Laboratory, Fort Monmouth, New Jersey, 1962.
8. Facy, L., Merlivat, L., Neif, G. and Roth, E., The Study of the Formation of a Hailstone By Means of Isotopic Analysis, Jour. of Geophysical Research, Vol. 68, No. 13, July 1, 1963.
9. Browning, K. A., Ludlam, F. H., Macklin, W. C., The Density and Structure of Hailstones, Quart. J. R. Meteorol. Sol. 89, 75-84, 1963.
10. Schleusener, Richard A. and Jennings, Paul C., An Energy Method for Relative Estimates of Hail Intensity, Bull. Amer. Meteorol. Soc. Vol. 41, No. 7, July 1960.
11. Thom, H. C. S., The Frequency of Hail Occurrence, Archivfur Meteorologie, Geophysik and Bioklimatologie, Serie B Allgemeine und Biologische klimatologie, Band 8, 2. Heft, 1957

12. Friedman, D. G., and Shortell, P. A., Prospective Weather Hazard Rating in the Midwest With Special Reference To Kansas and Missouri, Research Department, The Travelers Insurance Companies, August 28, 1967.
13. Fuchs, E. Rod, Hailstorm in Montana, American Roofer, Nov., 1955.
14. Bilham, E. G., Relf, E. F., The Dynamics of Large Hailstones, Quart. J. R. Meteorol. Soc. 63, 149-162, 1937.

